The Republic of the Sudan

Ministry of Higher Education and Scientific Research

Nile Valley University

Faculty of Post – Graduate Studies

Biaxial Buckling of Thin Laminated Composite Plates

A thesis Submitted in Fulfillment of the Requirements for the Ph.D. in Mechanical Engineering

By:
Assistant Professor Osama Mohammed Elmardi Suleiman Khayal

Supervised by:
Associate Professor Dr. Tagelsir Hassan

October 2017

The Republic of the Sudan

Ministry of Higher Education and Scientific Research

Nile Valley University

Faculty of Post – Graduate Studies

Biaxial Buckling of Thin Laminated Composite Plates

A thesis Submitted in Fulfillment of the Requirements for the Ph.D. in Mechanical Engineering

By:
Assistant Professor Osama Mohammed Elmardi Suleiman Khayal

Supervised by:
Associate Professor Dr. Tagelsir Hassan

October 2017

Dedication

In the name of Allah, the merciful, the compassionate

All praise is due to Allah and blessings and peace is upon his messenger and servant, Mohammed, and upon his family and companions and whoever follows his guidance until the day of resurrection.

To the memory of my mother **Khadra Dirar Taha**, my father **Mohammed Elmardi Suleiman**, and my dear aunt **Zaafaran Dirar Taha** and my second mother **Niemat Ibrahim Suleiman** who they taught me the greatest value of hard work and encouraged me in all my endeavors.

To my first wife **Nawal Abbas Abdelmajied** and my beautiful three daughters **Roa**, **Rawan** and **Aya** whose love, patience and silence are my shelter whenever it gets hard.

To my second wife **Limya Abdullah Ali** whose love and supplication to Allah were and will always be the momentum that boosts me through the thorny road of research.

To professor **Mahmoud Yassin Osman** for reviewing and modifying the manuscript before printing process.

To the memory of Professors **Elfadil Adam** and **Sabir Mohammed Salih.**

This thesis is dedicated mainly to undergraduate and postgraduate students, especially mechanical and civil engineering students plus mathematicians and mathematics students where most of the work is of mathematical nature.

To Mr. **Osama Mahmoud Mohammed Ali** of Daniya Center for Printing and Publishing Services whose patience in editing and re – editing the manuscript of this thesis was the momentum that pushed me in completing successfully the present work.

To my friend Professor **Elhassan Mohammed Elhassan Ishag**, Faculty of Medicine, University of Gezira, Medani, Sudan.

To my friend **Mohammed Ahmed Sambo**, Faculty of Engineering and Technology, Nile Valley University, Atbara, Sudan.

To my homeland, Sudan, hoping to contribute in its development and superiority.

Finally, may Allah accept this humble work and I hope that it will be beneficial to its readers.

Acknowledgement

I am grateful and deeply indebted to Associate Professor Dr. **Tagelsir Hassan** for close supervision, constructive criticism, and provision of useful parts of his papers and/ or other relevant materials during his stay in Russia, and also the valuable recommendations during the various stages of building up the present study, without which this work would not have been accomplished.

I am also grateful to Professor Dr. **Mahmoud Yassin Osman** who supervised me during the first period of this study.

I am also indebted to many people. Published texts in mechanics of materials, numerical techniques have been contributed to the author's thinking. Members of mechanical engineering department at Tehran University of Science and Technology, Nile Valley University, Red Sea University, Sudan University of Science and Technology and Blue Nile University have served to sharpen and refine the treatment of my topics. The author is extremely grateful to them for constructive criticisms and suggestions.

Special appreciation is due to the British Council's library for its response in ordering the requested reviews and papers.

Also, thanks are extended to the Faculty of Engineering and Technology, Atbara for enabling me to utilize its facilities in accessing the internet and printing out some papers, reviews and conference minutes concerning the present study.

Special gratitude is due to Professor **Mohammed Ibrahim Shukri** for the valuable gift "How to write a research", which assisted a lot in writing sequentially the present study. Thanks, are also due to Associate Professor **Izz Eldin Ahmed Abdellah** for helping with the internet.

Thanks, are also due to Faculty of Engineering and Technology, Nile Valley University administration for funding this research in spite of its financial hardships.

Abstract

Finite element (FE) method is presented for the analysis of thin rectangular laminated composite plates under the biaxial action of in – plane compressive loading. The analysis uses the classical laminated plate theory (CLPT) which does not account for shear deformations. In this theory it is assumed that the laminate is in a state of plane stress, the individual lamina is linearly elastic, and there is perfect bonding between layers. The classical laminated plate theory (CLPT), which is an extension of the classical plate theory (CPT) assumes that normal to the mid – surface before deformation remains straight and normal to the mid – surface after deformation. Therefore, this theory is only adequate for buckling analysis of thin laminates. A Fortran program has been compiled. The convergence and accuracy of the FE solutions for biaxial buckling of thin laminated rectangular plates are established by comparison with various theoretical and experimental solutions. New numerical results are generated for in – plane compressive biaxial buckling which serve to quantify the effects of lamination scheme, aspect ratio, material anisotropy, fiber orientation of layers, reversed lamination scheme and boundary conditions.

It was found that symmetric laminates are stiffer than the anti – symmetric one due to coupling between bending and stretching which decreases the buckling loads of symmetric laminates. The buckling load increases with increasing aspect ratio, and decreases with increase in modulus ratio. The buckling load will remain the same even when the lamination order is reversed. The buckling load increases with the mode number but at different rates depending on the type of end support. It is also observed that as the mode number increases, the plate needs additional support.

ملخص البحث

في هذا البحث تـمَّ استخدام أسلوب العنصر المحـدَّد (FE) لتحليل الألواح الشرائحية الرقيقة مستطيلة المقطع المسلَّط عليها حمل إنضغاط في محورين. يستخدم التحليل نظرية الألواح الشرائحية الكلاسيكية (CLPT) التي تتجاهل تأثيرات تشوه القص. في هذه النظرية يتم إفتراض أنَّ اللوح يكون في حالة إجهاد مستوٍ، وتكون الطبقة المفردة مرنة خطياً، ويكون هنالك رابط جيدّ بين الطبقات. نظرية الألواح الشرائحية الكلاسيكية التي هي إمتداد لنظرية الألواح الكلاسيكية (CPT) تفترض أن الخط المستقيم الوهمي المتعامد مع منتصف سطح اللوح قبل التشوه يظل مستقيماً ومتعامداً مع منتصف السطح بعد التشوه، بالتالي فإن هذه النظرية تتجاهل تشوه القص، عليه فهي تكون صالحة فقط لتحليل الألواح الرقيقة. لهذا الغرض تـمَّ تأليف برنامج فورتران (Fortran) وتـمَّ تأسيس تقارب ودقة برنامج أسلوب العنصر المحدد (FE) بمقارنته بالعديد من الحلول النظرية والمختبرية. تـمَّ الحصول على نتائج عددية جديدة للإنبعاج ثنائي المحور وذلك للتحقق من تأثيرات إتجاه الألياف، نسبة النطاق (a/b)، تباين الخواص للمادة (E_1/E_2)، عكس إتجاه الألياف والشروط الطرفية للوح.

وُجد في هذه الدراسة أنَّ الألواح المتماثلة تكون أكثر صلابة من الألواح الغير متماثلة وذلك نتيجة لتأثير الإزدواج بين الإنحناء والإستطالة الذي يخفِّض أحمال الإنبعاج للألواح المتماثلة. يزيد حمل الإنبعاج بزيادة نسبة النطاق (a/b) ويقل بزيادة نسبة المعاير (E_1/E_2). يظل حمل الإنبعاج ثابتاً حتى في حالة عكس إتجاه الألياف. يزيد الإنبعاج بزيادة عدد الأنماط بمعدلات مختلفة إعتماداً على نوع الإسناد الطرفي. يُلاحظ أيضاً أنه كلما زاد عدد الأنماط فإن اللوح سيحتاج لإسنادات إضافية.

Contents

List of Tables

List of Figures

Notations

a, b	Plate length and breadth
h	Plate thickness
$D_{ij}(i, j = 1, 2, 6)$	Plate flexural stiffnesses
E_1, E_2, G_{12}	Longitudinal, transverse, and in – plane shear moduli of a lamina
G_{13}, G_{23}	Transverse shear moduli in the $x - z$ and $y - z$ planes respectively
u, v	In – plane displacements
w	Out of plane displacements
ϕ, ψ	Rotations of the original normal to the plate mid - plane
ν_{12}	Poisson's ratio
Z_{k-1}, Z_k	Distance of upper and lower surfaces of the lamina from the plate mid – plane
$C_{ij}(i, j = 1, 2, 6)$	Transformed material properties
ϵ_j	Strain vector
σ_j	Stress vector
K^e	Element stiffness matrix
a_{ij}	Matrix of the coefficients of the shape functions
N_j	The shape function vector
r, s	The local co – ordinates
x, y	The global co – ordinates
K^D	Differential stiffness matrix

Preface

The objective of this thesis is to present a complete and up to date treatment of uniform cross section rectangular laminated plates on buckling. Finite element (FE) method is used for solving governing equations of thin laminated composite plates and their solution using classical laminated plate theory (CLPT). Plates are common structural elements of most engineering structures, including aerospace, automotive, and civil engineering structures, and their study from theoretical and experimental analyses points of view are fundamental to the understanding of the behavior of such structures.

The motivation that led to the writing of the present study has come from many years of studying classical laminated plate theory (CLPT) and its analysis by the finite element (FE) method, and also from the fact that there does not exist a publication that contains a detailed coverage of classical laminated plate theory and finite element method in one volume. The present study fulfills the need for a complete treatment of classical laminated theory of plates and its solution by a numerical solution.

The material presented is intended to serve as a basis for a critical study of the fundamentals of elasticity and several branches of solid mechanics including advanced mechanics of materials, theories of plates, composite materials and numerical methods. Chapter one includes certain properties of laminated composite plates, and at the end of this chapter the most important objectives of the present thesis are cited, this subject may be used either as a required reading or as a reference subject. Developments in the theories of laminated plates, several numerical methods and the past work of buckling analysis are presented in chapter two. Mathematical formulations and numerical modeling of rectangular laminated plates under biaxial buckling loads are introduced in chapter three. The present finite element (FE) results are validated with similar results generated by FE and/ or other numerical and

approximate analytical solutions in chapter four. Additional verification with ANSYS package and experimental results has been done in this chapter. In chapter five, the effects of lamination scheme, aspect ratio, material anisotropy, fiber orientations of layers, reversed lamination scheme and boundary conditions are investigated. In chapter six, the most important results have been summarized.

The present study is suitable as a textbook for an advanced course on theories of plates and finite element techniques in mechanical and civil engineering curricula. It can be used also as a reference by engineers and scientists working in industry and academic institutions.

CHAPTER (1)

Introduction

1.1 General Introduction

Composites were first considered as structural materials a little more than three quarters of a century ago. From that time to now, they have received increasing attention in all aspects of material science, manufacturing technology, and theoretical analysis.

The term composite could mean almost anything if taken at face value, since all materials are composites of dissimilar subunits if examined at close enough details. But in modern materials engineering, the term usually refers to a matrix material that is reinforced with fibers. For instance, the term "FRP" which refers to Fiber Reinforced Plastic usually indicates a thermosetting polyester matrix containing glass fibers, and this particular composite has the lion's share of today commercial market.

Many composites used today are at the leading edge of materials technology, with performance and costs appropriate to ultra-demanding applications such as space crafts. But heterogeneous materials combining the best aspects of dissimilar constituents have been used by nature for millions of years. Ancient societies, imitating nature, used this approach as well: The book of Exodus speaks of using straw to reinforce mud in brick making, without which the bricks would have almost no strength. Here in Sudan, people from ancient times dated back to Meroe civilization, and up to now used *zibala* (i.e. animals' dung) mixed with mud as a strong building material.

As seen in table (1.1) below, which is cited by David Roylance [1], Stephen et al. [2] and Turvey et al. [3], the fibers used in modern composites have strengths and stiffnesses far above those of traditional structural materials. The high strengths of the glass fibers are due to processing that

avoids the internal or external textures flaws which normally weaken glass, and the strength and stiffness of polymeric aramid fiber is a consequence of the nearly perfect alignment of the molecular chains with the fiber axis.

Table (1.1) Properties of composite reinforcing fibers

Material	E (GN/m²)	σ_b (GN/m²)	ε_b (%)	ρ (Mg/m³)	E/ρ (MN.m/kg)	σ_b/ρ (MN.m/kg)
E-glass	72.4	2.4	2.6	2.54	28.5	0.95
S-glass	85.5	4.5	2.0	2.49	34.3	1.8
Aramid	124	3.6	2.3	1.45	86	2.5
Boron	400	3.5	1.0	2.45	163	1.43
H S graphite	253	4.5	1.1	1.80	140	2.5
H M graphite	520	2.4	0.6	1.85	281	1.3

Where E is Young's modulus, σ_b is the breaking stress, ε_b is the breaking strain, and ρ is the mass density.

These materials are not generally usable as fibers alone, and typically they are impregnated by a matrix material that acts to transfer loads to the fibers, and also to protect the fibers from abrasion and environmental attack. The matrix dilutes the properties to some degree, but even so very high specific (weight – adjusted) properties are available from these materials. Polymers are much more commonly used, with unsaturated styrene – hardened polyesters having the majority of low to medium performance applications and Epoxy or more sophisticated thermosets having the higher end of the market. Thermoplastic matrix composites are increasingly attractive materials, with processing difficulties being perhaps their principal limitation.

Recently, composite materials are increasingly used in many mechanical, civil, and aerospace engineering applications due to two desirable features: the first one is their high specific stiffness (i.e. stiffness per unit density) and high specific strength (i.e. strength per unit density), and the second is their properties that can be tailored through variation of the fiber orientation and stacking sequence which gives the designers a wide spectrum of flexibility. The incorporation of high strength, high modulus and low-density filaments in a low strength and a low modulus matrix material is known to result in a structural composite material with a high strength to weight ratio. Thus, the potential of a two-material composite for use in aerospace, under-water, and automotive structures has stimulated considerable research activities in the theoretical prediction of the behavior of these materials. One commonly used composite structure consists of many layers bonded one on top of another to form a high-strength laminated composite plate. Each lamina is fiber reinforced along a single direction, with adjacent layers usually having different filament orientations. For these reasons, composites are continuing to replace other materials used in structures such as conventional materials. In fact, composites are the potential structural materials of the future as their cost continues to decrease due to the continuous improvements in production techniques and the expanding rate of sales.

1.2 Structure of Composites

There are many situations in engineering where no single material will be suitable to meet a particular design requirement. However, two materials in combination may possess the desired properties and provide a feasible solution to the materials selection problem. A composite can be defined as a material that is composed of two or more distinct phases, usually a reinforced material supported in a compatible matrix, assembled in prescribed amounts to achieve specific physical and chemical properties.

In order to classify and characterize composite materials, distinction between the following two types is commonly accepted; see Vernon [4], Jan Stegmann and Erik Lund [5], and David Roylance [1].

1. Fibrous composite materials: Which are composed of high strength fibers embedded in a matrix. The functions of the matrix are to bond the fibers together to protect them from damage, and to transmit the load from one fiber to another. {See Fig. (1.1)}.

2. Particulate composite materials: These are composed of particles encased within a tough matrix, e.g. powders or particles in a matrix like ceramics.
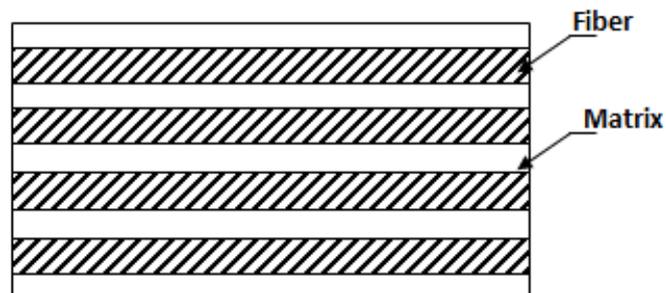
Fig. (1.1) Structure of a fibrous composite

In this study the focus will be on fiber reinforced composite materials, as they are the basic building element of a rectangular laminated plate structure. Typically, such a material consists of stacks of bonded-together layers (i.e. laminas or plies) made from fiber reinforced material. The layers will often be oriented in different directions to provide specific and directed strengths and stiffnesses of the laminate. Thus, the strengths and stiffnesses of the laminated fiber reinforced composite material can be tailored to the specific design requirements of the structural element being built.

1.2.1 Mechanical Properties of a Fiber Reinforced Lamina

Composite materials have many mechanical characteristics, which are different from those of conventional engineering materials such as metals. More precisely, composite materials are often both inhomogeneous and non-isotropic. Therefore, and due to the inherent heterogeneous nature of composite materials, they can be studied from a micromechanical or a macro mechanical point of view. In micromechanics, the behavior of the inhomogeneous lamina is defined in terms of the constituent materials; whereas in macro mechanics the material is presumed homogeneous and the effects of the constituent materials are detected only as averaged apparent macroscopic properties of the composite material. This approach is generally accepted when modeling gross response of composite structures. The micromechanics approach is more convenient for the analysis of the composite material because it studies the volumetric percentages of the constituent materials for the desired lamina stiffnesses and strengths, i.e. the aim of micromechanics is to determine the moduli of elasticity and strength of a lamina in terms of the moduli of elasticity, and volumetric percentage of the fibers and the matrix. To explain further, both the fibers and the matrix are assumed homogeneous, isotropic and linearly elastic.

1.2.1.1 Stiffness and Strength of a Lamina

The fibers may be oriented randomly within the material, but it is also possible to arrange for them to be oriented preferentially in the direction expected to have the highest stresses. Such a material is said to be anisotropic (i.e. different properties in different directions), and control of the anisotropy is an important means of optimizing the material for specific applications. At a microscopic level, the properties of these composites are determined by the orientation and distribution of the fibers, as well as by the properties of the fiber and matrix materials.

Consider a typical region of material of unit dimensions, containing a volume fraction, V_f of fibers all oriented in a single direction. The matrix volume fraction is then, $V_m = 1 - V_f$. This region can be idealized by gathering all the fibers together, leaving the matrix to occupy the remaining volume. If a stress σ_l is applied along the fiber direction, the fiber and matrix phases act in parallel to support the load. In these parallel connections the strains in each phase must be the same, so the strain ε_l in the fiber direction can be written as:

$$\varepsilon_l = \varepsilon_f = \varepsilon_m \tag{1.1}$$

(Where: the subscripts l, f and m denote the lamina, fibers and matrix respectively).

The forces in each phase must add to balance the total load on the material. Since the forces in each phase are the phase stresses times the area (here numerically equal to the volume fraction), we have

$$\sigma_l = \sigma_f V_f + \sigma_m V_m = E_f \varepsilon_l V_f + E_m \varepsilon_l V_m \tag{1.2}$$

The stiffness in the fiber direction is found by dividing the stress by the strain:

$$E_l = \frac{\sigma_l}{\varepsilon_l} = E_f V_f + E_m V_m \tag{1.3}$$

(Where: E is the longitudinal Young's modulus)

This relation is known as a rule of mixtures prediction of the overall modulus in terms of the moduli of the constituent phases and their volume fractions.

Rule of mixtures estimates for strength proceed along lines similar to those for stiffness. For instance, consider a unidirectional reinforced composite that is strained up to the value at which the fiber begins to fracture. If the matrix is more ductile than the fibers, then the ultimate tensile strength of the lamina in equation (1.2) will be transformed to:

$$\sigma_l^u = \sigma_f^u V_f + \sigma_m^f \left(1 - V_f\right) \tag{1.4}$$

Where the superscript u denotes an ultimate value, and σ_m^f is the matrix stress when the fibers fracture as shown in Fig. (1.2).
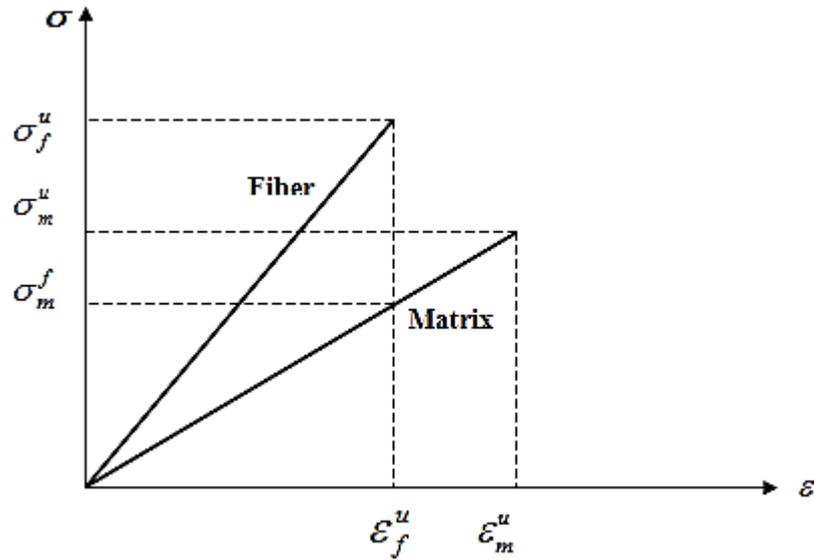
Fig. (1.2) Stress-strain relationships for fiber and matrix

It is clear that if the fiber volume fraction is very small, the behavior of the lamina is controlled by the matrix.

This can be expressed mathematically as follows:

$$\sigma_l^u = \sigma_m^u \left(1 - V_f\right) \tag{1.5}$$

If the lamina is assumed to be useful in practical applications, then there is a minimum fiber volume fraction that must be added to the matrix. This value is obtained by equating equations (1.4) and (1.5) i.e.

$$V_{min} = \frac{\sigma_m^u - \sigma_m^f}{\sigma_f^u + \sigma_m^u - \sigma_m^f} \tag{1.6}$$

The variation of the strength of the lamina with the fiber volume fraction is illustrated in Fig. (1.3). It is obvious that when $0 < V_f < V_{min}$ the strength of the lamina is dominated by the matrix deformation which is less than the matrix strength. But when the fiber volume fraction exceeds a critical

value (i.e. $V_f > V_{Critical}$), Then the lamina gains some strength due to the fiber reinforcement.
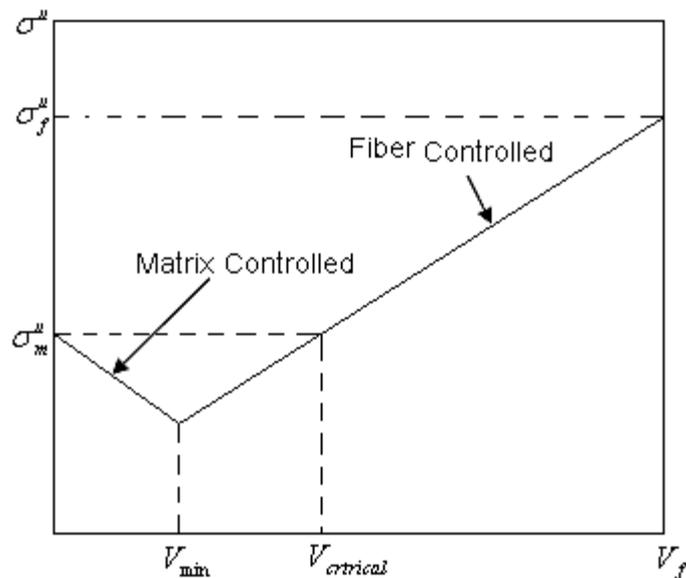
Fig. (1.3) Variation of unidirectional lamina strength with the fiber volume fraction

The micromechanical approach is not responsible for the many defects which may arise in fibers, matrix, or lamina due to their manufacturing. These defects, if they exist include misalignment of fibers, cracks in matrix, non-uniform distribution of the fibers in the matrix, voids in fibers and matrix, delaminated regions, and initial stresses in the lamina as a result of its manufacture and further treatment. The above-mentioned defects tend to propagate as the lamina is loaded causing an accelerated rate of failure. The experimental and theoretical results in this case tend to differ. Hence, due to the limitations necessary in the idealization of the lamina components, the properties estimated on the basis of micromechanics should be proved experimentally. The proof includes a very simple physical test in which the lamina is considered homogeneous and orthotropic. In this test, the ultimate strength and modulus of elasticity in a direction parallel to the fiber direction can be determined experimentally by loading the lamina longitudinally. When

the test results are plotted, as in Fig. (1.4) below, the required properties may be evaluated as follows: -

$$E_1 = \sigma_1 / \varepsilon_1 \quad ; \quad \sigma^u = P^u / A \quad ; \quad v_{12} = -\varepsilon_2 / \varepsilon_1$$
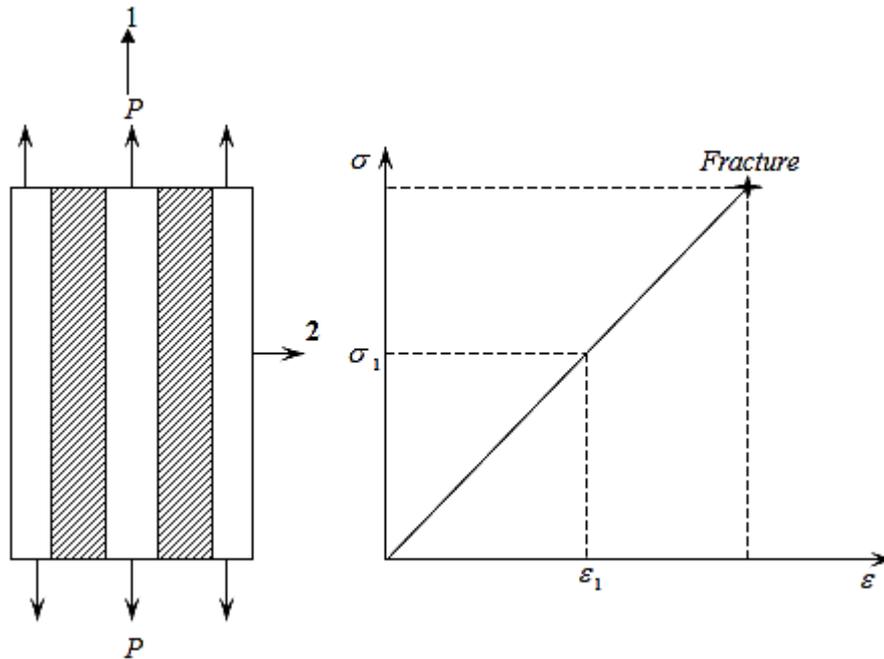
Fig. (1.4) Unidirectional lamina loaded in the fiber-direction

Similarly, the properties of the lamina in a direction perpendicular to the fiber direction can be evaluated in the same procedure.

1.2.1.2   Analytical Modeling of Composite Laminates

The properties of a composite laminate depend on the geometrical arrangement and the properties of its constituents. The exact analysis of such structure – property relationship is rather complex because of many variables involved. Therefore, a few simplifying assumptions regarding the structural details and the state of stress within the composite have been introduced.

It has been observed, that the concept of representative volume element and the selection of appropriate boundary conditions are very important in the discussion of micromechanics. The composite stress and strain are defined as the volume averages of the stress and strain fields,

respectively, within the representative volume element. By finding relations between the composite stresses and the composite strains in terms of the constituent properties, expressions for the composite moduli could be derived. In addition, it has been shown that, the results of advanced methods can be put in a form similar to the rule of mixtures equations.

Prediction of composite strengths is rather difficult because there are many unknown variables and also because failure critically depends on defects. However, the effects of constituents including fiber – matrix interface on composite strengths can be qualitatively explained. Certainly, failure modes can change depending on the material combinations. Thus, an analytical model developed for one material combination cannot be expected to work for a different one. Ideally a truly analytical model will be applicable to material combination. However, such an analytical model is not available at present. Therefore, it has been chosen to provide models each of which is applicable only to a known failure mode. Yet, they can explain many of the effects of the constituents. (Refer to Ref. [2]).

1.3 The Objectives of The Present Study

The present work involves a comprehensive study of the following objectives, which have been achieved over a period of five years:

1. A survey of various plate theories and techniques used to predict the response of laminated plates under buckling loads.

2. The development of a theoretical model capable of predicting buckling loads in a thin laminated plate.

3. The development and application of the finite element technique for the analysis of rectangular laminated plates subjected to a buckling load.

4. Investigation of the accuracy of the theoretical model through a wide range of theoretical and experimental comparisons.

5. Further investigations on the influence of coupling between bending and extension and/or twisting on the response of laminated plates could be carried out.

6. Generation of new results based on classical laminated plate theory (CLPT).

Chapter (2)

Literature Review

2.1 Developments in The Theories of Laminated Plates

From the point of view of solid mechanics, the deformation of a plate subjected to transverse and / or in plane loading consists of two components: flexural deformation due to rotation of cross – sections, and shear deformation due to sliding of section or layers. The resulting deformation depends on two parameters: the thickness to length ratio and the ratio of elastic to shear moduli. When the thickness to length ratio is small, the plate is considered thin, and it deforms mainly by flexure or bending; whereas when the thickness to length and the modular ratios are both large, the plate deforms mainly through shear. Due to the high ratio of in – plane modulus to transverse shear modulus, the shear deformation effects are more pronounced in the composite laminates subjected to transverse and / or in – plane loads than in the isotropic plates under similar loading conditions.

The three – dimensional theories of laminates, in which each layer is treated as homogeneous anisotropic medium, (see Reddy [6]) are intractable. Usually, the anisotropy in laminated composite structures causes complicated responses under different loading conditions by creating complex couplings between extensions and bending, and shears deformation modes. Expect for certain cases, it is inconvenient to fully solve a problem in three dimensions due to the complexity, size of computation, and the production of unnecessary data specially for composite structures.

Many theories which account for the transverse shear and normal stresses are available in the literature (see, for example Mindlin [7]). These are too numerous to review here. Only some classical papers and those which constitute a background for the present thesis will be considered. These theories are classified according to Phan and Reddy [8] into two major classes

on the basis of the assumed fields as: (1) stress based theories, and (2) displacement based theories. The stress – based theories are derived from stress fields which are assumed to vary linearly over the thickness of the plate:

$$\sigma_i = \frac{M_i}{\left(h^2/6\right)} \times \frac{z}{\left(h/2\right)} \quad (i = 1,2,6) \tag{2.1}$$

(Where M_i is the stress couples, h is the plate thickness, and z is the distance of the lamina from the plate mid – plane).

The displacement – based theories are derived from an assumed displacement field as:

$$u = u_\circ + zu_1 + z^2 u_2 + z^3 u_3 + \dots$$

$$v = v_\circ + zv_1 + z^2 v_2 + z^3 v_3 + \dots \tag{2.2}$$

$$w = w_\circ + zw_1 + z^2 w_2 + z^3 w_3 + \dots$$

Where: $u_\circ$, $v_\circ$ and $w_\circ$ are the displacements of the middle plane of the plate. The governing equations are derived using principle of minimum total potential energy. The theory used in the present work comes under the class of displacement – based theories. Extensions of these theories which include the linear terms in z in u and v and only the constant term in w, to account for higher – order variations and to laminated plates, can be found in the work of Yang, Norris and Stavsky [9] , Whitney and Pagano [10] and Phan and Reddy [8].

Based on different assumptions for displacement fields, different theories for plate analysis have been devised. These theories can be divided into three major categories, the individual layer theories (IL), the equivalent single layer (ESL) theories, and the three-dimensional elasticity solution procedures. These categories are further divided into sub – theories by the introduction of different assumptions. For example, the second category

includes the classical laminated plate theory (CLPT), the first order and higher order shear deformation theories (FSDT and HSDT) as stated in Refs. $\{[11] - [14]\}$.

In the individual layer laminate theories, each layer is considered as a separate plate. Since the displacement fields and equilibrium equations are written for each layer, adjacent layers must be matched at each interface by selecting appropriate interfacial conditions for displacements and stresses. In the ESL laminate theories, the stress or the displacement field is expressed as a linear combination of unknown functions and the coordinate along the thickness. If the in – plane displacements are expanded in terms of the thickness co – ordinate up to the nth power, the theory is named n^{th} order shear deformation theory. The simplest ESL laminate theory is the classical laminated plate theory (CLPT). This theory is applicable to homogeneous thin plates (i.e. the length to thickness ratio a / h > 20). The classical laminated plate theory (CLPT), which is an extension of the classical plate theory (CPT) applied to laminated plates was the first theory formulated for the analysis of laminated plates by Reissner and Stavsky [15] in 1961 , in which the Kirchhoff and Love assumption that normal to the mid – surface before deformation remain straight and normal to the mid – surface after deformation is used (see Fig.(2.1)) , but it is not adequate for the flexural analysis of moderately thick laminates. However, it gives reasonably accurate results for many engineering problems i.e. thin composite plates, as stated by Srinivas and Rao [16], Reissner and Stavsky [15]. This theory ignores the transverse shear stress components and models a laminate as an equivalent single layer. The classical laminated plate theory (CLPT) under – predicts deflections as proved by Turvey and Osman [17], [18], [19] and Reddy [6] due to the neglect of transverse shear strain. The errors in deflection are even higher for plates made of advanced filamentary composite materials like graphite – epoxy and boron – epoxy whose elastic modulus to shear modulus ratios are very large (i.e. of the order of 25 to 40, instead of 2.6 for typical isotropic

materials). However, these composites are susceptible to thickness effects because their effective transverse shear moduli are significantly smaller than the effective elastic modulus along the fiber direction. This effect has been confirmed by Pagano [20] who obtained analytical solutions of laminated plates in bending based on the three – dimensional theory of elasticity. He proved that classical laminated plate theory (CLPT) becomes of less accuracy as the side to thickness ratio decreases. In particular, the deflection of a plate predicted by CLPT is considerably smaller than the analytical value for side to thickness ratio less than 10. These high ratios of elastic modulus to shear modulus render classical laminate theory as inadequate for the analysis of composite plates. In the first order shear deformation theory (FSDT), the transverse planes, which are originally normal and straight to the mid – plane of the plate, are assumed to remain straight but not necessarily normal after deformation, and consequently shear correction factors are employed in this theory to adjust the transverse shear stress, which is constant through thickness (see Fig. (2.1)). Recently Reddy [6] and Phan and Reddy [8] presented refined plate theories that used the idea of expanding displacements in the powers of thickness coordinate. The main novelty of these works is to expand the in – plane displacements as cubic functions of the thickness coordinate, treat the transverse deflection as a function of the x and y coordinates, and eliminate the functions u_2, u_3, v_2 and v_3 from equation (2.2) by requiring that the transverse shear stress be zero on the bounding planes of the plate. Numerous studies involving the application of the first – order theory to bending, vibration and buckling analyses can be found in the works of Reddy [20], and Reddy and Chao [21].

In order to include the curvature of the normal after deformation, a number of theories known as higher – order shear deformation theories (HSDT) have been devised in which the displacements are assumed quadratic or cubic through the thickness of the plate. In this aspect, a variationally

Undeformed

x, u

y

z, w

Assumed deformation of normals (CLPT) (Shear stress neglected)

$\dfrac{dw}{dx}$

$\dfrac{dw}{dx}$

Assumed deformation of normals (FSDT) (shear stress assumed uniform)

ϕ

$\dfrac{dw}{dx}$

Assumed deformation of normals (HSDT) (parabolic shear stress distribution)

ϕ

$\dfrac{dw}{dx}$
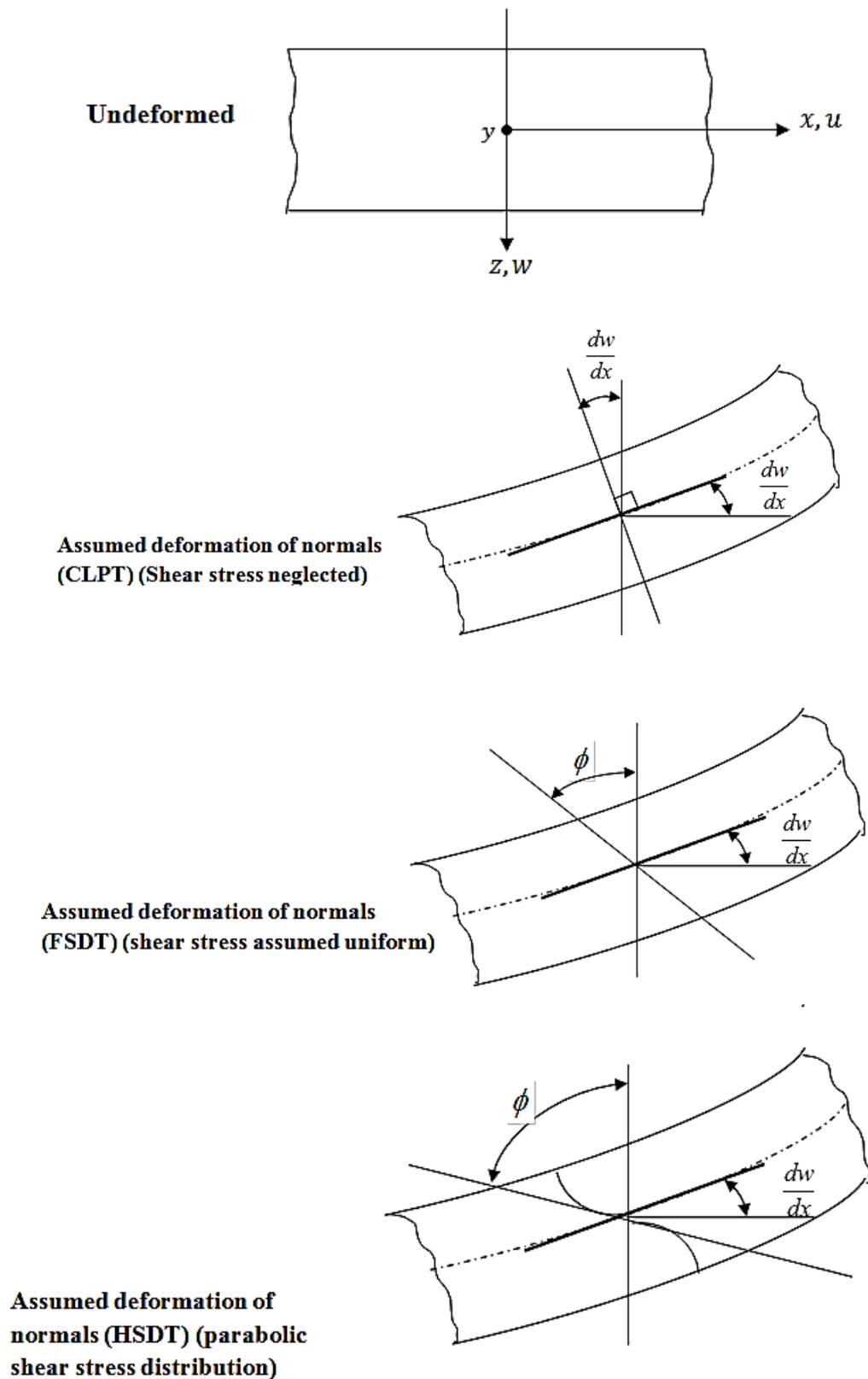
Fig. (2.1) Assumed deformation of the transverse normal in various displacement base plate theories

consistent higher – order theory which not only accounts for the shear deformation but also satisfies the zero transverse shear stress conditions on the top and bottom faces of the plate and does not require correction factors was suggested by Reddy [6]. Reddy's modifications consist of a more systematic derivation of displacement field and variationally consistent derivation of the equilibrium equations. The refined laminate plate theory predicts a parabolic distribution of the transverse shear stresses through the thickness, and requires no shear correction coefficients.

In the non – linear analysis of plates considering higher – order shear deformation theory (HSDT), shear deformation has received considerably less attention compared with linear analysis. This is due to the geometric non – linearity which arises from finite deformations of an elastic body and which causes more complications in the analysis of composite plates. Therefore, fiber – reinforced material properties and lamination geometry have to be taken into account. In the case of anti – symmetric and unsymmetrical laminates, the existence of coupling between stretching and bending complicates the problem further. Non – linear solutions of laminated plates using higher – order theories have been obtained through several techniques, i. e. perturbation method as in Ref. [22], finite element method as in Ref. [23], the increment of lateral displacement method as in Ref. [24], and the small parameter method as in Ref. [25].

In the present work, the analysis uses the classical laminated plate theory (CLPT) which does not account for transverse shear deformations. In this theory it is assumed that the laminate is in a state of plane stress, the individual lamina is linearly elastic, and there is perfect bonding between layers. The classical laminated plate theory assumes that normal to the mid – surface before deformation remains straight and normal to the mid – surface after deformation. Therefore, this theory is adequate for buckling analysis of thin laminates. A Fortran program has been compiled, the convergence and

accuracy of the FE solutions for biaxial buckling of thin laminated rectangular plates are established by comparison with various theoretical and experimental solutions and new numerical results are generated.

2.2 Numerical Techniques

Several numerical methods could be used in this study, but the main ones are finite difference method (FDM), dynamic relaxation coupled with finite difference method (DR), and finite element method (FEM).

In the finite difference method, the solution domain is divided into a grid of discrete points or nodes. The partial differential equation is then written for each node and its derivatives are replaced by finite divided differences. Although such point – wise approximation is conceptually easy to understand, it becomes difficult to apply for system with irregular geometry, unusual boundary conditions, and heterogeneous composition.

The DR method was first proposed in 1960th; see Rushton [26], Cassel and Hobbs [27], and Day [28]. In this method, the equations of equilibrium are converted to dynamic equations by adding damping and inertia terms. These are then expressed in finite difference form and the solution is obtained through iterations. The optimum damping coefficient and the time increment used to stabilize the solution depend on the stiffness matrix of the structure, the applied load, the boundary conditions and the size of mesh used.

In the present work, a numerical method known as finite element method (FEM) is used. It is a numerical procedure for obtaining solutions to many of the problems encountered in engineering analysis. It has two primary subdivisions. The first utilizes discrete elements to obtain the joint displacements and member forces of a structural framework. The second uses the continuum elements to obtain approximate solutions to heat transfer, fluid mechanics, and solid mechanics problem. The formulation using the discrete element is referred to as matrix analysis of structures and yields results identical with the classical analysis of structural frameworks. The second

approach is the true finite element method. It yields approximate values of the desired parameters at specific points called nodes. A general finite element computers program, however, is capable of solving both types of problems and the name" finite element method" is often used to denote both the discrete element and the continuum element formulations.

The finite element method combines several mathematical concepts to produce a system of linear and non – linear equations. The number of equations is usually very large, anywhere from 20 to 20,000 or more and requires the computational power of the digital computer.

It is impossible to document the exact origin of the finite element method because the basic concepts have evolved over a period of 150 or more years. The method as we know it today is an outgrowth of several papers published in the 1950th that extended the matrix analysis of structures to continuum bodies. The space exploration of the 1960th provided money for basic research, which placed the method of a firm mathematical foundation and stimulated the development of multi – purpose computer programs that implemented the method. The design of airplanes, unmanned drones, missiles, space capsules, and the like, provided application areas.

The finite element method (FEM) is a powerful numerical method, which is used as a computational technique for the solution of differential equations that arise in various fields of engineering and applied sciences. The finite element method is based on the concept that one can replace any continuum by an assemblage of simply shaped elements, called finite elements with well-defined force, displacement, and material relationships. While one may not be able to derive a closed – form solution for the continuum, one can derive approximate solutions for the element assemblage that replaces it. The approximate solutions or approximation functions are often constructed using ideas from interpolation theory, and hence they are

also called interpolation functions. For more details refer to Refs. {[29] – [31]}.

In a comparison between the finite element method (FEM) and dynamic relaxation method (DR), Aalami [32] found that the computer time required for the finite element method is eight times greater than for DR analysis, whereas the storage capacity for FEM is ten times or more than that for DR analysis. This fact is supported by Putcher and Reddy [23], and Turvey and Osman {[17] – [19]} who noted that some of the finite element formulations require large storage capacity and computer time. Hence due to the large computations involved in the present study, the finite element method (FEM) is considered more efficient than the DR method. In another comparison, Aalami [32] found that the difference in accuracy between one version of FEM and DR may reach a value of more than 15 % in favor of FEM. Therefore, the FEM can be considered of acceptable accuracy. The apparent limitation of the DR method is that it can only be applied to limited geometries, whereas the FEM can be applied to different intricate geometries and shapes.

2.3 The Past Work of Buckling Analysis

Composite materials are widely used in a broad spectrum of modern engineering application fields ranging from traditional fields such as automobiles, robotics, day to day appliances, building industry etc. This is due to their excellent high strength to weight ratio, modulus to weight ratio, and the controllability of the structural properties with the variation of fiber orientation, stacking scheme and the number of laminates. Among the various aspects of the structural performance of structures made of composite materials is the mechanical behavior of rectangular laminated plates which has drawn much attention. In particular, consideration of the buckling phenomena in such plates is essential for the efficient and reliable design and for the safe use of the structural element. Due to the anisotropic and coupled

material behavior, the analysis of composite laminated plates is generally more complicated than the analysis of homogeneous isotropic ones.

The members and structures composed of laminated composite material are usually very thin, and hence more prone to buckling. Buckling phenomenon is critically dangerous to structural components because the buckling of composite plates usually occurs at a lower applied stress and generates large deformations. This led to a focus on the study of buckling behavior in composite materials. General introductions to the buckling of elastic structures and of laminated plates can be found in e.g. Refs. {[33] – [46]}. However, these available curves and data are restricted to idealized loading, namely, uniaxial or biaxial uniform compression.

Due to the importance of buckling considerations, there is an overwhelming number of investigations available in which corresponding stability problems are considered by a wide variety of analysis methods which may be of a closed – form analytical nature or may be sorted into the class of semi – analytical or purely numerical analysis method.

Closed – form exact solutions for the buckling problem of rectangular composite plates are available only for limited combinations of boundary conditions and laminated schemes. These include cross – ply symmetric and angle – ply anti – symmetric rectangular laminates with at least two opposite edges simply supported, and similar plates with two opposite edges clamped but free to deflect (i.e. guided clamp) or with one edge simply supported and the opposite edge with a guided clamp. Most of the exact solutions discussed in the monographs of Whitney [47] who developed an exact solution for critical buckling of solid rectangular orthotropic plates with all edges simply supported, and of Reddy {[48] – [51]} and Leissa and Kang [52], and that of Refs. [39] and [53]. Bao et al. [54] developed an exact solution for two edges simply supported and two edges clamped, and Robinson [55] who developed

an exact solution for the critical buckling stress of an orthotropic sandwich plate with all edges simply supported.

For all other configurations, for which only approximated results are available, several semi – analytical and numerical techniques have been developed. The Rayleigh – Ritz method [53] and [56], the finite strip method (FSM) [36] and [57], the element free Galerkin method (EFG) [58], the differential quadrature technique [59], the moving least square differential quadrature method [60] and the most extensively used finite element method (FEM) [61] are the most common ones.

The Kantorovich method (KM) {[62] – [64]}, which is a different and in most cases advantageous semi – analytical method, combines a variation approach of closed – form solutions and an iterative procedure. The method assumes a solution in the form of a sum of products of functions in one direction and functions in the other direction. Then, by assuming the function in one direction, the variation problem of the plate reduces to a set of ordinary differential equations. In the case of buckling analysis, the variation problem reduces to an ordinary differential eigenvalue and eigenfunction problem. The solution of the resulting problem is an approximate one, and its accuracy depends on the assumed functions in the first direction. The extended Kantorovich method (EKM), which was proposed by Kerr [65], is the starting point for an iterative procedure, where the solution obtained in one direction is used as the assumed functions in the second direction. After repeating this process several times, convergence is obtained. The single term extended Kantorovich method was employed for a buckling analysis of rectangular plates by several researches. Eienberger and Alexandrov [66] used the method for the buckling analysis of isotropic plates with variable thickness. Shufrin and Eienberger [67] and [68] extended the solution to thick plates with constant and variable thickness using the first and higher order shear deformation theories. Ungbhakorn and Singhatanadgid [69] extended the

solution to buckling of symmetrically cross – ply laminated rectangular plates. The multi – term formulation of the extended Kantorovich approach to the simplest samples of rectangular isotropic plates was presented by Yuan and Jin [70]. This study showed that the additional terms in the expansion can be used in order to improve the solution.

March and Smith [71] found an approximate solution for all edges clamped. Also, Chang et al. [72] developed approximate solution to the buckling of rectangular orthotropic sandwich plate with two edges simply supported and two edges clamped or all edges clamped using the March – Erickson method and an energy technique. Jiang et al. [73] developed solutions for local buckling of rectangular orthotropic hat – stiffened plates with edges parallel to the stiffeners were simply supported or clamped and edges parallel to the stiffeners were free, and Smith [74] presented solutions bounding the local buckling of hat stiffened plates by considering the section between stiffeners as simply supported or clamped plates.

Many authors have used finite element method to predict accurate in – plane stress distribution which is then used to solve the buckling problem. Zienkiewicz [75] and Cook [76] have clearly presented an approach for finding the buckling strength of plates by first solving the linear elastic problem for a reference load and then the eigenvalue problem for the smallest eigenvalue which then multiplied by the reference load gives the critical buckling load of the structure. An excellent review of the development of plate finite elements during the past 35 years was presented by Yang et al. [77].

Many buckling analyses of composite plates available in the literature are usually realized parallel with the vibration analyses, and are based on two – dimensional plate theories which may be classified as classical and shear deformable ones. Classical plate theories (CPT) do not take into account the shear deformation effects and over predict the critical buckling loads for

thicker composite plates, and even for thin ones with a higher anisotropy. Most of the shear deformable plate theories are usually based on a displacement field assumption with five unknown displacement components. As three of these components corresponded to the ones in CPT, the additional ones are multiplied by a certain function of thickness coordinate and added to the displacements field of CPT in order to take into account the shear deformation effects. Taking these functions as linear and cubic forms leads to the so – called uniform or Mindlin shear deformable plate theory (USDPT) [78], and parabolic shear deformable plate theories (PSDPT) [79] respectively. Different forms were also employed such as hyperbolic shear deformable plate theory (HSDPT) [80], and trigonometric or sine functions shear deformable plate theory (TSDPT) [81] by researchers. Since these types of shear deformation theories do not satisfy the continuity conditions among many layers of the composite structures, the zig – zag type of the plate theories introduced by Di Sciuva [82], and Cho and Parmeter [83] in order to consider interlaminar stress continuities. Recently, Karama et al. [84] proposed a new exponential function {i.e. exponential shear deformable plate theory (ESDPT)} in the displacement field of the composite laminated structures for the representation of the shear stress distribution along the thickness of the composite structures and compared their result for static and dynamic problem of the composite beams with the sine model.

Within the classical lamination theory, Jones [85] presented a closed – form solution for the buckling problem of cross – ply laminated plates with simply supported boundary conditions. In the case of multi – layered plates subjected to various boundary conditions which are different from simply supported boundary conditions at all of their four edges, the governing equations of the buckling of the composite plates do not admit an exact solution, except for some special arrangements of laminated plates. Thus, for the solution of these types of problems, different analytical and / or numerical methods are employed by various researchers. Baharlou and Leissa [56] used

the Ritz method with simple polynomials as displacement functions, within the classical theory, for the problem of buckling of cross and angle – ply laminated plates with arbitrary boundary conditions and different in – plane loads. Narita and Leissa [86] also applied the Ritz method with the displacement components assumed as the double series of trigonometric functions for the buckling problem of generally symmetric laminated composite rectangular plates with simply supported boundary conditions at all their edges. They investigated the critical buckling loads for five different types of loading conditions which are uniaxial compression (UA – C), biaxial compression (BA – C), biaxial compression – tension (BA – CT), and positive and negative shear loadings.

The higher – order shear deformation theories can yield more accurate inter – laminate stress distributions. The introduction of cubic variation of displacement also avoids the need for shear correction displacement. To achieve a reliable analysis and safe design, the proposals and developments of models using higher order shear deformation theories have been considered. Lo et al. [87] and [88] reviewed the pioneering work on the field and formulated a theory which accounts for the effects of transverse shear deformation, transverse strain and non – linear distribution of the in – plane displacements with respect to the thickness coordinate. Third – order theories have been proposed by Reddy {[89] – [92]}, Librescu [93], Schmidt [94], Murty [95], Levinson [96], Seide [97], Murthy [98], Bhimaraddi [99], Mallikarjuna and Kant [100], Kant and Pandya [101], and Phan and Reddy [8], among others. Pioneering work and overviews in the field covering closed – form solutions and finite element models can be found in Reddy [90], [102], [103], Mallikarjuna and Kant [100], Noor and Burton [104], Bert [105], Kant and Kommineni [106], and Reddy and Robbins [107] among others.

For the buckling analysis of the cross – ply laminated plates subjected to simply supported boundary conditions at their opposite two edges and different boundary conditions at the remaining ones Khdeir [108] and Reddy and Khdeir [51] used a parabolic shear deformation theory and applied the state – space technique. Hadian and Nayfeh [109], on the basis of the same theory and for the same type of problem, needed to modify the technique due to ill – conditioning problems encountered especially for thin and moderately thick plates. The buckling analyses of completely simply supported cross – ply laminated plates were presented by Fares and Zenkour [110], who added a non – homogeneity coefficient in the material stiffnesses within various plate theories, and by Matsunaga [111] who employed a global higher order plate theory. Gilat el al. [112] also investigated the same type of problem on the basic of a global – local plate theory where the displacement field is composed of global and local contributions, such that the requirement of the continuity conditions and delamination effects can be incorporated into formulation.

Many investigations have been reported for static and stability analysis of composite laminates using different traditional methods. Pagano [113] developed an exact three – dimensional (3 – D) elasticity solution for static analysis of rectangular bi – directional composites and sandwich plates. Noor [114] presented a solution for stability of multi – layered composite plates based on 3 – D elasticity theory by solving equations with finite difference method. Also, 3 – D elasticity solutions are presented by Gu and Chattopadhyay [115] for the buckling of simply supported orthotropic composite plates. When the problem is reduced from a three – dimensional one (3 – D) to a two-dimensional case to contemplate more efficiently the computational analysis of plate composite structures, the displacement based theories and the corresponding finite element models receive the most attention [116].

Bifurcation buckling of laminated structures has been investigated by many researchers without considering the flatness before buckling [117]. This point was first clarified for laminated composite plates for some boundary conditions and for some lamina configurations by Leissa [117]. Qatu and Leissa [118] applied this result to identify true buckling behavior of composite plates. Elastic bifurcation of plates has been extensively studied and well documented in standard texts e.g. [33] and [119], research monographs {[120] – [122]} and journal papers {[123] – [126]}.

It is important to recognize that, with the advent of composite media, certain new material imperfections can be found in composite structures in addition to the better – known imperfections that one finds in metallic structures. Thus, broken fibers, delaminated regions, cracks in the matrix material, as well as holes, foreign inclusions and small voids constitute material and structural imperfections that can exist in composite structures. Imperfections have always existed and their effect on the structural response of a system has been very significant in many cases. These imperfections can be classified into two broad categories: initial geometrical imperfections and material or constructional imperfections.

The first category includes geometrical imperfections in the structural configuration (such as a local out of roundness of a circular cylindrical shell, which makes the cylindrical shell non – circular; a small initial curvature in a flat plate or rod, which makes the structure non – flat, etc.), as well as imperfections in the loading mechanisms (such as load eccentricities; an axially loaded column is loaded at one end in such a manner that a bending moment exists at that end). The effect of these imperfections on the response of structural systems has been investigated by many researchers and the result of these efforts can be easily found in books [3], as well in published papers [127] – [144].

The second class of imperfections is equally important, but has not received as much attentions as the first class; especially as far as its effect on the buckling response characteristics is concerned. For metallic materials, one can find several studies which deal with the effect of material imperfections on the fatigue life of the structural component. Moreover, there exist a number of investigations that deal with the effect of cut – outs and holes on the stress and deformation response of thin plates. Another material imperfection is the rigid inclusion. The effect of rigid inclusions on the stress field of the medium in the neighborhood of the inclusion has received limited attention. The interested reader is referred to the bibliography of Professor Naruoka [127].

There exist two important classes of material and constructional – type imperfections, which are very important in the safe design, especially of aircraft and spacecraft. These classes consist of fatigue cracks or cracks in general and delamination in systems that employ laminates (i.e. fiber – reinforced composites). There is considerable work in the area of stress concentration at crack tips and crack propagation. Very few investigations are cited, herein, for the sake of brevity. These include primarily those dealing with plates and shells and non – isotropic construction. Some deal with cracks in metallic plates and shells {[145] – [148]}. Others deal with non – isotropic construction and investigate the effects of non – isotropy {[149] – [154]}. In all of these studies, there is no mention of the effect of the crack presence on the overall stability or instability of the system.

Finally, delamination is one of the most commonly found defects in laminated structural components. Most of the work found in the literature deals with flat configurations.

Composite structures often contain delamination. Causes of delamination are many and include tool drops, bird strikes, runway debris hits and manufacturing defects. Moreover, in some cases, especially in the vicinity

of holes or close to edges in general, delamination starts because of the development of interlaminar stresses. Several analyses have been reported on the subject of edge delamination and its importance in the design of laminated structures. A few of these works are cited {[155] – [161]}. These and their cited references form a good basis for the interested reader. The type of delamination that comprises the basic and primary treatise is the one that is found to be present away from the edges (internal). This delaminating could be present before the laminate is loaded or it could develop after loading because of foreign body (birds, micrometer, and debris) impact. This is an extremely important problem especially for laminated structures that are subject to destabilizing loads (loads that can induce instability in the structure and possibly cause growth of the delamination; both of these phenomena contribute to failure of the laminate). The presence of delamination in these situations may cause local buckling and / or trigger global buckling and therefore induce a reduction in the overall load – bearing capacity of the laminated structure. The problem, because of its importance, has received considerable attention.

In the present study, the composite media are assumed free of imperfections i.e. initial geometrical imperfections due to initial distortion of the structure, and material and / or constructional imperfections such as broken fibers, delaminated regions, cracks in the matrix material, foreign inclusions and small voids which are due to inconvenient selection of fibers / matrix materials and manufacturing defects. Therefore, the fibers and matrix are assumed perfectly bonded.

Chapter (3)

Mathematical Formulations and Numerical Modeling

3.1 Introduction

The following assumptions were made in developing the mathematical formulations of laminated plates:

1. All layers behave elastically;

2. Displacements are small compared with the plate thickness;

3. Perfect bonding exists between layers;

4. The laminate is equivalent to a single anisotropic layer;

5. The plate is flat and has a constant thickness;

6. The plate buckles in a vacuum and all kinds of damping are neglected.

Unlike homogeneous plates, where the coordinates are chosen solely based on the plate shape, coordinates for laminated plates should be chosen carefully. There are two main factors for the choice of the coordinate system. The first factor is the shape of the plate. Where rectangular plates will be best represented by the choice of rectangular (i.e. cartesian) coordinates. It will be relatively easy to represent the boundaries of such plates with coordinates. The second factor is the fiber orientation or orthotropy. If the fibers are set straight within each lamina, then rectangular orthotropy would result. It is possible to set the fibers in a radial and circular fashion, which would result in circular orthotropy. Indeed, the fibers can also be set in elliptical directions, which would result in elliptical orthotropy.

The choice of the coordinate system is of critical importance for laminated plates. This is because plates with rectangular orthotropy could be set on rectangular, triangular, circular or other boundaries. Composite materials with rectangular orthotropy are the most popular, mainly because of

their ease in design and manufacturing. The equations that follow are developed for materials with rectangular orthotropy.

Fig. (3.1) below shows the geometry of a plate with rectangular orthotropy drawn in the cartesian coordinates X, Y, and Z or 1, 2, and 3. The parameters used in such a plate are: (1) the length in the X-direction, (a); (2) the length in the Y – direction (i.e. breadth), (b); and (3) the length in the Z – direction (i.e. thickness), (h).
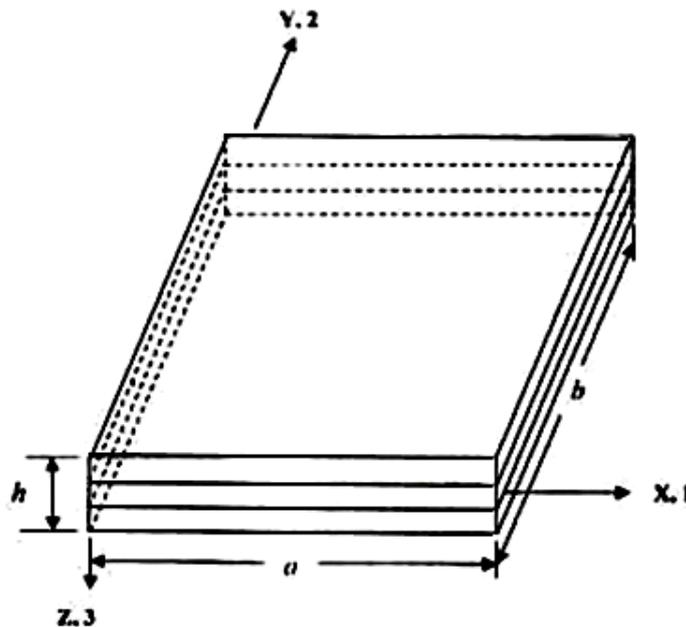
Fig. 3.1 The geometry of a laminated composite plate

3.2 Fundamental Equations of Elasticity

Classical laminated plate theory (CLPT) is selected to formulate the problem. Consider a thin plate of length a, breadth b, and thickness h as shown in Fig. (3.2(a)), subjected to in – plane loads R_x, R_y and R_{xy} as shown in Fig. (3.2(b)). The in – plane displacements $u\ (x, y, z)$ and $v\ (x, y, z)$ can be expressed in terms of the out of plane displacement $w\ (x, y)$ as shown below:

The displacements are:

$$
\left.\begin{array}{l}
u(x, y, z) = u_o(x, y) - z \dfrac{\partial w}{\partial x} \\[2mm]
v(x, y, z) = v_o(x, y) - z \dfrac{\partial w}{\partial y} \\[2mm]
w(x, y, z) = w_o(x, y)
\end{array}\right\}
\tag{3.1}
$$

Where u_o, v_o and w_o are mid – plane displacements in the direction of the x, y and z axes respectively; z is the perpendicular distance from mid – plane to the layer plane.

(a)   (b)
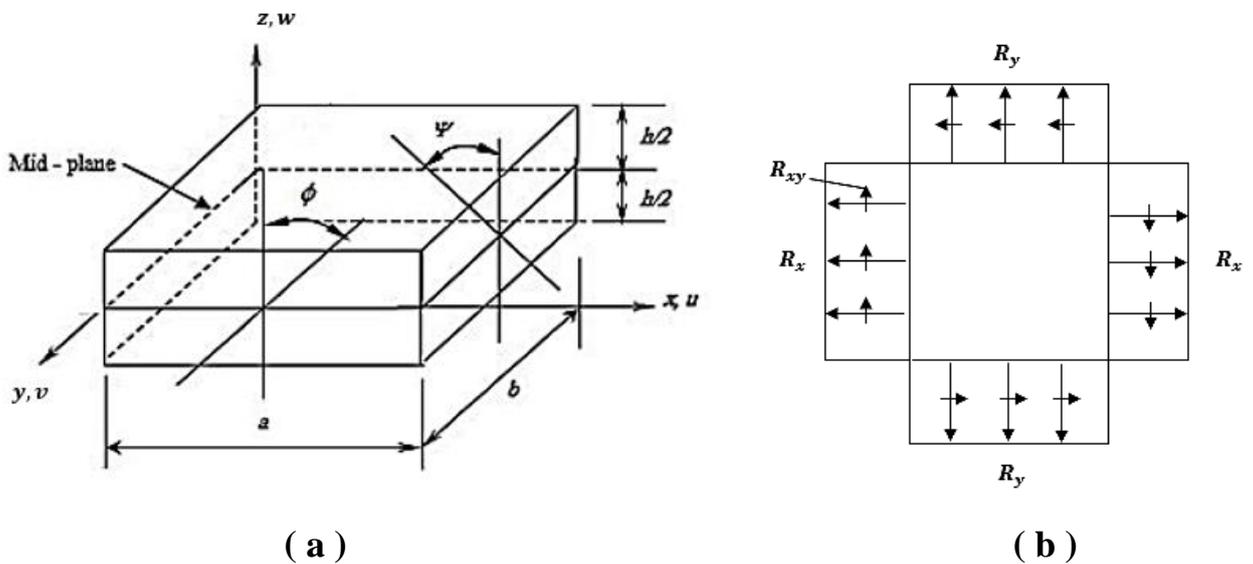
Fig. 3.2 A plate showing dimensions and deformations
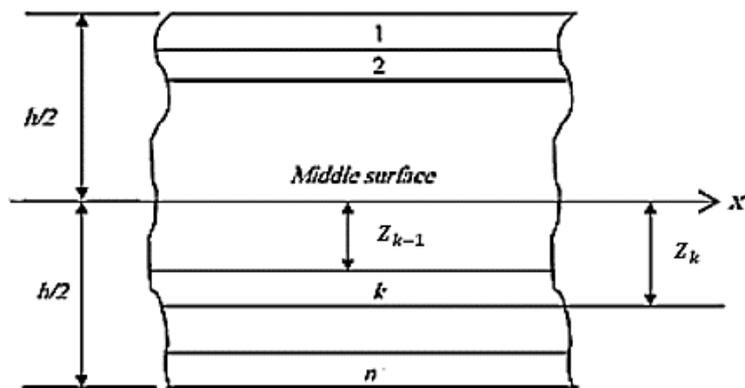
Fig. 3.3 Geometry of an n-layered laminate

The plate shown in Fig. (3.2(a)) is constructed of an arbitrary number of orthotropic layers bonded together as in Fig. (3.3) above.

The strains are:

$$\left.\begin{aligned}
\epsilon_x &= \frac{\partial u_o}{\partial x} - z\frac{\partial^2 w}{\partial x^2} + \frac{1}{2}\left(\frac{\partial w}{\partial x}\right)^2 \\
\epsilon_y &= \frac{\partial v_o}{\partial y} - z\frac{\partial^2 w}{\partial y^2} + \frac{1}{2}\left(\frac{\partial w}{\partial y}\right)^2 \\
\gamma &= \frac{\partial v_o}{\partial x} + \frac{\partial u_o}{\partial y} - 2z\frac{\partial^2 w}{\partial x\partial y} + \left(\frac{\partial w}{\partial x}\right)\left(\frac{\partial w}{\partial y}\right)
\end{aligned}\right\}
\tag{3.2}$$

The virtual strains:

$$\left.\begin{aligned}
\delta\epsilon_x &= \frac{\partial}{\partial x}\delta u_o - z\frac{\partial^2}{\partial x^2}\delta w + \frac{\partial w}{\partial x}\frac{\partial}{\partial x}\delta w \\
\delta\epsilon_y &= \frac{\partial}{\partial y}\delta v_o - z\frac{\partial^2}{\partial y^2}\delta w + \frac{\partial w}{\partial y}\frac{\partial}{\partial y}\delta w \\
\delta\gamma &= \frac{\partial}{\partial x}\delta v_o + \frac{\partial}{\partial y}\delta u_o - 2z\frac{\partial^2}{\partial x\partial y}\delta w + \frac{\partial w}{\partial x}\frac{\partial}{\partial y}\delta w + \frac{\partial}{\partial x}\delta w\frac{\partial w}{\partial y}
\end{aligned}\right\}
\tag{3.3}$$

The virtual strain energy:

$$\delta U = \int_V \delta\epsilon^T \sigma dV \tag{3.4}$$

But,

$$\sigma = C\epsilon$$

Where,

$$C = C_{ij}(i, j = 1, 2, 6)$$

$$\therefore \ \delta U = \int_V \delta\epsilon^T \ C \ \delta\epsilon \ dV \tag{3.5}$$

If we neglect the in-plane displacements u_o and v_o and considering only the linear terms in the strain – displacement equations, we write:

$$\delta\epsilon = -z\begin{vmatrix} \dfrac{\partial^2}{\partial x^2} \\ \dfrac{\partial^2}{\partial y^2} \\ 2\dfrac{\partial^2}{\partial x\partial y} \end{vmatrix}\delta w \tag{3.6}$$

33

3.3 The Numerical Method

The finite element is used in this analysis as a numerical method to predict the buckling loads and shape modes of buckling of laminated rectangular plates. In this method of analysis, four – noded type of elements is chosen. These elements are the four – noded bilinear rectangular elements of a plate. Each element has three degrees of freedom at each node. The degrees of freedom are the lateral displacement (w), and the rotations (ϕ) and (ψ) about the (X) and (Y) axes respectively.

The finite element method is formulated by the energy method. The numerical method can be summarized in the following procedures:

1. The choice of the element and its shape functions.
2. Formulation of finite element model by the energy approach to develop both element stiffness and differential matrices.
3. Employment of the principles of non – dimensionality to convert the element matrices to their non – dimensional forms.
4. Assembly of both element stiffness and differential matrices to obtain the corresponding global matrices.
5. Introduction of boundary conditions as required for the plate edges.
6. Suitable software can be used to solve the problem (here two software were utilized, FORTRAN and ANSYS).

For an n noded element, and 3 degrees of freedom at each node.

Now express w in terms of the shape functions N (given in Appendix (B)) and noded displacements a^e, equation (3.6) can be written as:

$$\delta\epsilon = -zB\delta a^e \qquad (3.7)$$

Where,

$$B^T = \left[\frac{\partial^2 N_i}{\partial x^2} \quad \frac{\partial^2 N_i}{\partial y^2} \quad 2\frac{\partial^2 N_i}{\partial x \partial y}\right]$$

and

$$N_i a_i^e = [w_i] \quad i = 1, n$$

The stress – strain relation is:

$$\sigma = C \, \epsilon$$

Where C are the material properties which could be written as follows:

$$C = \begin{bmatrix} C_{11} & C_{12} & C_{16} \\ C_{12} & C_{22} & C_{26} \\ C_{16} & C_{26} & C_{66} \end{bmatrix}$$

Where C_{ij} are given in Appendix (A).

$$\delta U = \int_V (B\delta a^e)^T (Cz^2) B a^e \, dV$$

Where V denotes volume.

$$\delta U = \delta a^{eT} \int_V B^T D B a^e \, dx \, dy = \delta a^{eT} K^e a^e \qquad (3.8)$$

Where $D_{ij} = \sum_{k=1}^{n} \int_{Z_{k-1}}^{Z_k} C_{ij} Z^2 \, dZ$ is the bending stiffness, and K^e is the element stiffness matrix which could be written as follows:

$$K^e = \int B^T D B \, dxdy \qquad (3.9)$$

The virtual work done by external forces can be expressed as follows: Refer to Fig. (3.4).

Denoting the nonlinear part of strain by $\delta\epsilon'$

$$\delta W = \iint \delta\epsilon'^T \sigma' dV = \int \delta\epsilon'^T N \, dxdy \qquad (3.10)$$

Where

$$N^T = [N_x \ N_y \ N_{xy}] = [\sigma_x \ \sigma_y \ \tau] \, dZ$$

$$\delta\epsilon' = \begin{bmatrix} \delta\epsilon_x \\ \delta\epsilon_y \\ \delta\gamma \end{bmatrix} = \begin{bmatrix} \dfrac{\partial}{\partial x}\delta w & 0 \\ 0 & \dfrac{\partial}{\partial y}\delta w \\ \dfrac{\partial}{\partial y}\delta w & \dfrac{\partial}{\partial x}\delta w \end{bmatrix} \begin{bmatrix} \dfrac{\partial w}{\partial x} \\ \dfrac{\partial w}{\partial y} \end{bmatrix} \qquad (3.11)$$
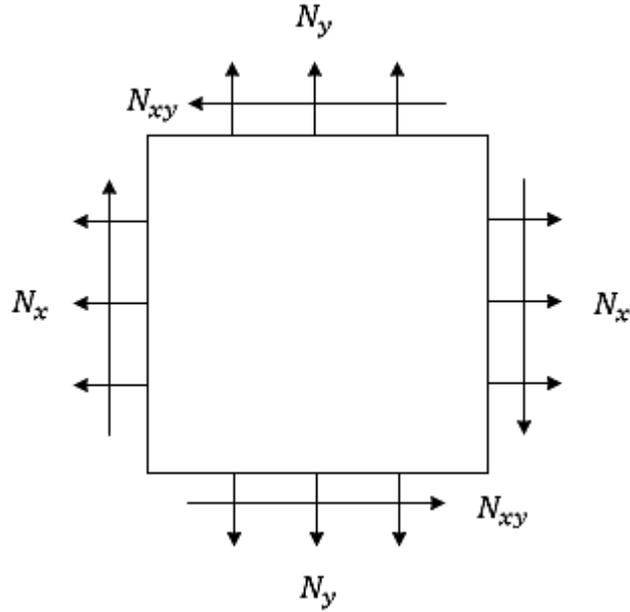
Fig. (3.4) External forces acting on an element

Hence

$$\delta W = \iint \begin{bmatrix} \dfrac{\partial w}{\partial x} \\ \dfrac{\partial w}{\partial y} \end{bmatrix}^T \begin{bmatrix} \dfrac{\partial}{\partial x}\delta w & 0 & \dfrac{\partial}{\partial y}\delta w \\ 0 & \dfrac{\partial}{\partial y}\delta w & \dfrac{\partial}{\partial x}\delta w \end{bmatrix} \begin{bmatrix} N_x \\ N_y \\ N_{xy} \end{bmatrix} dx\, dy \qquad (3.12)$$

This can be written as:

$$\delta W = \iint \begin{bmatrix} \dfrac{\partial}{\partial x}\delta w \\ \dfrac{\partial}{\partial y}\delta w \end{bmatrix}^T \begin{bmatrix} N_x & N_{xy} \\ N_{xy} & N_y \end{bmatrix} \begin{bmatrix} \dfrac{\partial w}{\partial x} \\ \dfrac{\partial w}{\partial y} \end{bmatrix} dx\, dy \qquad (3.13)$$

Now $w = N_i a_i^e$

$$\delta W = \delta a^{eT} \iint \begin{bmatrix} \dfrac{\partial N_i}{\partial x} \\[2mm] \dfrac{\partial N_i}{\partial y} \end{bmatrix}^T \begin{bmatrix} N_x & N_{xy} \\ N_{xy} & N_y \end{bmatrix} \begin{bmatrix} \dfrac{\partial N_i}{\partial x} \\[2mm] \dfrac{\partial N_i}{\partial y} \end{bmatrix} a^e \; dx \, dy \tag{3.14}$$

Substitute $P_x = -N_x, P_y = -N_y, P_{xy} = -N_{xy}$

$$\delta W = -\delta a^{eT} \iint \begin{bmatrix} \dfrac{\partial N_i}{\partial x} \\[2mm] \dfrac{\partial N_i}{\partial y} \end{bmatrix}^T \begin{bmatrix} P_x & P_{xy} \\ P_{xy} & P_y \end{bmatrix} \begin{bmatrix} \dfrac{\partial N_i}{\partial x} \\[2mm] \dfrac{\partial N_i}{\partial y} \end{bmatrix} a^e \; dx \, dy \tag{3.15}$$

Therefore, equation (3.15) could be written in the following form:

$$\delta W = -\delta a^{eT} K^D a^e \tag{3.16}$$

Where,

$$K^D = \iint \begin{bmatrix} \dfrac{\partial N_i}{\partial x} \\[2mm] \dfrac{\partial N_i}{\partial y} \end{bmatrix}^T \begin{bmatrix} P_x & P_{xy} \\ P_{xy} & P_y \end{bmatrix} \begin{bmatrix} \dfrac{\partial N_i}{\partial x} \\[2mm] \dfrac{\partial N_i}{\partial y} \end{bmatrix} dx \, dy$$

K^D is the differential stiffness matrix known also as geometric stiffness matrix, initial stress matrix, and initial load matrix.

The total energy:

$$\delta U + \delta W = 0 \tag{3.17}$$

Since δa^e is an arbitrary displacement which is not zero, then

$$K^e a^e - K^D a^e = 0 \tag{3.18}$$

Now let us compute the elements of the stiffness and the differential matrices.

$$K^e = \iint B^T D B \; dx \, dy$$

$$K^e = \iint \begin{bmatrix} \dfrac{\partial^2 N_i}{\partial x^2} \\[2mm] \dfrac{\partial^2 N_i}{\partial y^2} \\[2mm] 2\dfrac{\partial^2 N_i}{\partial x \partial y} \end{bmatrix}^T \begin{bmatrix} D_{11} & D_{12} & D_{16} \\ D_{12} & D_{22} & D_{26} \\ D_{16} & D_{26} & D_{66} \end{bmatrix} \begin{bmatrix} \dfrac{\partial^2 N_i}{\partial x^2} \\[2mm] \dfrac{\partial^2 N_i}{\partial y^2} \\[2mm] 2\dfrac{\partial^2 N_i}{\partial x \partial y} \end{bmatrix} dx \, dy$$

The elements of the stiffness matrix can be expressed as follows:

$$K_{ij}^e = \iint \left[D_{11} \frac{\partial^2 N_i}{\partial x^2} \frac{\partial^2 N_j}{\partial x^2} + D_{12} \left(\frac{\partial^2 N_i}{\partial y^2} \frac{\partial^2 N_j}{\partial x^2} + \frac{\partial^2 N_i}{\partial x^2} \frac{\partial^2 N_j}{\partial y^2} \right) \right.$$

$$+ 2D_{16} \left(\frac{\partial^2 N_i}{\partial x \partial y} \frac{\partial^2 N_j}{\partial x^2} + \frac{\partial^2 N_i}{\partial x^2} \frac{\partial^2 N_j}{\partial x \partial y} \right) + D_{22} \frac{\partial^2 N_i}{\partial y^2} \frac{\partial^2 N_j}{\partial y^2}$$

$$\left. + 2D_{26} \left(\frac{\partial^2 N_i}{\partial x \partial y} \frac{\partial^2 N_j}{\partial y^2} + \frac{\partial^2 N_i}{\partial y^2} \frac{\partial^2 N_j}{\partial x \partial y} \right) + 4D_{66} \frac{\partial^2 N_i}{\partial x \partial y} \frac{\partial^2 N_j}{\partial x \partial y} \right] dx\, dy \quad (3.19)$$

The elements of the differential stiffness matrix can be expressed as follows;

$$K_{ij}^D = \iint \left[P_x \frac{\partial N_i}{\partial x} \frac{\partial N_j}{\partial x} + P_{xy} \left(\frac{\partial N_i}{\partial y} \frac{\partial N_j}{\partial x} + \frac{\partial N_i}{\partial x} \frac{\partial N_j}{\partial y} \right) + P_y \frac{\partial N_i}{\partial y} \frac{\partial N_j}{\partial y} \right] dx dy \quad (3.20)$$

The integrals in equations (3.19) and (3.20) are given in Appendix (C).

The shape functions for a 4 – noded element is shown below in Fig. (3.5).
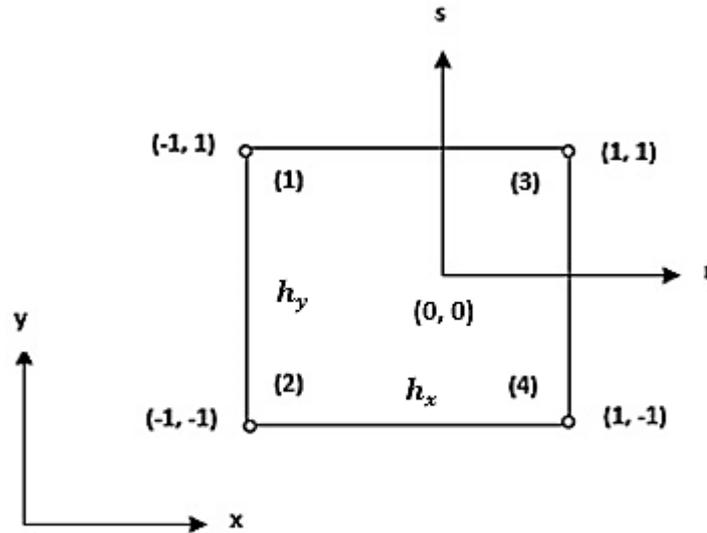
Fig. 3.5 A four noded element with local and global co – ordinates

The shape functions for the 4 – noded element expressed in global co – ordinates (x, y) are as follows:

$$w = N_1 w_1 + N_2 \phi_1 + N_3 \psi_1 + N_4 w_2 + N_5 \phi_2 + N_6 \psi_2$$

$$+ N_7 w_3 + N_8 \phi_3 + N_9 \psi_3 + N_{10} w_4 + N_{11} \phi_4 + N_{12} \psi_4$$

38

Where,

$$\phi = \frac{\partial w}{\partial x}, \qquad \psi = \frac{\partial w}{\partial y}$$

The shape functions in local co – ordinates are as follows:

$$N_i = a_{i1} + a_{i2}r + a_{i3}s + a_{i4}r^2 + a_{i5}rs + a_{i6}s^2 + a_{i7}r^3 + a_{i8}r^2 s + a_{i9}rs^2$$

$$+a_{i10}s^3 + a_{i11}r^3 s + a_{i12}rs^3$$

$$N_j = a_{j1} + a_{j2}r + a_{j3}s + a_{j4}r^2 + a_{j5}rs + a_{j6}s^2 + a_{j7}r^3 + a_{j8}r^2 s + a_{j9}rs^2$$

$$+a_{j10}s^3 + a_{j11}r^3 s + a_{j12}rs^3$$

The values of the coefficients a_{ij} are given in the table in Appendix (B).

$$q_1 = \iint \frac{\partial^2 N_i}{\partial r^2} \frac{\partial^2 N_j}{\partial r^2} \, dr \, ds = 16 \left[a_{i4}a_{j4} + 3a_{i7}a_{j7} + \frac{1}{3} a_{i8}a_{j8} + a_{i11}a_{j11} \right]$$

$$q_2 = \iint \frac{\partial^2 N_i}{\partial s^2} \frac{\partial^2 N_j}{\partial s^2} \, dr \, ds = 16 \left[a_{i6}a_{j6} + \frac{1}{3} a_{i9}a_{j9} + 3a_{i10}a_{j10} + a_{i12}a_{j12} \right]$$

$$q_3 = \iint \frac{\partial^2 N_i}{\partial r^2} \frac{\partial^2 N_j}{\partial s^2} \, dr \, ds = 16 \left[a_{i4}a_{j6} + a_{i7}a_{j9} + a_{i8}a_{j10} + a_{i11}a_{j12} \right]$$

$$q_4 = \iint \frac{\partial^2 N_i}{\partial s^2} \frac{\partial^2 N_j}{\partial r^2} \, dr \, ds = 16 \left[a_{i6}a_{j4} + a_{i9}a_{j7} + a_{i10}a_{j8} + a_{i12}a_{j11} \right]$$

$$q_5 = \iint \frac{\partial^2 N_i}{\partial r^2} \frac{\partial^2 N_j}{\partial r \partial s} \, dr \, ds = 8 \left[a_{i4}a_{j5} + a_{i4}a_{j11} + 2a_{i7}a_{j8} + a_{i4}a_{j12} \right.$$

$$\left. + \frac{2}{3} a_{i8}a_{j9} \right]$$

$$q_6 = \iint \frac{\partial^2 N_i}{\partial r \partial s} \frac{\partial^2 N_j}{\partial r^2} \, dr \, ds = 8 \left[a_{i5}a_{j4} + 2a_{i8}a_{j7} + a_{i11}a_{j4} + \frac{2}{3} a_{i9}a_{j8} \right.$$

$$\left. + a_{i12}a_{j4} \right]$$

$$q_7 = \iint \frac{\partial^2 N_i}{\partial s^2} \frac{\partial^2 N_j}{\partial r \partial s} \, dr \, ds = 8 \left[a_{i6}a_{j5} + a_{i6}a_{j11} + \frac{2}{3} a_{i9}a_{j8} \right]$$

$$q_8 = \iint \frac{\partial^2 N_i}{\partial r \partial s} \frac{\partial^2 N_j}{\partial s^2} \, dr \, ds = 8 \left[a_{i5}a_{j6} + \frac{2}{3} a_{i8}a_{j9} + a_{i11}a_{j6} \right]$$

$$q_9 = \iint \frac{\partial^2 N_i}{\partial r \partial s} \frac{\partial^2 N_j}{\partial r \partial s} \, dr \, ds = 4 \left[a_{i5}a_{j5} + a_{i5}a_{j11} + \frac{4}{3}a_{i8}a_{j8} + a_{i5}a_{j12} \right.$$

$$\left. + \frac{4}{3}a_{i9}a_{j9} + a_{i11}a_{j12} + a_{i12}a_{j11} + \frac{9}{5}a_{i12}a_{j12} \right]$$

$$q_{10} = \iint \frac{\partial N_i}{\partial r} \frac{\partial N_j}{\partial r} \, dr \, ds = 4 \left[a_{i2}a_{j2} + \frac{1}{3}(3a_{i2}a_{j7} + 4a_{i4}a_{j4} + 3a_{i7}a_{j2} \right.$$

$$+ a_{i7}a_{j9} + a_{i5}a_{j5} + a_{i9}a_{j2} + a_{i5}a_{j11} + a_{i7}a_{j9} + \frac{4}{3}a_{i8}a_{j8} + a_{i9}a_{j7}$$

$$a_{i11}a_{j5}) + \frac{1}{5}(a_{i5}a_{j12} + a_{i9}a_{j9} + a_{i12}a_{j5} + 9a_{i7}a_{j7} + 3a_{i11}a_{j11} + a_{i11}a_{j12}$$

$$\left. + a_{i12}a_{j11}) + \frac{1}{7}a_{i12}a_{j12} \right]$$

$$q_{11} = \iint \frac{\partial N_i}{\partial s} \frac{\partial N_j}{\partial s} \, dr \, ds = 4 \left[a_{i3}a_{j3} + \frac{1}{3}(a_{i3}a_{j8} + a_{i5}a_{j5} + a_{i8}a_{j3} \right.$$

$$+ 3a_{i3}a_{j10} + 4a_{i6}a_{j6} + 3a_{i10}a_{j3} + a_{i5}a_{j12} + a_{i8}a_{j10} + \frac{4}{3}a_{i9}a_{j9} + a_{i10}a_{j8}$$

$$+ a_{i12}a_{j5}) + \frac{1}{5}(a_{i5}a_{j11} + a_{i8}a_{j8} + a_{i11}a_{j5} + 9a_{i10}a_{j10} + a_{i11}a_{j12} + a_{i12}a_{j11}$$

$$\left. + 3a_{i2}a_{j12}) + \frac{1}{7}a_{i11}a_{j11} \right]$$

$$q_{12} = \iint \frac{\partial N_i}{\partial r} \frac{\partial N_j}{\partial s} \, dr \, ds = 4 \left[a_{i2}a_{j3} + \frac{1}{3}(a_{i2}a_{j8} + 2a_{i4}a_{j5} + 3a_{i7}a_{j8} \right.$$

$$+ 3a_{i2}a_{j10} + 2a_{i5}a_{j6} + a_{i9}a_{j3} + 2a_{i4}a_{j12} + 3a_{i7}a_{j10} + \frac{4}{3}a_{i8}a_{j9} + \frac{1}{3}a_{i9}a_{j8}$$

$$\left. + 2a_{i11}a_{j6}) \right]$$

$$q_{13} = \iint \frac{\partial N_i}{\partial s} \frac{\partial N_j}{\partial r} \, dr \, ds = 4 \left[a_{i3}a_{j2} + \frac{1}{3}(3a_{i3}a_{j7} + 2a_{i5}a_{j4} + a_{i8}a_{j2} \right.$$

$$+ a_{i3}a_{j9} + 2a_{i6}a_{j5} + 3a_{i10}a_{j2} + 2a_{i6}a_{j11} + \frac{1}{3}a_{i8}a_{j9} + \frac{4}{3}a_{i9}a_{j8} + 3a_{i10}a_{j7}$$

$$\left. + 2a_{i12}a_{j4}) + \frac{1}{5}(2a_{i6}a_{j12} + 3a_{i10}a_{j9} + 3a_{i8}a_{j7} + 2a_{i11}a_{j4}) \right]$$

The values of the integrals are converted from local co – ordinate (r, s) to global co – ordinates as follows:

$$r_1 = \iint \frac{\partial^2 N_i}{\partial x^2} \frac{\partial N_j}{\partial x^2} \, dx \, dy = \left(\frac{4h_y}{h_x^3}\right) q_1 = \frac{4n^3 b}{ma^3} q_1$$

$$r_2 = \iint \frac{\partial^2 N_i}{\partial y^2} \frac{\partial^2 N_j}{\partial y^2} \, dx \, dy = \left(\frac{4h_x}{h_y^3}\right) q_2 = \frac{4am^3}{nb^3} q_2$$

$$r_3 = \iint \frac{\partial^2 N_i}{\partial x^2} \frac{\partial^2 N_j}{\partial y^2} \, dx \, dy = \left(\frac{4}{h_y h_x}\right) q_3 = \frac{4mn}{ab} q_3$$

$$r_4 = \iint \frac{\partial^2 N_i}{\partial y^2} \frac{\partial^2 N_j}{\partial x^2} \, dx \, dy = \left(\frac{4}{h_y h_x}\right) q_4 = \frac{4mn}{ab} q_4$$

$$r_5 = \iint \frac{\partial^2 N_i}{\partial x^2} \frac{\partial^2 N_j}{\partial x \partial y} \, dx \, dy = \left(\frac{4}{h_x^2}\right) q_5 = \frac{4n^2}{a^2} q_5$$

$$r_6 = \iint \frac{\partial^2 N_i}{\partial x \partial y} \frac{\partial^2 N_j}{\partial x^2} \, dx \, dy = \left(\frac{4}{h_x^2}\right) q_6 = \frac{4n^2}{a^2} q_6$$

$$r_7 = \iint \frac{\partial^2 N_i}{\partial y^2} \frac{\partial^2 N_j}{\partial x \partial y} \, dx \, dy = \left(\frac{4}{h_y^2}\right) q_7 = \frac{4m^2}{a^2} q_7$$

$$r_8 = \iint \frac{\partial^2 N_i}{\partial x \partial y} \frac{\partial^2 N_j}{\partial y^2} \, dx \, dy = \left(\frac{4}{h_y^2}\right) q_8 = \frac{4m^2}{b^2} q_8$$

$$r_9 = \iint \frac{\partial^2 N_i}{\partial x \partial y} \frac{\partial^2 N_j}{\partial x \partial y} \, dx \, dy = \left(\frac{4}{h_y h_x}\right) q_9 = \frac{4mn}{ab} q_9$$

$$r_{10} = \iint \frac{\partial N_i}{\partial x} \frac{\partial N_j}{\partial x} \, dx \, dy = \left(\frac{h_y}{h_x}\right) q_{10} = \frac{bn}{am} q_{10}$$

$$r_{11} = \iint \frac{\partial N_i}{\partial y} \frac{\partial N_j}{\partial y} \, dx \, dy = \left(\frac{h_x}{h_y}\right) q_{11} = \frac{am}{bn} q_{11}$$

$$r_{12} = \iint \frac{\partial N_i}{\partial x} \frac{\partial N_j}{\partial y} \, dx \, dy = q_{12}$$

$$r_{13} = \iint \frac{\partial N_i}{\partial y} \frac{\partial N_j}{\partial x} \, dx \, dy = q_{13}$$

In the previous equations $h_x = \frac{a}{n}$ and $h_y = \frac{b}{m}$ where a and b are the lengths of the plate along the $x-$ and $y-$ axis respectively. n and m are the number of elements in the $x-$ and $y-$ directions respectively.

The elements of the stiffness matrix and the differential matrix can be written as follows:

$$K_{ij} = D_{11}r_1 + D_{12}r_4 + 2D_{16}r_3 + D_{12}r_3 + D_{22}r_2 + 2D_{66}r_8 + 2D_{16}r_5$$
$$+ 2D_{26}r_7 + 4D_{66}r_9$$

$$K_{ij}^D = P_x r_{10} + P_{xy}(r_{12} + r_{13}) + P_y r_{11}$$

or in the non $-$ dimensional form

$$K_{ij} = \frac{4n^3}{m}\left(\frac{b}{a}\right)\bar{D}_{11}q_1 + 4mn\left(\frac{a}{b}\right)\bar{D}_{12}q_4 + 4n^2\bar{D}_{16}q_6 + 4mn\left(\frac{a}{b}\right)\bar{D}_{12}q_3$$

$$+ \frac{4m^3}{n}\left(\frac{a}{b}\right)\bar{D}_{22}q_2 + 4m^2\left(\frac{a}{b}\right)^2\bar{D}_{26}q_8 + 4n^2\bar{D}_{16}q_5 + 4m^2\left(\frac{a}{b}\right)^2\bar{D}_{26}q_7$$

$$+4mn\left(\frac{a}{b}\right)\bar{D}_{66}q_9$$

$$K_{ij}^D = \bar{P}_x\frac{n}{m}\left(\frac{b}{a}\right)q_{10} + \bar{P}_{xy}(q_{12} + q_{13}) + \bar{P}_y\frac{m}{n}\left(\frac{a}{b}\right)q_{11}$$

where

$$\bar{D}_{ij} = \left(\frac{1}{E_1 h^3}\right)D_{ij}, \quad \bar{P}_i = \left(\frac{a}{E_1 h^3}\right)P_i$$

Also

$$\bar{w} = \left(\frac{1}{h}\right)w, \quad \bar{\phi} = \left(\frac{h}{a}\right)\phi, \quad \bar{\psi} = \left(\frac{h}{a}\right)\psi, \quad \bar{b} = b/a$$

The transformed stiffnesses are as follows:

$$C_{11} = C'_{11}c^4 + 2c^2s^2(C'_{11} + 2C'_{66}) + C'_{22}s^4$$

$$C_{12} = c^2s^2(C'_{11} + C'_{22} + 4C'_{66}) + C'_{12}(c^4 + s^4)$$

$$C_{16} = cs[C'_{11}c^4 + C'_{22}s^2 - (C'_{12} + 2C'_{66})(c^2 - s^2)]$$

$$C_{22} = C'_{11}s^4 + 2c^2s^2(C'_{12} + 2C'_{66}) + C'_{22}c^4$$

$$C_{26} = cs[C'_{11}s^2 - C'_{22}c^2 - (C'_{12} + 2C'_{66})(c^2 - s^2)]$$

$$C_{66} = (C'_{11} + C'_{22} - 2C'_{12})c^2s^2 + C'_{66}(c^2 - s^2)^2$$

Where

$$C'_{11} = \frac{E_1}{1 - v_{12}v_{21}}$$

$$C'_{12} = \frac{v_{21}E_1}{1 - v_{12}v_{21}} = \frac{v_{12}E_1}{1 - v_{12}v_{21}}$$

$$C'_{22} = \frac{E_2}{1 - v_{12}v_{21}}$$

$$C'_{44} = G_{23}, \qquad C'_{55} = G_{13} \quad \text{and} \quad C'_{66} = G_{12}$$

E_1 and E_2 are the elastic moduli in the direction of the fiber and the transverse directions respectively, v is the Poisson's ratio. G_{12}, G_{13}, and G_{23} are the shear moduli in the $x - y$ plane, $y - z$ plane, and $x - z$ plane respectively, and the subscripts 1 and 2 refer to the direction of fiber and the transverse direction respectively.

Chapter (4)

Verification of the Computer Program

4.1 Convergence Study

The optimum number of plate elements in the x any y directions (i.e. mesh size or discretization), to be used in order to compute the buckling loads with reasonable accuracy can be obtained by a convergence study. The suitable number of finite elements is determined by a number of factors which include material properties, plate dimensions, lamination scheme, boundary conditions and the storage capacity of the computer ram.

It can be observed that, as the mode order increases, the number of finite elements required increases. Therefore, it is expected that the higher modes need more number of elements.

All of the analyses described in the present thesis have been undertaken assuming the plate to be subjected to identical and/ or different support conditions on the four edges of the plate. The three sets of the of the edge conditions used here are designated as clamped – clamped (CC), simply – simply supported (SS), clamped – simply supported (CS), are shown in table (4.1) below.

Table (4.1) Boundary conditions

Boundary Conditions	Plate dimensions in y – coordinate $x = 0 , x = a$	Plate dimensions in x – coordinate $y = 0 , y = b$
CC	$w = \phi = \psi = 0$	$w = \phi = \psi = 0$
SS	$w = \psi = 0$	$w = \phi = 0$
CS	$w = \phi = \psi = 0$	$w = \phi = 0$

Table (4.2) shows the convergence study of non – dimensional buckling load of simply supported SS square isotropic plate with length to thickness ratio (a/h=20) having the following material properties: material 1:

$$E_y/E_x = 1.0 \,, G_{xy}/E_x = G_{yz}/E_x = G_{xz}/E_x = 0.4 \,, v_{xy} = 0.25$$

The discretization of elements used are:

1. $2 \times 2 = 4$ elements

2. $3 \times 3 = 9$ elements

3. $4 \times 4 = 16$ elements

4. $5 \times 5 = 25$ elements

5. $6 \times 6 = 36$ elements

6. $7 \times 7 = 49$ elements

7. $8 \times 8 = 64$ elements

8. $9 \times 9 = 81$ elements

9. $10 \times 10 = 100$ elements

It could be observed from table (4.2) that the values of the buckling parameter $\bar{P} = Pb^2/E_2h^3$ converge as the number of elements in the mesh are increased (i.e. as the mesh size is progressively reduced). These results suggest that a 6×6 mesh over the plate is adequate for the present work (i.e. less than 1.32% difference compared to the finest mesh result available). Therefore, a mesh size of 6×6 is found to be sufficient to predict the first seven modes of buckling load. In practice only the first three modes of buckling are sufficient.

Table (4.2) Convergence study of non – dimensional modes of buckling $\bar{P} = Pa^2/E_1h^3$ of simply supported (SS) isotropic square plate with a/h=20. (material 1)

Mesh Size	Mode Sequence Number						
	1	2	3	4	5	6	7
2×2	30.69	76.89	83.18	83.49	94.71	94.95	101.78
3×3	32.64	79.12	79.18	117.58	179.04	189.78	191.05
4×4	33.60	82.38	82.44	123.22	165.70	166.35	192.53
5×5	34.10	84.08	84.14	127.71	168.69	168.92	202.10
6×6	34.39	85.10	85.15	130.85	170.41	170.52	208.35
7×7	34.58	85.75	85.79	133.03	171.55	171.61	212.50
8×8	34.70	86.19	86.23	134.57	172.34	172.39	215.79
9×9	34.78	86.50	86.53	135.68	172.92	172.97	218.07
10×10	34.84	86.72	86.75	136.52	173.35	173.40	219.78

4.2 Validation of the Finite Element (FE) Program

In order to check the validity, applicability and accuracy of the present FE method, many comparisons were performed. The comparisons include theoretical, ANSYS simulation and experimental results.

4.2.1 Comparisons with Theoretical Results

In table (4.3) the non – dimensional critical buckling load is presented in order to compare with References [162], [163] and [164] for an isotropic plate of material 1 with different aspect ratios. As the table shows, the present results have a good agreement with References [162], [163] and [164].

Table (4.3) Comparison of the non – dimensional critical buckling load

$$\bar{P} = Pa^2/D \text{ for an isotropic plate (material 1)}$$

Aspect Ratio a/b	References			
	Ref. [162]	Ref. [163]	Ref. [164]	Present Study
0.5	12.33	12.3370	12.3370	12.3
1.0	19.74	19.7392	19.7392	19.7

Table (4.4) below shows the effect of plate aspect ratio and modulus ratio on non – dimensional critical loads $\bar{P} = P(b^2\pi^2/D_{22})$ of rectangular laminates under biaxial compression. The following material properties were used: material 2: $E_1/E_2 = 5, 10, 20, 25$ and 40; $G_{12} = G_{13} = G_{23} = 0.5\, E_2$; $\nu_{12} = 0.25$ and $a/h = 20$. It is observed that the non – dimensional buckling load increases for symmetric laminates as the modular ratio increases. The present results were compared with Osman [165] and Reddy [166]. The verification process showed good agreement especially as the aspect ratio increases and the modulus ratio decreases.

Table (4.4) Buckling load for (0/ 90/ 90/ 0) simply supported (SS) plate for different aspect and moduli ratios under biaxial compression (material 2)

Aspect Ratio a/b	Modular Ratio	Biaxial Compression				
	E_1/E_2	5	10	20	25	40
0.5	Present	10.864	12.122	13.215	13.726	14.000
	Ref. [165]	-	12.307	-	13.689	-
	Ref. [166]	11.120	12.694	13.922	14.248	14.766
1.0	Present	2.790	3.130	3.430	3.510	3.645
	Ref. [165]	-	3.137	-	3.502	-
	Ref. [166]	2.825	3.174	3.481	3.562	3.702

	Present	1.591	1.602	1.611	1.613	1.617
1.5	Ref. [165]	-	1.605	-	1.606	-
	Ref. [166]	1.610	1.624	1.634	1.636	1.641

Table (4.5) shows the effect of plate aspect ratio, and modulus ratio on non – dimensional critical buckling loads $\bar{P} = P(b^2/\pi^2 D_{22})$ of simply supported (SS) antisymmetric cross – ply rectangular laminates under biaxial compression. The properties of material 2 were used. It is observed that the non – dimensional buckling load decreases for antisymmetric laminates as the modulus ratio increases. The present results were compared with Reddy [166]. The validation process showed good agreement especially as the aspect ratio increases and the modulus ratio decreases.

Table (4.5) Buckling load for (0/ 90/ 90/ 0) simply supported (SS) plate for different aspect and moduli ratios under biaxial compression (material 2)

Aspect Ratio a/b	Modular Ratio	Biaxial Compression				
	E_1/E_2	5	10	20	25	40
0.5	Present	4.000	3.706	3.535	3.498	3.442
	Ref. [166]	3.764	3.325	3.062	3.005	2.917
1.0	Present	1.395	1.209	1.102	1.079	1.045
	Ref. [166]	1.322	1.095	0.962	0.933	0.889
1.5	Present	1.069	0.954	0.889	0.875	0.853
	Ref. [166]	1.000	0.860	0.773	0.754	0.725

Table (4.6) below shows the effect of plate aspect ratio, and modulus ratio on non – dimensional critical buckling loads of simply supported (SS) antisymmetric angle – ply rectangular laminates under biaxial compression.

The properties of material 2 were used. It is observed from table (4.6) that the prediction of the buckling loads by the present study is closer to that of Osman [165] and Reddy [166].

Table (4.6) Buckling load for antisymmetric angle – ply $(45/-45)_4$ plate with different moduli and aspect ratios under biaxial compression (material 2)

Aspect Ratio a/b	Modular Ratio	Biaxial Compression			
	E_1/E_2	10	20	25	40
0.5	Present	19.376	36.056	44.400	69.440
	Ref. [165]	19.480	-	44.630	-
	Ref. [166]	18.999	35.076	43.110	67.222
1.0	Present	9.028	17.186	21.265	33.512
	Ref. [165]	9.062	-	21.345	-
	Ref. [166]	8.813	16.660	20.578	32.343
1.5	Present	6.144	11.596	14.322	22.013
	Ref. [165]	6.170	-	14.383	-
	Ref. [166]	6.001	11.251	13.877	21.743

In tables (4.7) and (4.8), the buckling loads for symmetrically laminated composite plates of layer orientation (0/ 90/ 90/ 0) have been determined for three different aspect ratios ranging from 0.5 to 1.5 and two modulus ratios 40 and 5 of material 2. It is observed that the buckling load increases with increasing aspect ratio for biaxial compression loading. The buckling load is maximum for clamped – clamped (CC), and clamped – simply supported (CS) boundary conditions, while minimum for simply – simply supported (SS) boundary conditions. It is seen from tables (4.7) and (4.8) that the values of buckling loads by the present study is much closer to the of Osman [165].

Table (4.7) Buckling load for (0/ 90/ 90/ 0) plate with different boundary conditions and aspect ratios under biaxial compression $(\bar{P} = Pa^2/E_1h^3)$ (material 2) $E_1/E_2 = 40;\ G_{12} = G_{13} = G_{23} = 0.5\ E_2$; and $\nu_{12} = 0.25$

Aspect Ratio a/b	Comparisons of Results	Boundary Conditions		
		CC	SS	CS
0.5	Present	1.0742	0.4143	0.9679
	Ref. [165]	1.0827	0.4213	1.0022
1.0	Present	1.3795	0.4409	1.0723
	Ref. [165]	1.3795	0.4411	1.0741
1.5	Present	1.6402	0.4400	1.2543
	Ref. [165]	1.6367	0.4391	1.2466

Table (4.8) Buckling load for (0/ 90/ 90/ 0) plate with different boundary conditions and aspect ratios $(\bar{P} = Pa^2/E_1h^3)$ (material 2) $E_1/E_2 = 5;\ G_{12} = G_{13} = G_{23} = 0.5\ E_2$; and $\nu_{12} = 0.25$

Aspect Ratio a/b	Comparisons of Results	Boundary Conditions		
		CC	SS	CS
0.5	Present	1.7786	0.6787	1.6325
	Ref. [165]	1.8172	0.6877	1.6838
1.0	Present	2.1994	0.6972	1.8225
	Ref. [165]	2.2064	0.6985	1.8328
1.5	Present	2.7961	0.8943	1.7643
	Ref. [165]	2.8059	0.8962	1.7618

The same behavior of buckling load applies to symmetrically laminated composite plates (0/ 90/ 0) as shown in tables (4.9) and (4.10).

Table (4.9) Buckling load for (0/ 90/ 0) plate with different boundary conditions and aspect ratios ($\bar{P} = Pa^2/E_1h^3$) (material 2) $E_1/E_2 = 40$; $G_{12} = G_{13} = G_{23} = 0.5\,E_2$; and $\nu_{12} = 0.25$

Aspect Ratio a/b	Comparisons of Results	Boundary Conditions		
		CC	SS	CS
0.5	Present	1.7471	0.3238	0.6870
	Ref. [165]	0.7529	0.3325	0.7201
1.0	Present	0.9523	0.3485	0.7925
	Ref. [165]	0.9511	0.3489	0.7932
1.5	Present	1.1811	0.3530	0.8190
	Ref. [165]	1.1763	0.3514	0.8099

Table (4.10) Buckling load for (0/ 90/ 0) plate with different boundary conditions and aspect ratios ($\bar{P} = Pa^2/E_1h^3$) (material 2) $E_1/E_2 = 5$; $G_{12} = G_{13} = G_{23} = 0.5\,E_2$; and $\nu_{12} = 0.25$

Aspect Ratio a/b	Comparisons of Results	Boundary Conditions		
		CC	SS	CS
0.5	Present	1.6947	0.6772	1.5842
	Ref. [165]	1.7380	0.6871	1.6337
1.0	Present	2.1669	0.6970	1.7009
	Ref. [165]	2.1744	0.6984	1.7113
1.5	Present	2.5008	0.8224	1.7658
	Ref. [165]	2.5075	0.8235	1.7622

4.2.2 Comparisons with the Results of ANSYS Package

ANSYS is a general-purpose finite element modeling package for numerically solving a wide variety of mechanical problems. These problems include: static/ dynamic structural analysis (both linear and non – linear), heat transfer and fluid problems, as well as acoustic and electromagnetic problems. The problem of buckling in ANSYS is considered as static analysis. In this analysis, the following steps are done:

Step (1): Preprocessor:

Element type:

1. On the preprocessor menu, click "Element Type".

2. Click "Add/ Edit/ Delete".

3. Click "Add".

4. Choose the element type from the list on the right, then click "OK".

Real constants:

1. Click "Real Constants" on the Preprocessor menu.

2. Click "Add".

3. Click "OK" in the Element Type for Real Constant box.

4. Enter the number of layers, and the values of layers thickness, then click "OK".

Material properties:

1. Click "Material Props" on the Preprocessor menu.

2. Click "Material Models", then click "OK".

3. Double – click "Structural" in the right side of the window, then "Linear", then "Elastic", then finally "Orthotropic".

4. Enter values for Young's modulus, and for Poisson's ratio, then click "OK".

5. Double – click "Density" in the right side of the window, then enter its magnitude and click "OK".

Modeling:

1. Under the "-Modeling-" heading on the Preprocessor menu, click "Create".

2. Under the "-Areas-" heading, click "Rectangle".

3. Click "By Dimensions".

4. Enter in the values of (x) and (y) coordinates. This creates a rectangle, centered at the origin. Then click "OK".

Meshing:

1. On the Preprocessor menu, click "Mesh Tool".

2. Under Lines in the Size Controls section, click "Set".

3. In the pick box, click "Pick All".

4. Enter the number of element divisions, then click "OK".

5. In the Mesh Tool box, click "Mesh"; in the pick box that appears, click "Pick All". ANSYS will now mesh the model.

Step (2): Solution:

Defining the analysis:

1. On the Solution menu, click "New Analysis".

2. Choose "Static", then click "OK".

3. On the Solution menu, click "Analysis Options".

4. Enter the number of modes to extract and set the mode extraction method to "Subspace", then click "OK". Defining a fairly fine mesh, leads to easily get accurate results for the modes.

5. Click "OK" in the box for subspace modal analysis options.

Applying boundary conditions:

1. On the Solution menu under the "-Loads-" heading, click "Apply".

2. Click "Displacement".

3. Click "On Lines".

4. Click the top and bottom of the plate, then click "OK". (Both the top and bottom will have the same degrees of freedom constrained).

5. Select the type of constrains, then enter a displacement value of (0) and click "Apply".

6. Select the sides of the plate to be constrained, then click "Ok".

Solving the problem:

1. On the Solution menu under the "-Solve-" heading, click "Current LS".

2. Review the analysis summary information presented; in particular, make sure that the number of modes to extract is the number that you want. If everything is in order, click "OK" in the Solve Current Load Step window. ANSYS will now solve the problem. (For modal analysis, ANSYS may give a warning that the mode shapes found will be for viewing purposes only; you can ignore this).

Step (3): Postprocessor:

Viewing the mode shapes:

1. On the General Postprocessor menu under the – Read Results – heading, click "First Set".

2. Click "Plot Results".

3. Under the "-Contour Plot-" heading, click "Nodal Solu".

4. Choose "DOF Solution" in the box on the left, and "Translation UZ" in the right to see the out – of – plane displacements. The mode frequency will be displayed on the right side of the graphics window as "FREQ".

5. To view the other modes, go back to the General Postprocessor menu, click "Next Set" under the "-Read Results-" heading, then repeat steps 2 – 4 above.

To validate the present results with ANSYS, the present results were converted from its non – dimensional form to the dimensional form by using the formula $\bar{P} = Pa^2/E_1 h^3$. The E – glass/ Epoxy material is selected to obtain the numerical results for the comparisons. The mechanical properties of this material (material 3) is given in table (4.11) below.

Table (4.11) Mechanical Properties of the E – glass/ Epoxy material (material 3)

Property	Value
E_1 or E_x	38.6 GN/m^2
E_2 or E_y	8.27 GN/m^2
G_{12} or G_{xy}	4.14 GN/m^2
G_{13} or G_{xz}	4.14 GN/m^2
G_{23} or G_{yz}	3.4 GN/m^2
ν_{12} or ν_{xy}	0.28

Table (4.12) to (4.15) shows comparisons between the results of the present study and that simulated by ANSYS technique. Table (4.12) shows the effect of boundary conditions on dimensional buckling loads of symmetric angle – ply (30/ -30/ -30/ 30) of square thin laminates ($a/h = 20$) under biaxial compression. The properties of material 3 in table (4.11) were used. Small differences were shown between the results of the two techniques. The difference ranges between 0.6% to less than 2%. It is observed that as the mode serial number increases, the difference increases. The same behavior of buckling load of both techniques applies to symmetrically laminated composite plates of the order (45/ -45/ -45/ 45), (60/ -60/ -60/ 60) and (0/ 90/ 90/ 0) shown in tables (4.13), (4.14) and (4.15).

Table (4.12) Dimensional buckling load of symmetric angle–ply (30/ -30/ -30/ 30) square thin laminates with different boundary conditions (a/h=20) (material 3)

Boundary Conditions	Method	Mode Serial Number		
		1	2	3
SS	Present	109.5 N	193.4 N	322.8 N
	ANSYS	109.4 N	206.5 N	315.8 N

		1	2	3
CS	Present	234.7 N	257.2 N	371.41 N
	ANSYS	233.21 N	255.6 N	378.7 N

Table (4.13) Dimensional buckling load of symmetric angle–ply (45/-45/-45/45) square thin laminates with different boundary conditions (a/h=20) (material 3)

Boundary Conditions	Method	Mode Serial Number		
		1	2	3
SS	Present	115.24 N	219.5 N	305.4 N
	ANSYS	116.3 N	225.5 N	312.7 N
CS	Present	196.33 N	282.8 N	439.53 N
	ANSYS	194.7 N	287.6 N	444.51 N

Table (4.14) Dimensional buckling load of symmetric angle–ply (60/-60/-60/60) square thin laminates with different boundary conditions (a/h=20) (material 3)

Boundary Conditions	Method	Mode Serial Number		
		1	2	3
SS	Present	109.39 N	193.213 N	322.19 N
	ANSYS	109.6 N	191.13 N	325.37 N
CS	Present	161.4 N	279.1 N	370.5 N
	ANSYS	160.6 N	280.4 N	377.7 N

Table (4.15) Dimensional buckling load of symmetric cross–ply (0/ 90/ 90/ 0) square thin laminates with different boundary conditions (a/h=20) (material 3)

Boundary Conditions	Method	Mode Serial Number		
		1	2	3
SS	Present	93.4 N	170.4 N	329 N
	ANSYS	94.4 N	181.4 N	315 N

CS	Present	244.5 N	263.7 N	366.23 N
	ANSYS	244.4 N	265.8 N	369.6 N

4.2.3 Comparisons with Experimental Results

Many numerical and mathematical models exist which can be used to describe the behavior of a laminate under the action of different forces. When it comes to buckling, a mathematical model can be developed which is used to model the phenomenon of buckling. But numerical methods become complicated as the number of assumptions and variables increase. Also, once the model is formed, it takes a lot of time to solve the partial differential equations and then arrive to the final result. This process becomes very cumbersome and time consuming. In view of the above-mentioned limitations, experimental methods are followed. The experimental process needs less time and less computational work. Also, the results obtained in experiments are fairly close to that which is obtained theoretically.

The composites have two components. The first is the matrix which acts as the skeleton of the composite and the second is the hardener which acts as the binder for the matrix. The reinforcement that was used for the present study was woven glass fibers. Glass fibers are materials which consist of numerous extremely fine fibers of glass. The hardener that utilized was epoxy which functions as a solid cement to keep fiber layers together.

To manufacture the composites the following steps were taken:

1. The weight of the fiber was noted down, then approximately $1/3^{rd}$ mass of epoxy was prepared for further use.

2. A clean plastic sheet was taken and the mold releasing spray was sprayed on it. After that, a generous coating of the hardener mixture was coated on the sheet. A woven fiber sheet was taken and placed on top of the coating. A second coating was done again, and a second layer of fiber was placed, and the process continued until the required thickness was obtained. The fiber was pressed with the help of rollers.

3. Another plastic sheet was taken and the mold releasing spray was sprayed on it. The plastic sheet was placed on top of the fiber with hardener coating.
4. The plate obtained was placed under weights for a period of 24 hours.
5. After that the plastic sheets were removed and the plates separated.

The buckling test rig for biaxial compression was developed in Tehran University of Science and Technology, College of Engineering, Iran. The frame was built using rectangular shaped mild steel channels. The channels were welded to one another and then the frame was prepared. A two-ton hydraulic jacks were assembled into the frame to provide the necessary hydraulic forces for biaxial compression of the plates. The setup can be easily assembled and disassembled. Thus, the setup offers flexibility over the traditional buckling setups.

It is proposed to undertake some study cases and obtain experimental results of non – dimensional buckling of rectangular laminated plates subjected to in – plane biaxial Compressive loads. The plates are assumed to be either simply supported on all edges (SS), or a combined case of clamped and simply supported (CS), or clamped on all edges (CC).

The effects of various parameters like material anisotropy, fiber orientation, aspect ratio, and edge conditions on the buckling load of laminated plates are to be investigated and compared with the present finite element results. The plates are made of graphite – epoxy material (material 3), and generally square with side $a = b = 250mm$ and length to thickness ratio (a/h)=20. The required experiments are explained below:

Experiment (1): Effect of Material Anisotropy (E_1/E_2)

Cross – ply symmetric laminates with length to thickness ratio of ($a/h = 20$) are to be tested. The ratio of longitudinal to transverse modulus (E_1/E_2) is to be increased from 10 to 50. The required number of plies is 8. The plate is simply – supported (SS) on all edges. The experimental values of buckling

load were compared with the present theoretical results as shown in table (4.16).

Table (4.16) Effect of material anisotropy on buckling load $a/h = 20$

E_1/E_2	Method	Buckling loads
10	Present	0.5537
	Experimental	0.4985
20	Present	0.4789
	Experimental	0.4310
30	Present	0.4536
	Experimental	0.4082
40	Present	0.4418
	Experimental	0.3976
50	Present	0.4343
	Experimental	0.3908

It is observed that the buckling load decreases with the increase in material anisotropy (E_1/E_2). The present theoretical results were about 10% higher than the experimental values which is considered to be acceptable.

Experiment (2): Effect of Fiber Orientation (θ)

Symmetric and anti – symmetric cross – ply laminated plates (0/ 90/ 90/ 0) and (0/ 90/ 0/ 90) with length to thickness ratio (a/h) are to be tested. The required number of plies is 8. The plate is simply supported (SS) on four edges. As shown in table (4.17) below, the theoretical buckling load was found to be 10% above the experimental value.

Table (4.17) **Effect of fiber orientation on buckling load $E_1/E_2 = 40$,**

$$a/h = 20$$

Orientation	Method	Buckling loads
Symmetric	Present	0.4418
	Experimental	0.3976
Anti – Symmetric	Present	0.4417
	Experimental	0.3975

Experiment (3): Effect of Aspect Ratio (a/b)

The effect of aspect ratio (a/b) on the buckling load is studied by testing cross – ply symmetric (0/ 90/ 90/ 0) laminates with length to thickness ratio $(a/h = 20)$. The aspect ratios 0.5, 1, 1.5 and 2.0 are to be tested. The required number of plies is 8. The plate is simply supported on four edges and the modulus ratio is taken to be $(E_1/E_2 = 40)$. As shown in table (4.18) below, the difference between the theoretical and experimental buckling was found to be about 10%.

Table (4.18) Effect of aspect ratio on buckling load $E_1/E_2 = 40$,

$$a/h = 20$$

Aspect Ratio (a/b)	Method	Buckling loads
0.5	Present	0.4192
	Experimental	0.3773
1.0	Present	0.4418
	Experimental	0.3976
1.5	Present	0.7187
	Experimental	0.6468
2.0	Present	1.2324
	Experimental	1.1092

Experiment (4): Effect of Boundary Conditions

Cross – ply symmetric laminates (0/ 90/ 90/ 0) can be used to study the effect of the boundary conditions on the buckling load. The length to thickness ratio is taken to be ($a/h = 20$). The boundary conditions used are SS, CS and CC. The required number of plies is 8 and the modulus ratio (E_1/E_2) is selected to be 40. As shown in table (4.19) below, the same difference between the theoretical and experimental results was observed.

Table (4.19) Effect of boundary conditions on buckling load $E_1/E_2 = 40$, $a/h = 20$

Boundary Conditions	Method	Buckling loads
SS	Present	0.4418
	Experimental	0.3976
CS	Present	1.2882
	Experimental	1.1594
CC	Present	1.3812
	Experimental	1.2431

Chapter (5)

Numerical Results and Discussions

With confidence in the finite element (FE) program proved through the various verification exercises undertaken, it was decided to undertake some study cases and generate new results for biaxial loaded laminated composite rectangular plates. The plates were assumed to be simply supported (SS), clamped (CC) and clamped – simply supported (CS) on all four edges.

The problem of critical buckling loads of laminated composite plates is analyzed and solved using the energy method which is formulated by a finite element model. In that model, a four noded rectangular elements of a plate is considered. Each element has three degrees of freedom at each node. The degrees of freedom are the lateral displacement w, and the rotations ϕ and ψ about the y and x axes respectively.

The effects of lamination scheme, aspect ratio, material anisotropy, fiber orientation of layers, reversed lamination scheme and boundary conditions on the non – dimensional critical buckling loads of laminated composite plates are investigated.

The material chosen has the following properties: material 2: $E_1/E_2 = 5, 10, 20, 25, 40$; $G_{12} = G_{13} = G_{23} = 0.5E_2$; $v_{12} = 0.25$.

5.1 Effect of Lamination Scheme

In the present analysis the lamination scheme of plates is supposed to be symmetric, anti – symmetric and quasi – isotropic.

Four lamination schemes were considered which are symmetric and anti – symmetric cross – ply and angle – ply laminates. Table (5.1) gives a comparison between the non – dimensional buckling loads for all lamination schemes. The results are shown graphically in Fig. (5.1). The thickness of all layers is assumed equal, the length to thickness ratio ($a/h = 20$), and the modulus ratio ($E_1/E_2 = 5$). It is noticed from table (5.1) and Figs. (5.1), (5.2)

and (5.3) that the values of the non – dimensional buckling loads for both symmetric and anti – symmetric lamination are slightly different, except for symmetric and anti – symmetric angle – ply laminates which are exactly the same. Because of this fact, the rest of the upcoming effects will be discussed for symmetric case only. The results indicate that the symmetric laminate is stiffer than the anti – symmetric one. This phenomenon is caused by coupling between bending and stretching which lowers the buckling loads of symmetric laminate.

Table (5.1) The first five non – dimensional buckling loads $\overline{P} = Pa^2/E_1h^3$ of symmetric cross – ply (0/ 90/ 90/ 0) and anti – symmetric cross – ply (0/ 90/ 0/ 90), and symmetric angle – ply (45/ -45/ -45/ 45) and anti – symmetric angle – ply (45/ -45/ 45/ -45) laminated plates with $a/h = 20$, and $E_1/E_2 = 5$, (material 2)

Lamination Scheme	Mode Number	Boundary Conditions		
		SS	CC	CS
0/ 90/ 90/ 0	1	0.6972	2.1994	1.8225
	2	1.2522	2.5842	2.0097
	3	2.4284	4.1609	2.7116
	4	2.6907	4.7431	4.3034
	5	2.7346	5.0168	4.4536
0/ 90/ 0/ 90	1	0.6973	2.2273	1.5591
	2	1.9947	3.9687	2.3391
	3	1.9958	3.9732	3.7581
	4	2.6912	4.7871	3.8290
	5	4.3962	7.0544	4.5402

	1	0.8729	1.9505	1.4756
	2	1.6400	2.8534	2.1162
45/-45/-45/45	3	2.3130	3.8941	3.3039
	4	2.7100	4.3753	3.3068
	5	3.5488	5.2694	4.4166
	1	0.8729	2.2010	1.6554
	2	1.6400	3.7616	2.5672
45/-45/45/-45	3	2.3130	3.7654	3.4642
	4	2.7100	5.6599	4.2174
	5	3.5488	5.9540	4.8091
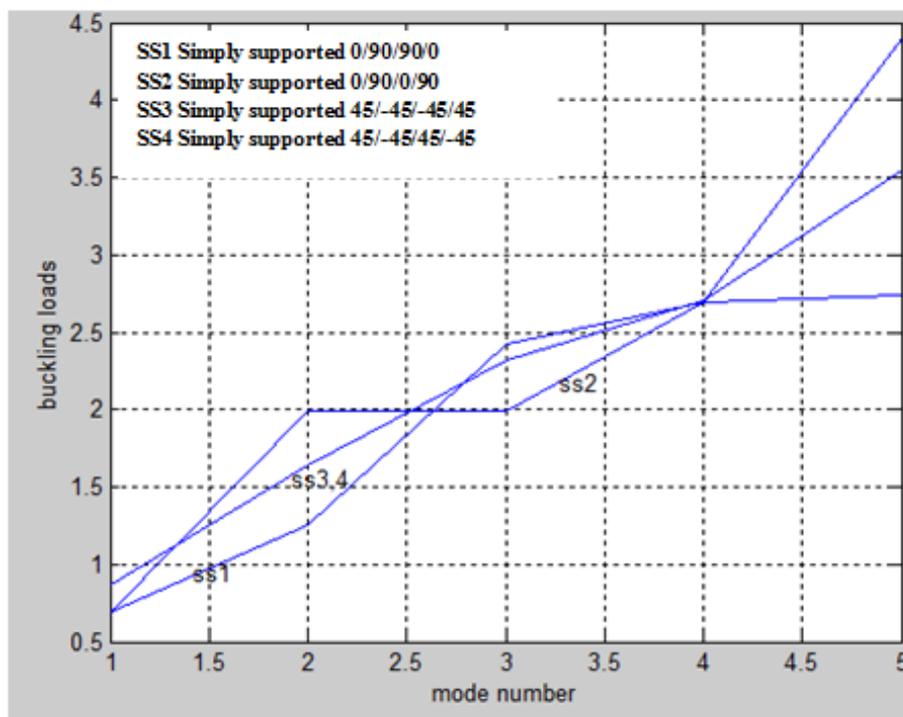
Fig. (5.1) Effect of lamination scheme for simply supported laminates
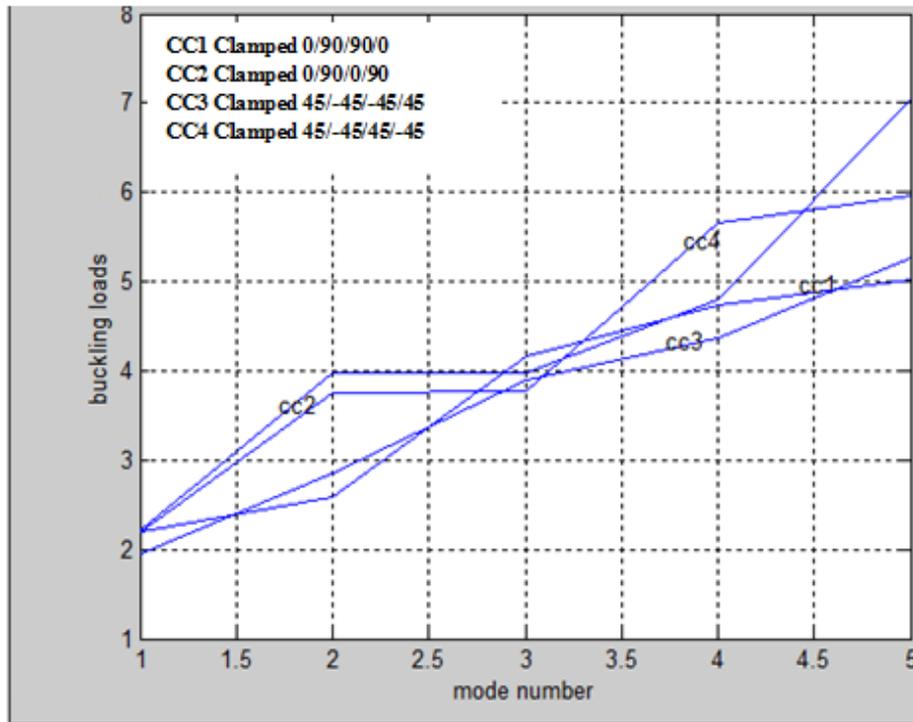
Fig. (5.2) Effect of lamination scheme for clamped – clamped laminates
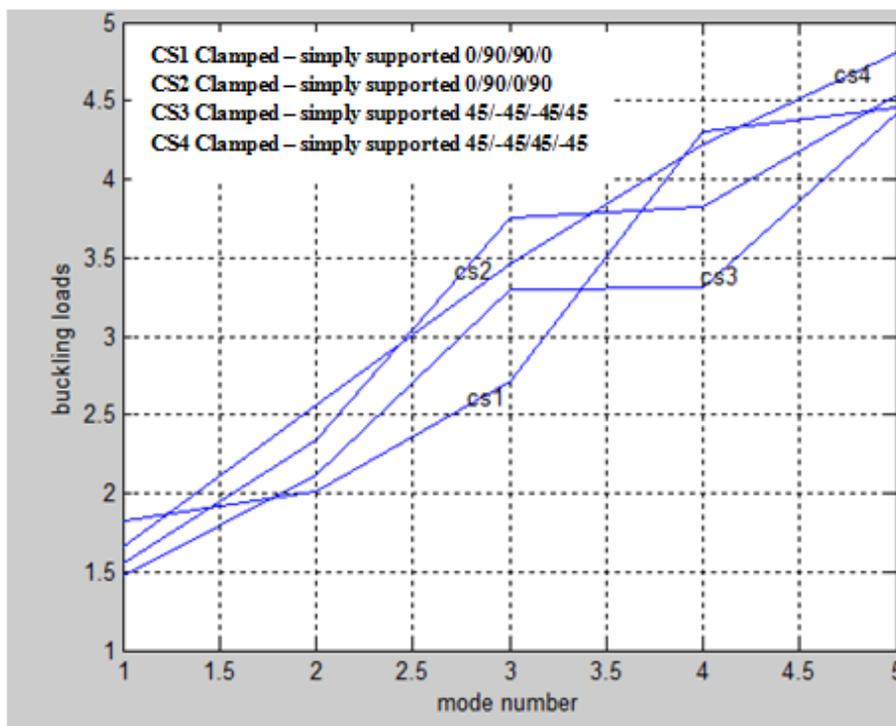
Fig. (5.3) Effect of lamination scheme for clamped – simply supported laminates

Tables (5.2) and (5.3) show the buckling load of quasi – isotropic rectangular composite plate with $a/h = 20$, $a/b = 1$ and different modulus ratios ($E_1/E_2 = 40$ and 5). The buckling load is highly influenced by its boundary conditions. The buckling load of the quasi – isotropic (0/+45/-45/90) rectangular composite plate with CC type boundary condition is 1.5 times higher than the buckling load of the composite plate with CS type boundary condition and more than 3 times of SS type boundary condition.

Table (5.2) The first three non – dimensional buckling loads of quasi – isotropic (0/+45/-45/90) laminated plates with a/h=20, and $E_1/E_2 = 40$, (material 2)

Mode Number	Boundary Conditions		
	SS	CC	CS
1	0.4905	1.6878	1.1683
2	1.4842	3.0187	1.7359
3	1.4850	3.0229	2.7673

Table (5.3) The first three non – dimensional buckling load of quasi – isotropic (0/+45/-45/90) laminated plates with a/h=20, and $E_1/E_2 = 5$, (material 2)

Mode Number	Boundary Conditions		
	SS	CC	CS
1	0.7338	2.2255	1.5717
2	2.0202	3.9506	2.3714
3	2.0214	3.9549	3.7214

5.2 Effect of Aspect Ratio

In this study, the buckling loads for symmetrically loaded laminated composite plates of layer orientation 0/90/90/0 have been determined for seven different aspect ratios ranging from 0.5 to 2.0 and two modulus ratios 40 and 5 as shown in tables (5.4) and (5.5) and Figs. (5.4) and (5.5). The first mode of buckling loads was considered. It is observed that the buckling load increases continuously with increasing aspect ratio but the rate of increase is not uniform. This may be due to the effect of bending – extensional twisting stiffness which increases the critical load. The buckling load is maximum for clamped – clamped (CC), clamped – simply supported (CS) while minimum for simply – simply supported (SS) boundary conditions. This means that as the plate becomes more restrained, its resistance to buckling increases. The reason is that the structural stiffness reduces due to its constrains.

Table (5.4) The first three non – dimensional buckling loads $\overline{P} = Pa^2/E_1h^3$ of symmetric cross – ply (0/ 90/ 90/ 0) laminated plates with $a/h = 20$, and $E_1/E_2 = 40$, (material 2)

Aspect Ratio (a/b)	Mode Number	SS	CC	CS
	1	0.4143	1.0742	0.9679
0.5	2	0.4236	1.0941	1.0484
	3	0.5408	1.3751	1.1257
	1	0.4300	1.2389	1.0444
0.75	2	0.4978	1.2691	1.2043
	3	0.6520	1.8354	1.2921
	1	0.4409	1.3795	1.0723
1.0	2	0.5580	1.5286	1.3105
	3	1.0763	2.1648	1.6946

Aspect Ratio (a/b)	Mode Number	SS	CC	CS
1.25	1	0.4224	1.5549	1.1349
	2	0.7795	1.7455	1.4327
	3	1.6164	3.0019	1.8042
1.5	1	0.4400	1.6402	1.2543
	2	1.0787	2.2999	1.3330
	3	1.6841	3.2702	2.4753
1.75	1	0.4885	1.8361	1.1494
	2	1.4473	3.0138	1.6342
	3	1.8520	3.6574	2.7310
2.0	1	0.5642	2.1358	1.1054
	2	1.7525	3.7696	2.0207
	3	1.8813	3.8703	2.8553

Table (5.5) The first three non – dimensional buckling loads $\bar{P} = Pa^2/E_1 h^3$ of symmetric cross – ply (0/ 90/ 90/ 0) laminated plates with $a/h = 20$, and $E_1/E_2 = 5$, (material 2)

Aspect Ratio (a/b)	Mode Number	Boundary Conditions		
		SS	CC	CS
0.5	1	0.6787	1.7786	1.6325
	2	0.6841	1.8364	1.7192
	3	0.8672	2.2141	1.9284
0.75	1	0.6698	2.0107	1.7117
	2	0.8831	2.1504	1.9339
	3	1.4912	2.7694	2.2689
1.0	1	0.6972	2.1994	1.8225
	2	1.2552	2.5842	2.0097
	3	2.4284	4.1609	2.7116

1.25	1	0.7726	2.3958	1.8397
	2	1.7753	3.5341	2.1821
	3	2.6844	5.1641	3.8539
1.5	1	0.8943	2.7961	1.7643
	2	2.4305	4.8034	2.7358
	3	2.6675	5.2420	4.6305
1.75	1	1.0588	3.3873	1.7741
	2	2.6919	5.4542	3.4532
	3	3.2171	6.3629	4.7373
2.0	1	1.2630	4.1517	1.8578
	2	2.7619	5.8342	4.3179
	3	4.1301	8.1942	4.6131
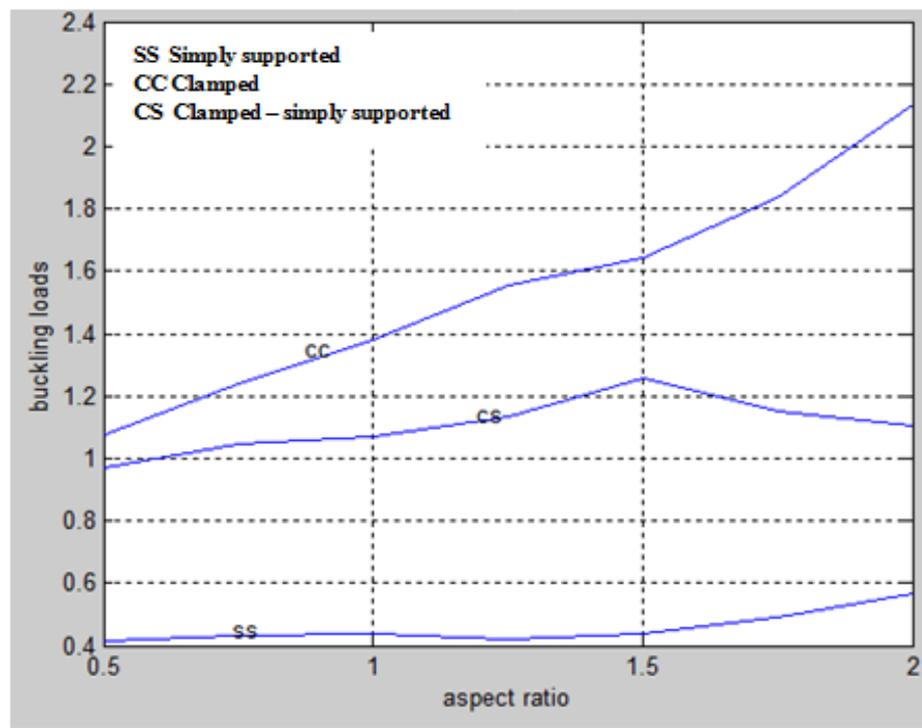
Fig. (5.4) Effect of aspect ratio for different boundary conditions,

$$E_1/E_2 = 40$$
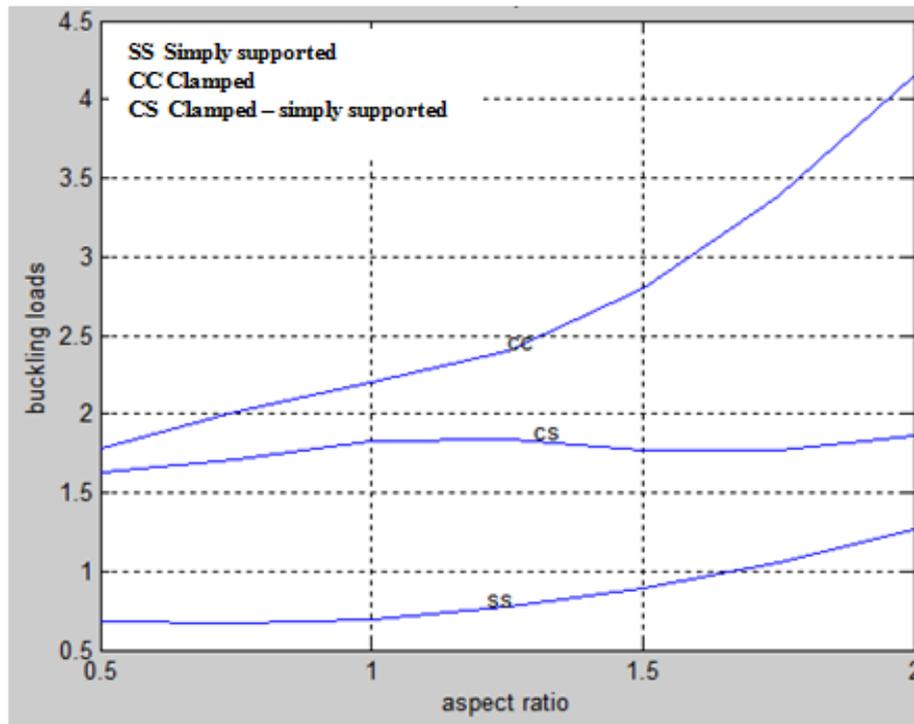
Fig. (5.5) Effect of aspect ratio for different boundary conditions,

$$E_1/E_2 = 5$$

5.3 Effect of Material Anisotropy

The buckling loads as a function of modulus ratio of symmetric cross – ply plates (0/ 90/ 90/ 0) are illustrated in table (5.6) and Fig. (5.6). As confirmed by other investigators, the buckling load decreases with increase in modulus ratio. Therefore, the coupling effect on buckling loads is more pronounced with the increasing degree of anisotropy. It is observed that the variation of buckling load becomes almost constant for higher values of elastic modulus ratio.

Table (5.6) The first three non – dimensional buckling loads $\bar{P} = Pa^2/E_1 h^3$ of symmetric cross – ply (0/ 90/ 90/ 0) square laminated plates for different modulus ratios with $a/h = 20$, (material 2)

E_1/E_2	Mode Number	Boundary Conditions		
		SS	CC	CS
5	1	0.6972	2.1994	1.8225
	2	1.2552	2.5842	2.0097
	3	2.4284	4.1609	2.7116
10	1	0.5505	1.8548	1.3928
	2	0.8557	1.8951	1.8292
	3	1.6532	2.9814	1.9089
15	1	0.5019	1.6663	1.2505
	2	0.7232	1.7248	1.6428
	3	1.3966	2.6049	1.7694
20	1	0.4775	1.5515	1.1791
	2	0.6569	1.6524	1.5096
	3	1.2683	2.4228	1.7394
25	1	0.4629	1.4828	1.1365
	2	0.6172	1.6055	1.4299
	3	1.1916	2.3171	1.7214
30	1	0.4531	1.4366	1.1078
	2	0.5907	1.5723	1.3766
	3	1.1402	2.2481	1.7094
35	1	0.4462	1.4044	1.0877
	2	0.5723	1.5479	1.3391
	3	1.1043	2.2006	1.7009

	1	0.4409	1.3795	1.0723
40	2	0.5580	1.5286	1.3105
	3	1.0763	2.1648	1.6946
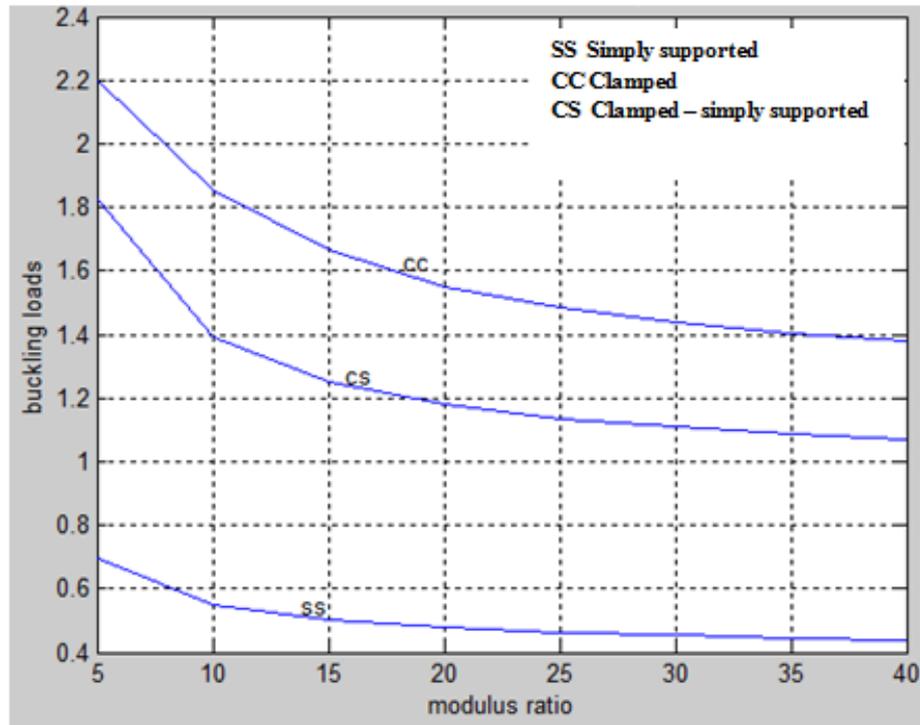
Fig. (5.6) Effect of material anisotropy

5.4 Effect of Fiber Orientations of Layers

The variation of the buckling load, $\bar{P}$ with fiber orientation (θ) of square laminated plate is shown in tables (5.7) and (5.8), and Figs. (5.7) and (5.8). Three boundary conditions SS, CC and CS are considered in this case. The buckling loads have been determined for two modulus ratios 40 and 5. The curves of simply – simply supported (SS) boundary conditions show maximum value of buckling load at $\theta = 45^o$. However, this trend is different for a plate under clamped – clamed (CC) boundary conditions which show minimum buckling load at $\theta = 45^o$. For clamped – simply supported, it is observed that the buckling load decreases continuously with θ, this may be due to the total and partial fixed rotation ($\phi \ and \ \psi$) in the two later cases.

Table (5.7) The first three non – dimensional buckling loads $\bar{P} =$ Pa^2/E_1h^3 of laminated plates for different fiber orientations (θ) with $a/h = 20$, and $E_1/E_2 = 40$, (material 2)

Orientation Angle (θ)	Mode Number	Boundary Conditions		
		SS	CC	CS
0	1	0.2604	0.6134	0.5561
	2	0.2825	0.6398	0.5729
	3	0.3960	0.8738	0.6745
15	1	0.2759	0.5957	0.5496
	2	0.3171	0.6123	0.5855
	3	0.4771	0.8638	0.7570
30	1	0.2823	0.5636	0.5114
	2	0.3125	0.5834	0.5352
	3	0.4861	0.9552	0.7902
45	1	0.2773	0.5207	0.4230
	2	0.3253	0.5842	0.4490
	3	0.5135	0.9793	0.7093
60	1	0.2834	0.5574	0.3073
	2	0.3116	0.5788	0.3895
	3	0.4783	0.9107	0.6362
75	1	0.2762	0.5859	0.3137
	2	0.3153	0.6043	0.3297
	3	0.4161	0.8252	0.4924
90	1	0.2602	0.6061	0.3069
	2	0.2811	0.6260	0.3438
	3	0.3908	0.8429	0.4801

Table (5.8) The first three non – dimensional buckling loads $\bar{P} = Pa^2/E_1h^3$ of laminated plates for different fiber orientations (θ) with $a/h = 20$, and $E_1/E_2 = 5$, (material 2)

Orientation Angle (θ)	Mode Number	Boundary Conditions		
		SS	CC	CS
0	1	0.6970	2.1130	1.6496
	2	1.0086	2.1396	2.0991
	3	1.7709	3.1397	2.1597
15	1	0.7108	2.0261	1.6665
	2	1.0908	2.1400	1.9833
	3	1.8704	3.2340	2.2141
30	1	0.7457	1.8142	1.6326
	2	1.2613	2.2494	1.7099
	3	2.0671	3.4809	2.4700
45	1	0.7665	1.7189	1.3114
	2	1.3477	2.3567	1.7689
	3	2.1557	3.5899	2.7032
60	1	0.7457	1.8147	1.0893
	2	1.2602	2.2457	1.7913
	3	2.0637	3.4650	2.6452
75	1	0.7110	2.0264	0.9824
	2	1.0898	2.1366	1.6562
	3	1.8659	3.2178	2.7338
90	1	0.6970	2.1101	0.9573
	2	1.0080	2.1389	1.5827
	3	1.7666	3.1269	2.7322
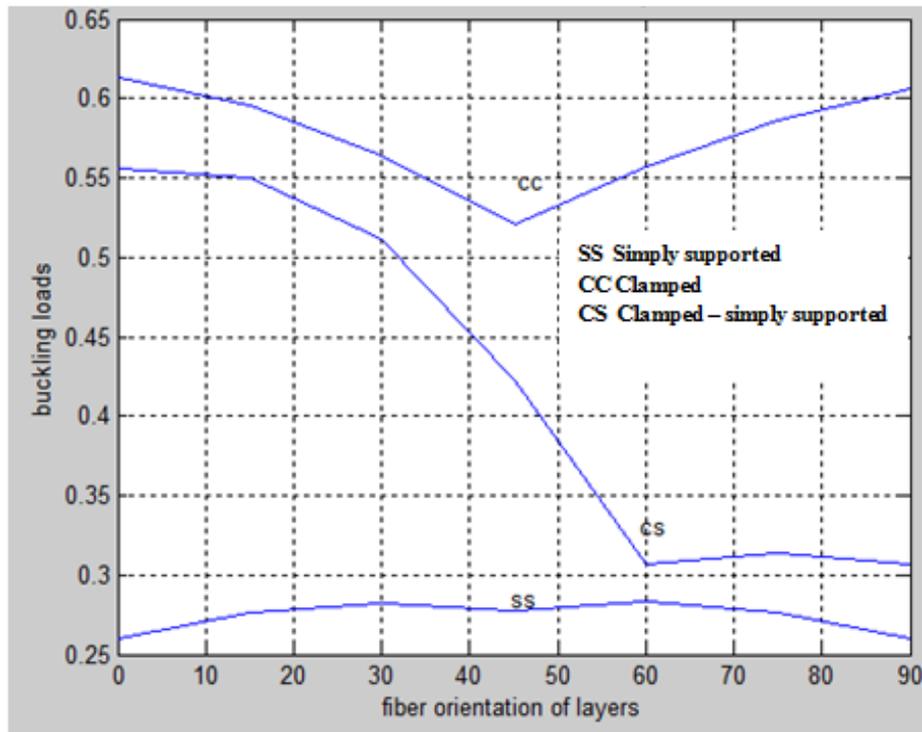
Fig. (5.7) Effect of fiber orientation of layers, $E_1/E_2 = 40$
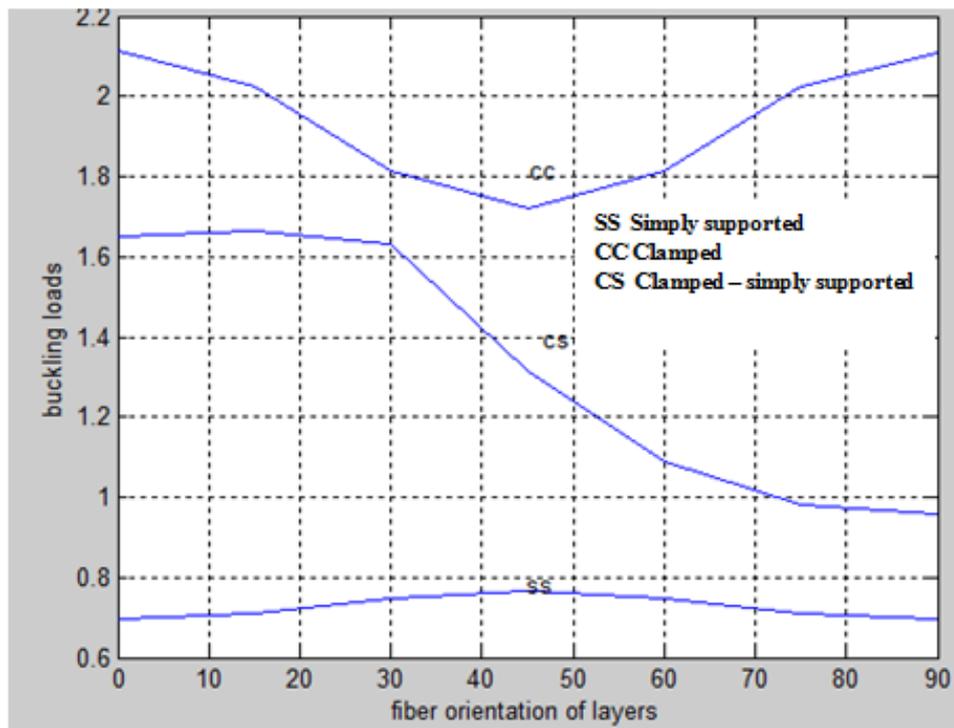
Fig. (5.8) Effect of fiber orientation of layers, $E_1/E_2 = 5$

5.5 Effect of Reversing Lamination Scheme

In order to study the stacking sequence of laminated plates, two lamination schemes of cross – ply (0/ 90) and (90/ 0) and two other lamination of angle ply (45/ -45) and (-45/ 45) were considered. The results of their buckling loads of parameter ($\bar{P} = Pa^2/E_1h^3$) are given in tables (5.9), (5.10), (5.11) and (5.12). Three boundary conditions SS, CC and CS are considered in this case. The buckling loads have been determined for two modulus ratios 40 and 5. It is observed that, the buckling loads are completely the same for the given first three modes.

Therefore, it can be concluded that the buckling load of laminated plates will remain the same even if the lamination order is reversed. The reason behind this is that the transformed elastic coefficients, $[C_{ij}]$, are equal for both lamination schemes.

Table (5.9) Non – dimensional buckling loads $\bar{P} = Pa^2/E_1h^3$ of (0/ 90) and (90/ 0) lamination schemes of square laminated plates with $a/h = 20$, and $E_1/E_2 = 40$, (material 2)

Lamination order	Mode Number	Boundary Conditions		
		SS	CC	CS
0/90	1	0.4410	1.6885	1.1512
	2	0.4494	3.0311	1.6881
	3	1.4502	3.0349	2.5982
90/0	1	0.4410	1.6885	1.1512
	2	0.4494	3.0311	1.6881
	3	1.4502	3.0349	2.5982

Table (5.10) Non – dimensional buckling loads $\bar{P} = Pa^2/E_1 h^3$ of (0/ 90) and (90/ 0) lamination schemes of square laminated plates with $a/h = 20$, and $E_1/E_2 = 5$, (material 2)

Lamination order	Mode Number	Boundary Conditions		
		SS	CC	CS
0/90	1	0.6970	2.2275	1.5593
	2	1.9943	3.9687	2.3388
	3	1.9954	3.9733	3.7581
90/0	1	0.6970	2.2274	1.5594
	2	1.9944	3.9688	2.3393
	3	1.9957	3.9733	3.7580

Table (5.11) Non – dimensional buckling loads $\bar{P} = Pa^2/E_1 h^3$ of (45/ -45) and (-45/ 45) lamination schemes of square laminated plates with $a/h = 20$, and $E_1/E_2 = 40$, (material 2)

Lamination order	Mode Number	Boundary Conditions		
		SS	CC	CS
45/-45	1	0.8375	1.6524	1.2806
	2	1.7263	2.7630	1.9965
	3	1.7285	2.7659	2.5358
-45/45	1	0.8372	1.6527	.2805
	2	.7262	2.7631	19963
	3	1.7283	2.7660	2.5355

Table (5.12) Non – dimensional buckling loads $\bar{P} = Pa^2/E_1 h^3$ of (45/ -45) and (-45/ 45) lamination schemes of square laminated plates with $a/h = 20$, and $E_1/E_2 = 5$, (material 2)

Lamination order	Mode Number	Boundary Conditions		
		SS	CC	CS
45/-45	1	0.9907	2.2010	1.6553
	2	2.1995	3.7613	2.5668
	3	2.2015	3.7652	2.4640
-45/45	1	0.9908	2.2010	1.6553
	2	2.1995	3.7613	2.5671
	3	2.2015	3.7652	3.4636

5.6 Effect of Boundary Conditions

The type of boundary support is an important factor in determining the buckling loads of a plate along with other factors such as aspect ratio, modulus ratio, … etc.

Three sets of boundary conditions, namely simply – simply supported (SS), clamped – clamped (CC), and clamped – simply supported (CS) were considered in this study.

The variations of buckling load, $\bar{P}$ with the mode number for thin $(a/h = 20)$ symmetrically loaded laminated cross – ply (0/90/90/0) plate with modulus ratio $(E_1/E_2 = 5)$ were computed and the results are given in table (5.13) and Fig. (5.9).

It is observed that, for all cases the buckling load increases with the mode number but at different rates depending on whether the plate is simply supported, clamped or clamped – simply supported. The buckling load is a minimum when the plate is simply supported and a maximum when the plate is clamped. Because of the rigidity of clamped boundary condition, the

buckling load is higher than in simply supported boundary condition. It is also observed that as the mode number increases, the plate needs additional support.

Table (5.13) The first five non – dimensional buckling loads $\overline{P} =$ Pa^2/E_1h^3 of symmetric (0/90/90/0) square laminated plates with $a/h =$ 20, and $E_1/E_2 = 5$

Mode Number	Boundary Conditions		
	SS	CC	CS
1	0.6972	2.1994	1.8225
2	1.2552	2.5842	2.0097
3	2.4284	4.1609	2.7116
4	2.6907	4.7431	4.3034
5	2.7346	5.0168	4.4536
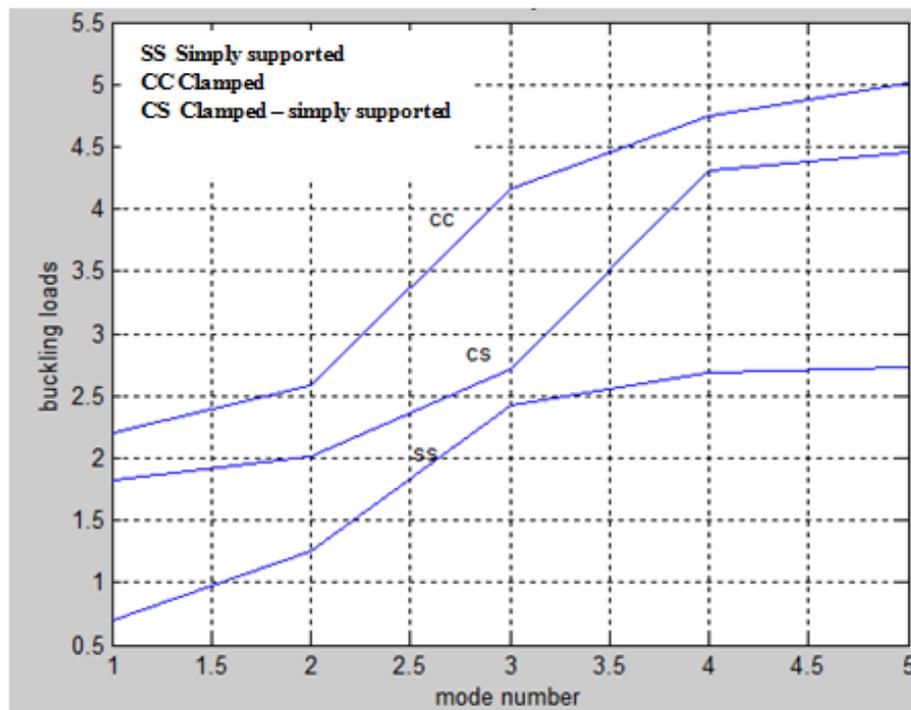
Fig. (5.9) Effect of boundary conditions

Chapter (6)

6. Concluding Remarks

A Fortran program based on finite elements (FE) has been developed for buckling analysis of thin rectangular laminated plates using classical laminated plate theory (CLPT). The problem of buckling loads of generally layered composite plates has been studied. The problem is analyzed and solved using the energy approach, which is formulated by a finite element model. In this method, quadrilateral elements are applied utilizing a four noded model. Each element has three degrees of freedom at each node. The degrees of freedom are: lateral displacement (w), and rotation (ϕ) and (ψ) about the x and y axes respectively. To verify the accuracy of the present technique, buckling loads are evaluated and validated with other works available in the literature. Further comparisons were carried out and compared with the results obtained by the ANSYS package and the experimental result. The good agreement with available data demonstrates the reliability of finite element method used.

The finite element model has been formulated to compute the buckling loads of laminated plates with rectangular cross – section and to study the effects of lamination scheme, aspect ratio, material anisotropy, fiber orientation of layers, reversed lamination scheme and boundary conditions on the non – dimensional critical buckling loads of laminated composite plates. Finally, a series of new results have been presented. These results show the following:

1. The symmetric laminate is stiffer than the anti – symmetric one. This phenomenon is caused by coupling between bending and stretching which lowers the buckling loads of symmetric laminate.

2. The buckling load is highly influenced by the end support. The buckling load of the quasi – isotropic (0/+45/-45/90) rectangular composite plate with

clamped – clamped type boundary condition is 1.5 times higher than the buckling load of the composite plate with clamped – simply supported (CS) type boundary condition, and more than 3 times of simply – simply supported (SS) type boundary condition.

3. The buckling load increases continuously with increasing aspect ratio, but the rate of increase is not uniform. This may be due to the effect of bending – extensional twisting stiffness which increases the critical load.

4. As the plate becomes more restrained, its resistance to buckling increases. The reason is that the structural stiffness reduces due to its constraints.

5. The buckling load decreases with increase in modulus ratio. It is also observed that the variation of buckling load becomes almost constant for higher values of elastic modulus. This may be attributed to the coupling effect which increases with the increasing degree of anisotropy.

6. The curves of simply – simply supported (SS) boundary conditions show maximum value of buckling load at $\theta = 45^o$. However, this trend is different for a plate under clamped – clamped (CC) boundary conditions which show minimum load at $\theta = 45^o$. For clamped – simply supported, it is observed that the buckling load decreases continuously with θ. This may be due to the total and partial fixed rotation ϕ and ψ in the two later cases.

7. The buckling load of laminated plates will remain the same even if the lamination order is reversed. The reason behind this is that the transformed elastic coefficients, $[C_{ij}]$, are equal for both lamination schemes.

8. The buckling load increases with the mode number but at different rates depending on whether the plate is simply supported (SS), clamped (CC) or clamped – simply supported. The buckling load is a minimum when the plate is simply supported and a maximum when the plate is clamped. Because of the rigidity of clamped boundary condition, the buckling load is higher than in

simply supported boundary condition. It is also observed that as the mode number increases, the plate needs additional support.

Bibliography

[1] David Roylance, ' an introduction to composite materials', Department of material science and engineering, Massachusetts Institute of Technology, Cambridge; (2000).

[2] Stephen W. Tsai, Thomas Hahn H., ' introduction to composite materials', Technomic publishing company; (1980).

[3] Turvey G.J., Marshall I.H., 'buckling and post buckling of composite plates', Great Britain, T.J. press Ltd, Padstow, Cornwall; (1995).

[4] Vernon B. John, ' introduction to engineering materials', second edition; (1972).

[5] Jan Stegmann and Erik Lund, ' notes on structural analysis of composite shell structures', Aalborg University, Denmark; (2001).

[6] Reddy J.N., ' A simple higher – order theory for laminated composite plates', Journal of applied mechanics, vol. 51, No. 745; (1984): pp. (13–19).

[7] Mindlin R.D., 'Influence of rotatory inertia and shear on flexural motions of isotropic elastic plates', Journal of applied mechanics; (1951): PP. (31–38).

[8] Phan N.D. and Reddy J.N., 'Analysis of laminated composite plate using higher – order shear deformation theory', International Journal of numerical methods in engineering, vol.21; (1985): pp. (2201–2219).

[9] Constance P. Yang, Charles H. Norris and Yehuda Stavsky,' Elastic wave propagation in heterogeneous plates', International Journal of solids and structures, vol.2 ;(1966): PP. (665 – 684).

[10] Whitney J.M. and Pagano N.J.,' Shear deformation in heterogeneous anisotropic plates', Journal of applied mechanics, vol.4; (1970): PP. (1031 – 1036).

[11] Seloodeh A.R., Karami G.,' Static, free vibration and buckling analysis of anisotropic thick laminated composite plates on distributed and point elastic supports using a 3–D layer-wise FEM', Engineering structures (26); (2004): pp. (211–220).

[12] Noor A.K.,'Free vibration of multi-layered composite plates', AIAA Journal; (1973), 11: PP. (1038–1039).

[13] Dorgruoglu A.N., Omurtag M.H.,' Stability analysis of composite plate foundation interaction by mixed FEM', Journal of engineering mechanics, ASCE; (2000), 126(9): PP. (928–936).

[14] Huang M.H., Thambiratnum D.P.,' Analysis of plate resting on elastic supports and elastic foundation by finite strip method', computers and structures; (2001), 79: PP. (2547–2557).

[15] Reissner E. and Stavsky Y.,' Bending and stretching of certain types of heterogeneous Aeolotropic plates', Journal of applied mechanics, vol.28; (1961): PP. (402– 408).

[16] Srinivas S. and Rao A.K.,' Bending, vibration and buckling of simply supported thick orthotropic rectangular plates and laminates', vol.6; (1970): PP. (1463 –1481).

[17] Turvey G.J. and Osman M.Y.,' Elastic large deflection analysis of isotropic rectangular Mindlin plates', International Journal of mechanical sciences, vol.22; (1990): PP. (1 –14).

[18] Turvey G.J. and Osman M.Y., 'Large deflection analysis of orthotropic Mindlin plates', proceedings of the 12th Energy resource technology conference and exhibition, Houston, Texas; (1989): PP. (163–172).

[19] Turvey G.J. and Osman M.Y.,' Large deflection effects in anti-symmetric cross-ply laminated strips and plates', I.H. Marshall, composite structures, vol.6, Paisley College, Scotland, Elsevier Science publishers; (1991): PP. (397– 413).

[20] Reddy J.N.,' a penalty plate – bending element for the analysis of laminated anisotropic composite plates', International Journal for numerical methods in engineering, vol.15; (1980): PP. (1187–1206).

[21] Reddy J.N. and Chao W.C.,' Non-linear bending of thick rectangular laminated composite plates', International Journal of non – linear mechanics, vol.16, No. 314;(1981): PP. (291–301).

[22] Chia C.Y. and Prabhakara M.K.,' Large deflection of unsymmetrical cross – ply and angle – ply plates', Journal of mechanical engineering science, vol.18, No.4;(1976): PP. (179–183).

[23] Putcha N.S. and Reddy J.N.,' A refined mixed shear flexible finite element for the non – linear analysis of laminated plates', computers and structures, vol.22, No.4 ;(1986): PP. (529–538).

[24] Gorji M.,' On large deflection of symmetric composite plates under static loading', Institution of mechanical engineering, vol. 200; (1986) : PP. (13–19).

[25] Zenkour A.M. and Fares M.E.,' Non – homogenous response of cross – ply laminated elastic plates using a higher order theory', Composite structures, vol. 44; (1999): PP. (297 – 305).

[26] Rushton K.R.,' large deflection of variable thickness plates', International Journal of mechanical sciences, vol.10; (1968): PP. (723 – 735).

[27] Cassell A.C. and Hobbs R.E.,' Numerical stability of dynamic relaxation analysis of nonlinear structures', International Journal for numerical methods in engineering, vol.35, No.4; (1966): PP. (1407 – 1410).

[28] Day A.S.,' An introduction to dynamic relaxation', the engineer, vol.219, No.5683; (1965): PP. (218 – 221).

[29] Larry J. Segelind, 'applied finite element analyses', Agricultural engineering department, Michigan state University, John Wiley and sons' publishers; (1984).

[30] Amir Wadi Al – khafaji and John R. Tooley,' Numerical methods in engineering practice', University of Evansville, CBS publishing Japan Ltd; (1986).

[31] Eastop T.D., McConkey A.,' Applied thermodynamics for engineering technologists', fifth edition, John wiley and sons, New York ;(1993).

[32] Aalami B.,' Large deflection of elastic plates under patch loading', Journal of the structural division, ASCE, vol.98, No.ST 11; (1972): PP. (2567 – 2586).

[33] Timoshenko S.P., Gere J.M.,' Theory of elastic stability', second edition, New York: McGraw Hill book company, Inc.; (1961).

[34] Chai G.B., Hoon K.H.,' buckling of generally laminated composite plates', Composite science technology; (1992), 45: PP. (125 – 133).

[35] Liew K.M., Wang C.M.,' Pb – 2 Rayleigh – Ritz method for general plate analyses', Engineering structures; (1993), 15: PP. (55 – 60).

[36] Chai G.B., Khong P.W.,' The effect of varying support conditions on the buckling of laminated composite plates', Composite structures; (1993), No.24(2): PP. (99 – 106).

[37] Narita Y. Fukushi K.,' Analysis program for generally laminated rectangular plates based on classical plate theory', Trans. J. SME, (A); (1996), PP. (2621 – 2627).

[38] Ashton J.E., Whitney J.M,' theory of laminated plates', Stamford: Technomic publishing co., Inc.; (1970).

[39] Jones R.M.,' Mechanics of composite materials', Washington: Scripta Book Co.; (1975).

[40] Turvey G.J., Marshall I.H.,' Buckling and post buckling of composite plates', London: Chapman and Hall; (1995).

[41] Singer J., Arbocz J., Weller T.,' Buckling experiments: Experimental methods in buckling of thin walled strictures', vol.1, New York: John Willey and sons ;(1998).

[42] Singer J., Arbocz J., Wetter T.,' buckling experiments: Experimental methods in buckling of thin walled structures: shells, Built up structures, composites and additional topics', vol.2., New York: John Willey and Sons; (2002).

[43] Reddy J.N., second edition,' Mechanics of laminated composite plates and shells', Boca Raton CRC press; (2004).

[44] Leissa A.W.,' Buckling of laminated composite plates and shells panels', Air force Wright – Patterson aeronautical laboratories, final report ;(1985).

[45] Herakovich C.T., Tarnopolskii Y.M.,' Hand book of composites structures and design', vol.2, Amsterdam: North Holland; (1989).

[46] Berthelot J.M.,' Composite materials mechanical behavior and structural analyses', New York: Springer; (1999).

[47] Whitney J.M.,' Structural analysis of laminated anisotropic plates', Lancaster, PA: Technomic Publishing; (1987).

[48] Reddy J.N.,' Mechanics of laminated composite plates: Theory and Analyses', Boca Raton: CRC press; (1997).

[49] Reddy J.N.,' Energy and variational methods in applied mechanics', New York: Wiley; (1984).

[50] Reddy J.N., Phan N.S.,' Stability and natural vibration of isotropic, orthotropic and laminated plates according to a higher order shear deformable theory', Journal of sound and vibration; (1985), 9 (82): PP. (157 – 170).

[51] Reddy J.N., Khdeir A.A.,' Buckling and vibration of laminated composite plates using various plate theories', AIAA; (1989), 27 (12): PP. (1808 – 1817).

[52] Leissa A.W., Kang J.,' Exact solutions for vibration and buckling of an SS – C – SS – C rectangular plate loaded by linearly varying in – plane stresses', International Journal of mechanical sciences;(2002),44: PP. (1925 – 1945).

[53] Iyengar N.G.,' Structural stability of columns and plates', Chichester, England: Ellis Horwood limited publishers; (1988).

[54] Bao G., Jiang W., Roberts J.C.,' Analytic and finite element solutions for bending and buckling of orthotropic rectangular plates', International Journal of solids and structures; (1997),34(14): PP. (1792 – 1821).

[55] Robinson J.R.,' The buckling and bending of orthotropic sandwich panels with all edges- simply supported', Aero Q; (1955), 6(2): PP. (125).

[56] Baharlou B., Leissa A.W.,' Vibration and buckling of generally laminated composite plates with arbitrary edge conditions', International Journal of mechanical sciences;(1987),29(8): PP. (545 – 555).

[57] Dawe D.J., Wang S.,' Spline finite strip analysis of the buckling and vibration of rectangular composite laminated plates', International Journal of mechanical sciences; (1995),37(6): PP. (645 – 667).

[58] Liu G.R., Chen X.L., Reddy J.N.,' Buckling of symmetrically laminated composite plates using the element free Galerkin method', International Journal of structural stability dynamics; (2002), 2(3): PP. (281 – 294).

[59] Bert C.W., Malik M.,' Differential quadrature: A powerful new technique for analysis of composite structures', composite structures; (1997), 39(3– 4): PP. (179 – 189).

[60] Huang Y.Q., Li Q.S.,' Bending and buckling analysis of anti – symmetric laminates using the least square differential quadrature method', Computer methods in applied mechanics and engineering, 193; (2004): PP. (3471 – 3492).

[61] Kim Y.S., Hoa S.V.,' biaxial buckling behavior of composite rectangular plates', composite structures; (1995), 31(4): PP. (247 – 252).

[62] Kantorovich L.V., Krylov I.V.,' approximate method of higher analyses', Groningen: P. Noordhoff Ltd; (1958).

[63] Shufrin I., Rabinovitch O., Eisenberger M.,' Buckling of symmetrically laminated rectangular plates with general boundary conditions – A semi analytical approach', composite structures; (2007).

[64] Kantorovich L.V., Krylov I.V.,' approximate method of higher analyses', New York: Interscience publishers Inc.; (1964).

[65] Kerr A.D.,' An extended Kantorovich method for solution of Eigen value problem', International Journal of solids and structures; (1969), 5 (7): PP. (559– 572).

[66] Eisenberger M., Alexandrov A.,' Buckling loads of variable thickness thin isotropic plates', thin – walled structures; (2003), 41(9): PP. (871 – 889).

[67] Shufrin I., Eisenberger M.,' stability and vibration of shear deformable plates – first order and higher order analyses', International Journal of solid structures; (2005), 42(3 – 4): PP. (1225 – 1251).

[68] Shufrin I., Eisenberger M.,' stability of variable thickness shear deformable plates – first order and higher order analyses', Thin – walled structures;(2005),43(2): PP. (189 – 207).

[69] Ungbhakorn V., singhatanadgid P.,' Buckling analysis of symmetrically laminated composite plates by extended Kantorovich method', Composite structures; (2006); 73(1): PP. (120 – 128).

[70] Yuan S., Jin Y.,' Computation of elastic buckling loads of rectangular thin plates using the extended Kantorovich method', computer structures; (1998), 66(6): PP. (861 – 867).

[71] March H.W., Smith C.B.,' Buckling loads of flat sandwich panels in compression', Forest products research laboratory report No.1525, Madison, WI; (1945).

[72] Chang C.C., Ebcioglu I.K., Haight C.H.,' General stability analysis of orthotropic sandwich panels for four different boundary conditions', Zeitschr Angew, Math. Mech.; (1962), 43: PP. (373 – 389).

[73] Jiang W., Bao G., Roberts J.C.,' Finite element modeling of stiffened and unstiffened orthotropic plates', Computer and structures Journal; (1977), 63(1): PP. (105 – 117).

[74] Smith C.S.,' Design of marine structures in composite materials', Amsterdam: Elsevier science publishers Ltd; (1990).

[75] Zienkiewicz O.C.,' The finite element method', England: McGraw Hill; (1977).

[76] Cook R.D.,' Concepts and applications of finite element analyses', New York: Wiley; (1981).

[77] Yang H.T.Y., Saigal S., Masud A., Kapania R.K.,' A survey of recent shell element', International Journal for numerical methods in engineering,47 (1–3); (2000): PP. (101 – 127).

[78] Mindlin R.D.,' Influence of rotatory inertia and shear on flexural motions of isotropic elastic plates', Trans. ASME Journal of applied mechanics; (1951), 18: PP. (31 – 38).

[79] Reddy J.N.,' A refined non – linear theory of laminated plates with transverse shear deformation', International Journal of solids and structures; (1984), 51: PP. (319 – 330).

[80] Soladatos K.P.,' a transverse shear deformation theory for homogeneous monoclinic plates', Acta Mech.; (1992), 94: PP. (195 – 220).

[81] Touratier M.,' An efficient standard plate theory', International Journal of engineering sciences; (1991), 29(8): PP. (901 – 916).

[82] Di sciuva M.,' An improved shear deformation theory for moderately thick multi – layered anisotropic shells and plates', Journal of applied mechanics; (1987), 54: PP. (589 – 596).

[83] Cho M., Parmerter R.R.,' Efficient higher – order composite plate theory for laminated composites', AIAA Journal; (1993), 31 – 7: PP. (1299 – 1306).

[84] Karama M., Afaqk S., Mistou S.,' Mechanical behavior of laminated composite beam by the new multi – layered laminated composite structures model with transverse shear stress continuity', International Journal of solids and structures;(2003),40: PP. (1525 – 1546).

[85] Jones R.M.,' Buckling and vibration of unsymmetrical laminated cross – ply rectangular plates', AIAA Journal; (1973), 12(11) : PP. (1626 – 1632).

[86] Narita Y., Leissa W.L.,' Buckling studies for simply supported symmetrically laminated rectangular plates', Composite structures; (1989), 12: PP. (113 – 132).

[87] Lo K.H., Christensen R.M., Wu E.M.,'A high – order theory of plate deformation', part 1: homogeneous plates, Journal of applied mechanics, Trans. ASME; (1977), 44(4): PP. (663 – 668).

[88] Lo K.H., Christensen R.M., Wu E.M.,' A high – order theory of plate deformation', part 2: Laminated plates, Journal of applied mechanics; (1977), 44 (4): PP. (669 – 676).

[89] Reddy J.N.,' an evaluation of equivalent single layer and layer wise theories of composite laminates', Composite structures; (1993), 25: PP. (21–35).

[90] Reddy J.N.,' a simple higher – order theory for laminated composite plates', Journal of applied mechanics; (1984), 51: PP. (745 – 752).

[91] Reddy J.N.,' A refined non – linear theory of plates with transverse shear deformation', International Journal of solids and structures; (1984), 20(9/10): PP. (881 – 896).

[92] Reddy J.N.,' A general non – linear third – order theory of plates with transverse shear deformation', Journal of Non – linear mechanics; (1990), 25(6): PP. (677 – 686).

[93] Librescu L.,' Electrostatics and kinetics of anisotropic and heterogeneous shell – type structures', Noordhoff: Leyden; (1975).

[94] Schmidt R.,' A refined non – linear theory of plates with transverse shell deformation', Journal of India mathematical society; (1977), 27(1): PP. (23 – 38).

[95] Krishna Murty A.V.,' higher order theory for vibration of thick plates', AIAA Journal; (1977), 15(12): PP. (1823 – 1824).

[96] Levinson M.,' an accurate simple theory of the statics and dynamics of elastic plates', Mechanical research community; (1980), 7(6): PP. (343 – 350).

[97] Seide P.,' an improved approximate theory for the bending theory of laminated plates', Mechanics today; (1980), 5: PP. (451 – 466).

[98] Murthy M.V.V.,' an improved transverse shear deformation theory for laminated anisotropic plates', NASA technical paper, 1903; (1981) : PP. (1 – 37).

[99] Bhimaraddi A., Stevens L.K.,' A higher – order theory for free vibration of orthotropic, homogeneous, and laminated rectangular plates', Journal of applied mechanics; (1984), 51: PP. (195 – 198).

[100] Mallikarjuna, Kant T.,' A critical review and some results of recently developed refined theories of fibers – reinforced laminated composites and sandwich plates', Composite structures; (1993),23: PP. (293 – 312).

[101] Kant T., Pandya,' A simple finite element formulation of higher – order theory for unsymmetrical laminated composite plates', Composite structures; (1988), 98: PP. (215 – 224).

[102] Reddy J.N.,' An evaluation of equivalent single layer and layer wise theories of composite laminates', Composite structures; (1993), 25: PP. (21 – 35).

[103] Reddy J.N.,' On refined theories of composite laminates', Mechanical; (1980), 25(4): PP. (230 – 238).

[104] Noor A.K., Burton W.S.,' Assessment of computational models for multi – layered anisotropic plates', Composite structures; (1990), 14: PP. (233 – 265).

[105] Bert C.W.,'A critical evaluation of new plate theories applied to laminated composites', Composite structures; (1984),2: PP. (329 – 347).

[106] Kant T., Kommineni J.R.,' geometrically non – linear analysis of symmetrically laminated composite and sandwich shells with higher – order theory and C^o finite elements', composite structures; (1984), 27: PP. (403 – 418).

[107] Reddy J.N., Robbins Jr D.H.,' Theories and computational models for composite laminates', Applied mechanics review, part 1; (1994), 47(6): PP. (147 – 165).

[108] Khdeir A.A.,' Free vibration and buckling of unsymmetrical cross – ply laminated plates using a refined theory', Journal of sound and vibration; (1989), 128: PP. (377 – 395).

[109] Hadian J., Nayfeh A.H,' Free vibration and buckling of shear deformable cross – ply laminated plates using state – space concept', Computer and structures;(1993),4: PP. (677 – 693).

[110] Fares M.E., Zenkour A.M.,' Buckling and vibration of non – homogeneous composite cross – ply laminated plates with various plate theories', Composite structures; (1999), 44: PP. (279 – 287).

[111] Matsunaga H.,' Vibration and stability of cross – ply laminated composite plates according to a global higher – order plate theory', composite structures; (2000), 48: PP. (231 – 244).

[112] Gilat R., Williams T.O., Aboudi J.,' Buckling of composite plates by global – local plate theory', Composite part B – Engineering; (2001), 32: PP. (229 – 236).

[113] Pagano N.J.,' Exact solution for rectangular bi – directional composite and sandwich plates', Journal of composite materials; (1970), 4: PP. (20 – 34).

[114] Noor A.K.,' Stability of multi – layered composite plates', Fiber science technology; (1975), 8: PP. (81 – 89).

[115] GU H., Chattopadhyay A.,' Three – dimensional elasticity solution for buckling of composite laminates', Composite structures; (2000), 50: PP. (29 – 35).

[116] Reddy J.N.,' An evaluation of equivalent single layer and layer wise theories of composite laminates', Composites structures; (1993), 25: PP. (21 – 35).

[117] Leissa A.W.,' Conditions for laminated plates to remain flat under in – plane loading', Composite structures; (1986), 6: PP. (261 – 270).

[118] Qatu M.S., Leissa A.W.,' Buckling of transverse deflections of unsymmetrically laminated plates subjected to in – plane loads', AIAA Journal; (1993),31(1): PP. (189 – 194).

[119] Bazant Z.P., Gedolin L.,' Stability of structures', New York: Oxford University press; (1991).

[120] Column research committee of Japan,' Handbook of structural stability', Tokyo: Corona; (1971).

[121] Gerard G., Becker H.,' Handbook of structural stability: part 1, Buckling of flat plates', Technical report, NASA TN 3781; (1957).

[122] Leissa A.W.,' Vibration of plates', (Nasa Sp-169), Washington (DC): Office of technology utilization; (1969).

[123] Cox H.L., Klein B.,' The buckling of isosceles triangular plates', Journal of Aeronautical science; (1955), 22: PP. (321 – 325).

[124] Ramaiah G.K.,' Flexural vibrations and elastic stability of annular plates under uniform in – plane tensile forces along inner edge', Journal of sound and vibration ;(1980), 72: PP. (11 – 23).

[125] Harik I.E.,' Stability of annular sector plates with clamped radial edges', Journal of applied mechanics, ASME; (1985).

[126] Su G.H., Xiang y.,' A non – discrete approach for the analysis of plates with multiple sub domains', Engineering structures, 24; (2002): PP. (563 – 575).

[127] Naruoka M., 'Bibliography on theory of plates', Gihodo, Tokyo; (1981).

[128] Winterstetter Th. A. and Schmidt H., 'Stability of circular cylindrical steel shells under combined loading', Thin – walled structures; (2002), 40: PP. (893 –909).

[129] Pircher M., and Bridge R., ' The influence of circumferential weld – induced imperfections on the buckling of silos and tanks', Journal of constructional steel research; (2001), 57 (5): PP. (569 – 580).

[130] Deml M., and Wunderlich W.,' Direct evaluation of the worst imperfection shape in shell buckling', Computer methods in applied mechanics and engineering; (1997), 149 [1 – 4]: PP. (201 – 222).

[131] Arbocz J., and Starnes J.H.,' Future   directions and challenges in shell stability analysis', Thin – walled structures; (2002), 40: PP. (729 – 754).

[132] Arbocz J.,' The effect of imperfect boundary conditions on the collapse behavior of anisotropic shells', International Journal of solids and structures; (2000), 37: PP. (6891 – 6915).

[133] Huhne C., Zimmermann R., Rolfes R., and Geier B., 'loading imperfections – experiments and Computations', Euromech Colloquium 424 ;(2001), the Netherlands.

[134] Geier B., Klein H., and Zimmermann R.,' Buckling tests with axially Compressed unstiffened cylindrical shells made from CFRP', proceedings, International Colloquium on buckling of shell structures on land, in the sea, and in the air, Elsevier applied sciences; (1991), London and New York: PP. (498– 507).

[135] Geier B., Klein H., and Zimmermann,' Experiments on buckling of CFRP Cylindrical shells under non – uniform axial load', proceedings of international conference on Composites engineering; (1994).

[136] Albus J., Gomez – Garcia J., and oery H.,' Control of assembly induced stresses and deformations due to the waviness of the interface flanges of the ESC – An upper stage', 52nd International astronautical   congress; (2001), Toulouse, France.

[137] Zimmermann R.,' Buckling research for imperfection tolerant fiber composite structures', proceeding of the conference on spacecraft structures, material and mechanical testing, Nordwijk, The Netherlands: (1996).

[138] Meyer – Piening H.R., Farshad M., Geier B., and Zimmermann, 'Buckling loads of CFRP Composite cylinders under combined axial and torsion loading – experiments and computations', Composite structures; (2001), 52: PP. (427 – 435).

[139] CMH – 17 (Composite Material Handbook – 17), Material science corporation; (2010).

[140] Guo S.J.,' Stress concentration and buckling behaviour of shear loaded composite panels with reinforced cutouts', Composite structures ;(2007): PP. (1– 9).

[141] Remmers J.J.C., and de Borst R.,' Delamination buckling of fiber – metal laminates', Composite science and technology; (2001): PP. (2207 – 2213).

[142] Vit obdrzalek, and Jan Vrbka,' Buckling and post buckling of a large delaminated plate subjected to shear loading', Engineering mechanics, vol. 16; (2009), No.4: PP. (297 – 312).

[143] Vit obdrzalek, and Jan Vrbka,' On buckling of a plate with multiple delaminations', Engineering mechanics, vol.17; (2010), No. 1: PP. (37 – 47).

[144] Keiichi Nemoto, Hirakazu Kasuya, Hisao Kikugawa, and Takashi Asaka,' post buckling behavior of composite laminated plates with initial imperfections under biaxial compression', Materials transactions, vol.50, No.2;(2009): PP. (299 – 304).

[145] Takao Y., Taya M., and Chou T.W.,' Stress field due to cylindrical inclusion with constant axial eigenstrain in an infinite elastic body', Journal of applied mechanics; (1981), 48(4): PP. (853 – 858).

[146] Lakshminarayana H.V., and Murthy M.V.V.,' On stresses around an arbitrarily oriented Crack in cylindrical shell', International Journal of fracture; (1976), 12(4): PP. (547 – 566).

[147] Twee J., and Rooke D.P,' The stress intensity factor for a crack at the edge of a loaded hole', International Journal of solids and structures; (1979), 15: PP. (899 – 906).

[148] Dyshel M.S.,' Fracture of plates with cracks under tension after loss of stability', Journal of applied mathematics and mechanics (PMM); (1981), 17(4): PP. (77 – 83).

[149] Erdogan F., Ratwani M., and Yuceoglu U.,' On the effect of orthotropy in cracked cylindrical plates', International Journal of fracture; (1974), 10 (4): PP. (369 – 374).

[150] Krenk S.,' Influence of transverse shear on an axial crack in a cylindrical shell', International Journal of fracture; (1978), 14(2): PP. (123 – 142).

[151] Delale F., and Erdogan F.,' Effect of transverse shear and material orthotropy in a cracked spherical cap', International Journal of solids and structures; (1979), 15: PP. (907 – 926).

[152] Lakshminarayana H.V., and Murthy M.V.V,' On a finite element model for the analysis of through cracks in laminated anisotropic cylindrical shells', Engineering fracture mechanics; (1981), 14(4): PP. (697 – 712).

[153] Theocaris P.S., and Milios J.,' Crack – arrest at a bimaterial interface', International Journal of solids and structures; (1981), 17: PP. (217 – 230).

[154] Rogers T.G.,' Crack extension and energy release rates in finitely deformed sheet reinforced with inextensible fibers', International Journal of solids and structures; (1982), 18: PP. (705 – 721).

[155] Kachanov L.M.,' Separation failure of composite materials', polymer mechanics; (1976), 6 (12): PP. (812 – 815).

[156] Williams J.G., and et al.,' Recent developments in the design, testing and impact damage – tolerance of stiffened composite plates', Nasa TM 80077; (1979), April.

[157] Wilkins D.J, and et al.,' characterizing delamination growth in graphite – epoxy', Damage in composite materials; (1982): PP. (168 – 183).

[158] Wang S.S.,' Edge delamination in angle – ply composite laminates', AIAA Journal; (1984), 22(2): PP. (256 – 264).

[159] Scott W. Beckwith,' Manufacturing defects in composite structures', Sample Journal, volume 48, No.5; September/October (2012).

[160] M. Vable,' Stability of columns', Mechanics of materials; (2014): chapter eleven: PP. (496 – 528).

[161] CPNI EBP,' Influence of delamination of laminated glass on its blast performance', July (2013).

[162] L. H. Yu, and C. Y. Wang, 'Buckling of rectangular plates on an elastic foundation using the levy solution', American Institute of Aeronautics and Astronautics, 46; (2008): PP. (3136 – 3167).

[163] M. Mohammadi, A. R. Saidi, and E. Jomehzadeh, 'Levy solution for buckling analysis of functionally graded rectangular plates', International Journal of Applied Composite Materials, 10; (2009): PP. (81 – 93).

[164] Moktar Bouazza, Djamel Ouinas, Abdelaziz Yazid and Abdelmadjid Hamouine, 'Buckling of thin plates under uniaxial and biaxial compression', Journal of Material Science and Engineering B2, 8; (2012): PP. (487 – 492).

[165] Mahmoud Yassin Osman and Osama Mohammed Elmardi Suleiman, 'Buckling analysis of thin laminated composite plates using finite element method', International Journal of Engineering Research and Advanced Technology (I JERAT), Volume 3, Issue 3; March (2017): PP. (1 – 18).

[166] J. N. Reddy, 'Mechanics of laminated composite plates and shells, theory and analysis', second edition, CRC press, Washington; (2004).

APPENDICES

Appendix (A)

Transformed Material Properties

The transformed material properties are:

$$C_{11} = C'_{11}cos^4\theta + C'_{22}sin^4\theta + 2(C'_{12} + 2C'_{66})sin^2\theta cos^2\theta$$

$$C_{12} = (C'_{11} + C'_{22} - 4C'_{66})sin^2\theta cos^2\theta + C^1_{12}(cos^4\theta + sin^4\theta)$$

$$C_{22} = C'_{11}sin^4\theta + C'_{22}cos^4\theta + 2(C'_{12} + 2C'_{66})sin^2\theta cos^2\theta$$

$$C_{16} = (C'_{11} - C'_{12} - 2C'_{66})cos^3\theta sin\theta - (C'_{22} - C'_{12} - 2C'_{66})sin^3\theta cos\theta$$

$$C_{26} = (C'_{11} - C'_{12} - 2C'_{66})cos\theta sin^3\theta - (C'_{22} - C'_{12} - 2C'_{66})sin\theta cos^3\theta$$

$$C_{66} = (C'_{11} + C'_{22} - 2C'_{12} - 2C'_{66})sin^2\theta cos^2\theta + C'_{66}(sin^4\theta + cos^4\theta)$$

$$\text{where} \quad C'_{11} = \frac{E_1}{1 - \nu_{12}\nu_{21}}, C'_{22} = \frac{E_2}{1 - \nu_{12}\nu_{21}}, C'_{12} = \frac{\nu_{12} E_2}{1 - \nu_{12}\nu_{21}}, C'_{16}$$

$$= G_{12}$$

Appendix (B)

Coefficients of Shape Functions

$$a_{i,j}/8$$

N_i \ i	$i,1$	$i,2$	$i,3$	$i,4$	$i,5$	$i,6$	$i,7$	$i,8$	$i,9$	$i,10$	$i,11$	$i,12$
N_1	2	-3	3	0	-4	0	1	0	0	-1	1	1
N_2	1	-1	1	-1	-1	0	1	-1	0	0	1	0
N_3	-1	1	-1	0	1	1	0	0	-1	1	0	-1
N_4	2	-3	-3	0	4	0	1	0	0	1	-1	-1
N_5	1	-1	-1	-1	1	0	1	1	0	0	-1	0
N_6	1	-1	-1	0	1	-1	0	0	1	1	0	-1
N_7	2	3	3	0	4	0	-1	0	0	-1	-1	-1
N_8	-1	-1	-1	1	-1	0	1	1	0	0	1	0
N_9	-1	-1	-1	0	-1	1	0	0	1	1	0	1
N_{10}	2	3	-3	0	-4	0	-1	0	0	1	1	1
N_{11}	-1	-1	1	1	1	0	1	-1	0	0	-1	0
N_{12}	1	1	-1	0	-1	-1	0	0	-1	1	0	1

Appendix (C)

Transformation of Integrals from Local to Global Co – ordinates

The integrals in equations (3.19) and (3.20) are given in non - dimensional form as follows (limits of integration $r, s = -1$ to 1):

$$\iint \frac{\partial^2 N_i}{\partial x^2} \frac{\partial^2 N_j}{\partial x^2} \, dx \, dy = \frac{4h_y}{h_x{}^3} \iint \frac{\partial^2 N_i}{\partial r^2} \frac{\partial^2 N_j}{\partial r^2} \, dr \, ds$$

$$= \frac{4n^3}{mR} \left(16a_{i,4} \, a_{j,4} + 48a_{i,7}a_{j,7} + 16a_{i,8}a_{j,8}/3 + 16a_{i,11}a_{j,11} \right)$$

$$\iint \frac{\partial^2 N_i}{\partial y^2} \frac{\partial^2 N_j}{\partial y^2} \, dx \, dy = \frac{4h_x}{h_y{}^3} \iint \frac{\partial^2 N_i}{\partial s^2} \frac{\partial^2 N_j}{\partial s^2} \, dr \, ds$$

$$= \frac{4m^3 R^3}{n} \left(16a_{i,6} \, a_{j,6} + 16a_{i,9}a_{j,9}/3 + 48a_{i,10}a_{j,10} + 16a_{i,12}a_{j,12} \right)$$

$$\iint \frac{\partial^2 N_i}{\partial x^2} \frac{\partial^2 N_j}{\partial y^2} \, dx \, dy = \frac{4}{h_y h_x} \iint \frac{\partial^2 N_i}{\partial r^2} \frac{\partial^2 N_j}{\partial s^2} \, dr \, ds$$

$$= 4mnR \left(16a_{i,4} \, a_{j,6} + 16a_{i,7}a_{j,9} + 16a_{i,8}a_{j,10} + 16a_{i,11}a_{j,12} \right)$$

$$\iint \frac{\partial^2 N_i}{\partial y^2} \frac{\partial^2 N_j}{\partial x^2} \, dx \, dy = \frac{4}{h_y h_x} \iint \frac{\partial^2 N_i}{\partial s^2} \frac{\partial^2 N_j}{\partial r^2} \, dr \, ds$$

$$= 4mnR \left(16a_{i,6} \, a_{j,4} + 16a_{i,9}a_{j,7} + 16a_{i,10}a_{j,8} + 16a_{i,12}a_{j,11} \right)$$

$$\iint \frac{\partial^2 N_i}{\partial x \partial y} \frac{\partial^2 N_j}{\partial x \partial y} \, dx \, dy = \frac{4}{h_y h_x} \iint \frac{\partial^2 N_i}{\partial r \partial s} \frac{\partial^2 N_j}{\partial r \partial s} \, dr \, ds =$$

$$4mnR \Big[4a_{i,5} \, a_{j,5} + 4(3a_{i,5}a_{j,11} + 4a_{i,8}a_{j,8})/3$$

$$+4(3a_{i,5} \, a_{j,12} + 4a_{i,9}a_{j,9})/3 + 4(a_{i,11} \, a_{j,12} + a_{i,12}a_{j,11}) + 36a_{i,12}a_{j,12}/5 \Big]$$

$$\iint \frac{\partial N_i}{\partial x} \frac{\partial N_j}{\partial x} \, dx \, dy = \frac{h_y}{h_x} \iint \frac{\partial N_i}{\partial r} \frac{\partial N_j}{\partial r} \, dr \, ds$$

$$= \frac{n}{mR} \Big[4a_{i,2} \, a_{j,2} + 4(3a_{i,2}a_{j,7} + 4a_{i,4}a_{j,4} + 3a_{i,7}a_{j,2})/3$$

$$+4(a_{i,2}a_{j,9} + a_{i,5}a_{j,5} + a_{i,9}a_{j,2})/3 + 4(3a_{i,5} \, a_{j,11} + 3a_{i,7}a_{j,9} + 4a_{i,8}a_{j,8}$$

$$+3a_{i,9}a_{j,7} + 3a_{i,11}a_{j,5})/9 + 4(a_{i,5}a_{j,12} + a_{i,9}a_{j,9} + a_{i,12}a_{j,5})/5$$
$$+36a_{i,7}a_{j,7}/5 + 12a_{i,11}a_{j,11}/5 + 4(a_{i,11}a_{j,12} + a_{i,12}a_{j,11})/5$$

$$+ 4a_{i,12}a_{j,12}/7\big]$$

$$\iint \frac{\partial N_i}{\partial y}\frac{\partial N_j}{\partial y}\,dx\,dy = \frac{h_x}{h_y}\iint \frac{\partial N_i}{\partial s}\frac{\partial N_j}{\partial s}\,dr\,ds$$

$$= \frac{mR}{n}\big[4a_{i,3}\,a_{j,3} + 4(a_{i,3}a_{j,8} + a_{i,5}a_{j,5} + a_{i,8}a_{j,3})/3$$
$$+4(3a_{i,3}a_{j,10} + 4a_{i,6}a_{j,6} + 3a_{i,10}a_{j,3})/3 + 4(3a_{i,5}\,a_{j,11} + a_{i,8}a_{j,8}$$
$$+ a_{i,11}a_{j,5})/5$$
$$+4(3a_{i,5}a_{j,12} + 3a_{i,8}a_{j,10} + 4a_{i,9}a_{j,9} + 3a_{i,10}a_{j,8} + 3a_{i,12}a_{j,5})/9$$
$$+36a_{i,10}a_{j,10}/5 + 4(a_{i,11}a_{j,12} + a_{i,12}a_{j,11})/5 + 12a_{i,12}a_{j,12}/5$$

$$+ 4a_{i,11}a_{j,11}/7\big]$$

$$\iint \frac{\partial N_i}{\partial x}\frac{\partial N_j}{\partial y}\,dx\,dy = \iint \frac{\partial N_i}{\partial r}\frac{\partial N_j}{\partial s}\,dr\,ds$$

$$= 4a_{i,2}a_{j,3} + 4(a_{i,2}a_{j,8} + 2a_{i,4}a_{j,5} + 3a_{i,7}\,a_{j,8})/3 + 4(3\,a_{i,2}a_{j,10}$$
$$+ 2a_{i,5}a_{j,6}$$
$$+a_{i,9}a_{j,3})/3 + 4(2a_{i,4}a_{j,11} + 3a_{i,7}a_{j,8})/5 + 4(6a_{i,4}a_{j,12} + 9a_{i,7}a_{j,10}$$
$$+4a_{i,8}a_{j,9} + a_{i,9}a_{j,8} + 6a_{i,11}a_{j,6})/9 + 4(3a_{i,9}a_{j,10} + 2a_{i,12}a_{j,6})/5$$

$$\iint \frac{\partial N_i}{\partial y}\frac{\partial N_j}{\partial x}\,dx\,dy = \iint \frac{\partial N_i}{\partial s}\frac{\partial N_j}{\partial r}\,dr\,ds$$

$$= 4a_{i,3}a_{j,2} + 4(3a_{i,3}a_{j,7} + 2a_{i,5}a_{j,4} + a_{i,8}\,a_{j,2})/3 + 4(\,a_{i,3}a_{j,9} + 2a_{i,6}a_{j,5}$$
$$+3a_{i,10}a_{j,2})/3 + 4(6a_{i,6}a_{j,11} + a_{i,8}a_{j,9} + 4a_{i,9}a_{j,8} + 9a_{i,10}a_{j,7}$$
$$+ 6a_{i,2}a_{j,4})/9$$
$$+4(2a_{i,6}a_{j,12} + 3a_{i,10}a_{j,9})/5 + 4(3a_{i,8}a_{j,7} + 2a_{i,11}a_{j,4})/5$$

$$\iint \frac{\partial^2 N_i}{\partial x^2}\frac{\partial^2 N_j}{\partial x\partial y}\,dx\,dy = \frac{4}{h_x{}^2}\iint \frac{\partial^2 N_i}{\partial r^2}\frac{\partial^2 N_j}{\partial r\partial s}\,dr\,ds$$
$$= 4n^2\big[8a_{i,4}\big(a_{j,5} + a_{j,11} + a_{j,12}\big) + 16(a_{i,7}a_{j,8} + a_{i,8}a_{j,9}/3)\big]$$

$$\iint \frac{\partial^2 N_i}{\partial x\partial y}\frac{\partial^2 N_j}{\partial x^2}\,dx\,dy = \frac{4}{h_x{}^2}\iint \frac{\partial^2 N_i}{\partial r\partial s}\frac{\partial^2 N_j}{\partial r^2}\,dr\,ds$$
$$= 4n^2\big[8a_{j,4}\big(a_{i,5} + a_{i,11} + a_{i,12}\big) + 16a_{i,8}a_{j,7} + 16a_{i,9}a_{j,8}/3\big]$$

$$\iint \frac{\partial^2 N_i}{\partial y^2} \frac{\partial^2 N_j}{\partial x \partial y} \, dx \, dy = \frac{4}{h_y{}^2} \iint \frac{\partial^2 N_i}{\partial s^2} \frac{\partial^2 N_j}{\partial r \partial s} \, dr \, ds$$

$$= 4m^2 R^2 \left[8a_{i,6}\left(a_{j,5} + a_{j,11} + a_{j,12}\right) + 16a_{i,10}a_{j,9} + 16a_{i,9}a_{j,8}/3 \right]$$

$$\iint \frac{\partial^2 N_i}{\partial x \partial y} \frac{\partial^2 N_j}{\partial y^2} \, dx \, dy = \frac{4}{h_y{}^2} \iint \frac{\partial^2 N_i}{\partial r \partial s} \frac{\partial^2 N_j}{\partial s^2} \, dr \, ds$$

$$= 4m^2 R^2 \left[8a_{j,6}\left(a_{i,5} + a_{i,11} + a_{i,12}\right) + 16a_{i,9}a_{j,10} + 16a_{i,8}a_{j,9}/3 \right]$$

In the above expressions $h_x = \frac{a}{n}$, $h_y = \frac{b}{m}$ where a and b are the dimensions of the plate in the x – and y – directions respectively. n and m are the number of elements in the x – and y – directions respectively. Note that $dx = \frac{h_x}{2} dr$ and $dy = \frac{h_y}{2} ds$ where r and s are the normalized coordinates, and $R = a/b$.

Appendix (D)

The Fortran Program

C*** This program computes the modes and buckling load.


```fortran
      PARAMETER (M1=500, M2=100, M3=12, M4=121, M5=7, M6=11,
     +M7=4, M8=3)
      REAL LAM,IM
      INTEGER FLAG,DOF,E,EE
      DIMENSION ESM(M1,M1),EMM(M1,M1),EMMI(M1,M1),REF(M1,M1),
     +INDX(M1),E(M2,M3),VAL(M1),RE(M1),IM(M1),W(M5,M6,M6),
     +PHI(M5,M6,M6),THI(M5,M6,M6),VECT(M1,M5),NODE(M4,M7),EE(M4
     ,M8)

      OPEN(UNIT=5,FILE='BUCK.DAT',STATUS='OLD')
      OPEN(UNIT=6,FILE='BUCK.OUT',STATUS='UNKNOWN')
```

C*** Read number of buckling loads required
```fortran
      READ(5,*)NLOAD
```

C*** Relate local nodes to global nodes
```fortran
      CALL NODEN(NODE,NEI,NEJ,FLAG,M4,M7)
      IF(FLAG.EQ.0) GO TO 444
```

C*** Read boundary conditions

    CALL COMP(NEI,NEJ,E,DOF,NODE,EE,M2,M3,M4,M7,M8)

    IF(FLAG.EQ.0) GO TO 444

C*** Compute stiffnesses

    CALL STFN(D11,D12,D22,D16,D26,D66,LAM,M4,FLAG)

    IF(FLAG.EQ.0) GO TO 444

C*** Compute element matrices and global matrices

    CALL GLOBAL(ESM,EMM,D11,D12,D22,D16,D26,D66,NEI,NEJ,
LAM,ASR,

    +E,DOF,M1,M2,M3,FLAG)

    IF(FLAG.EQ.0) GO TO 444

C*** Factorize matrix into upper and lower matrices.

    CALL LUCOM(EMM,DOF,INDX,FLAG,M1)

    IF(FLAG.EQ.0) GO TO 444

C*** Inversion of matrix

    CALL LUSOL(EMM,DOF,INDX,EMMI,M1)

C*** Multiplication of matrices

    CALL MULT(EMMI,ESM,EMM,DOF,M1)

C*** Save plate matrix as it will be destroyed later.

    DO 12 I=1,DOF

```
      DO 12 J=1,DOF

    REF(I,J)=EMM(I,J)

  12 CONTINUE


C***  Balancing of the plate matrix

    CALL BAL(EMM,DOF,M1)


C***  Reduction of plate matrix to Heisenberg form

    CALL HES(EMM,DOF,M1)


C***  Find eigenvalues of an upper Heisenberg matrix

    CALL HQR(EMM,RE,IM,DOF,FLAG,M1)

    IF(FLAG.EQ.0) GO TO 444


C***  Sort eigenvalues in ascending order

    CALL ESORT(RE,VAL,DOF,M1)

C    CALL NATF1(RE,VAL,DOF,M1)


C***  Compute eigenvectors

    CALL SIL(REF,VECT,VAL,DOF,FLAG,M1,M5)

    IF(FLAG.EQ.0) GO TO 444


C***  Arrange eigenvalues and eigenvectors for printing

    CALL PNATF(VECT,DOF,NEI,NEJ,EE,W,PHI,THI,M1,M4,M5,M6,

    +M7,M8,NODE)
```

```fortran
C***  Print result

      CALL PRINT(VAL,DOF,NLOAD,W,PHI,THI,NEI,NEJ,M1,M5,M6)
  444 STOP
      END

C*********************************************

C    This subroutine does node numbering.

      SUBROUTINE NODEN(NODE,NEI,NEJ,FLAG,M4,M7)

      PARAMETER (M11=100)

      INTEGER FLAG

      DIMENSION NODE(M4,M7),NEL(M11)


C    Read number of elements

      READ(5,*)NEI,NEJ


      NE=NEI*NEJ

      FLAG=1

      IF(NE.GT.100)THEN

      WRITE(*,*)'Number of elements must not exceed 100'

      FLAG=0

      RETURN

      ENDIF


      K=1

      DO 70 N=1,NEI
```

```
      IF(N.GT.1)K=K-(NEJ+1)

      IMIN=1+NEJ*(N-1)

      IMAX=IMIN+NEJ-1

      DO 10 I=IMIN,IMAX

      DO 20 J=2,4,2

      NODE(I,J)=K

      K=K+1

20 CONTINUE

      NNEJ=N*NEJ

      IF(I.LT.NNEJ) K=K-1

10 CONTINUE


      DO 50 I=IMIN,IMAX

      DO 60 J=1,3,2

      NODE(I,J)=K

      K=K+1

60 CONTINUE

      NNEJ=N*NEJ

      IF(I.LT.NNEJ) K=K-1

50 CONTINUE

70 CONTINUE

      DO 80 I=1,NE

      NEL(I)=I

80 CONTINUE

      RETURN
```

```
      END
c*****************************
C***  This subroutine reads boundary conditions.


      SUBROUTINE COMP(NEI,NEJ,E,DOF,NODE,EE,M2,M3,M4,M7,M8)
      INTEGER WI1,PI1,TI1,WI2,PI2,TI2,WJ1,PJ1,TJ1,WJ2,PJ2,TJ2,E,
     +EE,DOF,COUNT


      DIMENSION E(M2,M3),EE(M4,M8),NODE(M4,M7)
C***  Read boundary conditions
      READ(5,*)WI1,PI1,TI1
      READ(5,*)WI2,PI2,TI2
      READ(5,*)WJ1,PJ1,TJ1
      READ(5,*)WJ2,PJ2,TJ2


      NE=NEI*NEJ


      DO 6 I=1,NE
      DO 6 J=1,4
      L=NODE(I,J)
      DO 6 K=1,3
      EE(L,K)=1000000
    6 CONTINUE


      IM=NE+1-NEJ
```

```fortran
      DO 10 I=1,IM,NEI
      DO 10 J=1,2
      L=NODE(I,J)
      IF(WI1.EQ.0) EE(L,1)=0
      IF(PI1.EQ.0) EE(L,2)=0
      IF(TI1.EQ.0) EE(L,3)=0
   10 CONTINUE

      DO 20 I=NEJ,NE,NEI
      DO 20 J=3,4
      L=NODE(I,J)
      IF(WI2.EQ.0) EE(L,1)=0
      IF(PI2.EQ.0) EE(L,2)=0
      IF(TI2.EQ.0) EE(L,3)=0
   20 CONTINUE

      DO 30 I=1,NEJ
      DO 30 J=2,4,2
      L=NODE(I,J)
      IF(WJ1.EQ.0) EE(L,1)=0
      IF(PJ1.EQ.0) EE(L,2)=0
      IF(TJ1.EQ.0) EE(L,3)=0
   30 CONTINUE

      DO 40 I=IM,NE
```

```
    DO 40 J=1,3,2

    L=NODE(I,J)

    IF(WJ2.EQ.0) EE(L,1)=0

    IF(PJ2.EQ.0) EE(L,2)=0

    IF(TJ2.EQ.0) EE(L,3)=0

 40 CONTINUE


    COUNT=0

    DO 220 I=1,NE

    DO 220 J=1,4

    L=NODE(I,J)

    DO 220 K=1,3

    IF(EE(L,K).EQ.1000000) THEN

    COUNT=COUNT+1

    EE(L,K)=COUNT

    ENDIF

220 CONTINUE


    DO 260 I=1,NE

    DO 260 J=1,4

    L=NODE(I,J)

    DO 260 K=1,3

    M=K+3*(J-1)

    E(I,M)=EE(L,K)

260 CONTINUE
```

```fortran
      DOF=COUNT

      WRITE(*,*)'Degrees of freedom =',DOF

      RETURN

      END
```

C***

C*** This subroutine computes the stiffness parameters

```fortran
      SUBROUTINE STFN(D11,D12,D22,D16,D26,D66,LAM,M4,FLAG)

      REAL NUXY,NUYX,LAM

      INTEGER FLAG

      PARAMETER(M44=20)

      DIMENSION ZK(M44),THETA(M44)
```

C   Read material properties
```fortran
      READ(5,*)EY,GXY,GYZ,GXZ,NUXY,LAM
```
C   Read number of layers and orientations
```fortran
      READ(5,*)NL,(THETA(I),I=1,NL)


      FLAG=1

      IF(NL.GT.20)THEN

      WRITE(*,*)'Number of layers must not exceed 20'

      FLAG=0

      RETURN
```

```fortran
      ENDIF

c     IF(LAM.GT.50)THEN

c           WRITE(*,*)'LENGTH-TO-THICKNESS RATIO MUST NOT
EXCEED 50'

c     FLAG=0

c     RETURN

c     ENDIF


      SCF=5.0/6.0

      PI=22.0/7.0

      NUYX=NUXY*EY

      C11=1.0/(1.0-NUXY*NUYX)

      C12=NUXY*EY/(1.0-NUXY*NUYX)

      C22=EY/(1.0-NUXY*NUYX)

      C66=GXY

      C44=GYZ

      C55=GXZ


      D11=0.0

      D12=0.0

      D22=0.0

      D16=0.0

      D26=0.0

      D66=0.0
```

```
      TH=1.0/NL
      DO 1 I=1,NL+1
      ZK(I)=-0.5+(I-1)*TH
    1 CONTINUE


      DO 134 I=1,NL
      CO=COS(THETA(I)*PI/180.0)
      SI=SIN(THETA(I)*PI/180.0)


      CB11=C11*CO**4+C22*SI**4+2.0*(C12+2.0*C66)*SI**2*CO**2
      CB12=(C11+C22-4.0*C66)*SI**2*CO**2+C12*(CO**4+SI**4)
      CB22=C11*SI**4+C22*CO**4+2.0*(C12+2.0*C66)*SI**2*CO**2
      CB16=(C11-C12-2.0*C66)*CO**3*SI-(C22-C12-2.0*C66)*SI**3*CO
      CB26=(C11-C12-2.0*C66)*CO*SI**3-(C22-C12-2.0*C66)*SI*CO**3
      CB66=(C11+C22-2.0*C12 2.0*C66)*SI**2*CO**2+C66*(SI**4+
     CO**4)
      CB44=C44*CO**2+C55*SI**2
      CB45=(C44+C55)*SI*CO
      CB55=C44*SI**2+C55*CO**2


      SZ1=ZK(I+1)-ZK(I)
      SZ2=(ZK(I+1)**2-ZK(I)**2)/2.0
      SZ3=(ZK(I+1)**3-ZK(I)**3)/3.0


      D11=CB11*SZ3+D11
      D12=CB12*SZ3+D12
```

```fortran
      D22=CB22*SZ3+D22

      D16=CB16*SZ3+D16

      D26=CB26*SZ3+D26

      D66=CB66*SZ3+D66

  134 CONTINUE

      write(*,*)D11,D22

      RETURN

      END
```

C***


```fortran
      SUBROUTINE GLOBAL(ESM,EMM,D11,D12,D22,D16,D26,D66,
     NEI,NEJ,
     +LAM,ASR,ED,DOF,M1,M2,M3,FLAG)


      PARAMETER (M11=12, M33=12)

      REAL LAM

      INTEGER ED,T,DOF,FLAG

      DIMENSION ESM(M1,M1),EMM(M1,M1),ED(M2,M3),A(M11),
     B(M11),C(M11),

     +D(M11),E(M11),F(M11),G(M11),H(M11),P(M11),Q(M11),R(M11),S(M11
     ),
     +ST(M33,M33),ZT(M33,M33)


C    Read aspect ratio and edge loads
      READ(5,*)ASR,PX,PY,PXY
```

```fortran
      FLAG=1
      IF(ASR.GT.5)THEN
      WRITE(*,*)'ASPECT RATIO MUST NOT EXCEED 5'
      FLAG=0
      RETURN
      ENDIF

      NE=NEI*NEJ
      DO 5 L=1,DOF
      DO 5 T=1,DOF
      ESM(L,T)=0.0
      EMM(L,T)=0.0
5     CONTINUE

      A(1)=1.0/4.0
      A(2)=1.0/8.0
      A(3)=-1.0/8.0
      A(4)=1.0/4.0
      A(5)=1.0/8.0
      A(6)=1.0/8.0
      A(7)=1.0/4.0
      A(8)=-1.0/8.0
      A(9)=-1.0/8.0
      A(10)=1.0/4.0
      A(11)=-1.0/8.0
```

A(12)=1.0/8.0

B(1)=-3.0/8.0

B(2)=-1.0/8.0

B(3)=1.0/8.0

B(4)=-3.0/8.0

B(5)=-1.0/8.0

B(6)=-1.0/8.0

B(7)=3.0/8.0

B(8)=-1.0/8.0

B(9)=-1.0/8.0

B(10)=3.0/8.0

B(11)=-1.0/8.0

B(12)=1.0/8.0

C(1)=3.0/8.0

C(2)=1.0/8.0

C(3)=-1.0/8.0

C(4)=-3.0/8.0

C(5)=-1.0/8.0

C(6)=-1.0/8.0

C(7)=3.0/8.0

C(8)=-1.0/8.0

C(9)=-1.0/8.0

C(10)=-3.0/8.0

C(11)=1.0/8.0

C(12)=-1.0/8.0

D(1)=0

D(2)=-1.0/8.0

D(3)=0

D(4)=0

D(5)=-1.0/8.0

D(6)=0

D(7)=0

D(8)=1.0/8.0

D(9)=0

D(10)=0

D(11)=1.0/8.0

D(12)=0

E(1)=-1.0/2.0

E(2)=-1.0/8.0

E(3)=1.0/8.0

E(4)=1.0/2.0

E(5)=1.0/8.0

E(6)=1.0/8.0

E(7)=1.0/2.0

E(8)=-1.0/8.0

E(9)=-1.0/8.0

E(10)=-1.0/2.0

E(11)=1.0/8.0

E(12)=-1.0/8.0

F(1)=0

F(2)=0

F(3)=1.0/8.0

F(4)=0

F(5)=0

F(6)=-1.0/8.0

F(7)=0

F(8)=0

F(9)=1.0/8.0

F(10)=0

F(11)=0

F(12)=-1.0/8.0

G(1)=1.0/8.0

G(2)=1.0/8.0

G(3)=0

G(4)=1.0/8.0

G(5)=1.0/8.0

G(6)=0

G(7)=-1.0/8.0

G(8)=1.0/8.0

G(9)=0

G(10)=-1.0/8.0

G(11)=1.0/8.0

G(12)=0

H(1)=0

H(2)=-1.0/8.0

H(3)=0

H(4)=0

H(5)=1.0/8.0

H(6)=0

H(7)=0

H(8)=1.0/8.0

H(9)=0

H(10)=0

H(11)=-1.0/8.0

H(12)=0

P(1)=0

P(2)=0

P(3)=-1.0/8.0

P(4)=0

P(5)=0

P(6)=1.0/8.0

P(7)=0

P(8)=0

P(9)=1.0/8.0

P(10)=0

P(11)=0

P(12)=-1.0/8.0

Q(1)=-1.0/8.0

Q(2)=0

Q(3)=1.0/8.0

Q(4)=1.0/8.0

Q(5)=0

Q(6)=1.0/8.0

Q(7)=-1.0/8.0

Q(8)=0

Q(9)=1.0/8.0

Q(10)=1.0/8.0

Q(11)=0

Q(12)=1.0/8.0

R(1)=1.0/8.0

R(2)=1.0/8.0

R(3)=0

R(4)=-1.0/8.0

R(5)=-1.0/8.0

R(6)=0

R(7)=-1.0/8.0

R(8)=1.0/8.0

R(9)=0

R(10)=1.0/8.0

R(11)=-1.0/8.0

R(12)=0

S(1)=1.0/8.0

S(2)=0

S(3)=-1.0/8.0

S(4)=-1.0/8.0

S(5)=0

S(6)=-1.0/8.0

S(7)=-1.0/8.0

S(8)=0

S(9)=1.0/8.0

S(10)=1.0/8.0

S(11)=0

S(12)=1.0/8.0

ASR=ASR*NEI/NEJ

C   D11=4.0*D11*(NEI/NEJ)/ASR

C   D12=4.0*D12*(NEJ/NEI)*ASR

C   D16=4.0*D16

C   D22=4.0*D22*(NEJ/NEI)**3*ASR**3

C   D26=4.0*D26*(NEJ/NEI)**2*ASR**2

C   D66=4.0*D66*(NEJ/NEI)*ASR

    D11=4.0*D11/ASR

    D12=4.0*D12*ASR

    D16=8.0*D16

    D22=4.0*D22*ASR**3

    D26=8.0*D26*ASR**2

    D66=16.0*D66*ASR

    DO 110 I=1,12

    DO 110 J=1,12

    RR=2.0*B(I)*(B(J)+G(J)+P(J)/3.0)+8.0*D(I)*D(J)/3.0+2.0*E(I)*(

    +E(J)/3.0+R(J)/3.0+S(J)/5.0)+2.0*G(I)*(B(J)+9.0*G(J)/5.0+P(J)/3.0)+

    +8.0*H(I)*H(J)/9.0+2.0*P(I)*(B(J)/3.0+G(J)/3.0+P(J)/5.0)+

    +2.0*R(I)*(E(J)/3.0+3.0*R(J)/5.0+S(J)/5.0)+2.0*S(I)*(E(J)/5.0+

    +R(J)/5.0+S(J)/7.0)

    RR=2.0*RR

    SS=2.0*C(I)*(C(J)+Q(J)+H(J)/3.0)+8.0*F(I)*F(J)/3.0+2.0*E(I)*

    +(E(J)/3.0+S(J)/3.0+R(J)/5.0)+2.0*Q(I)*(C(J)+9.0*Q(J)/5.0+H(J)/

    +3.0)+8.0*P(I)*P(J)/9.0+2.0*H(I)*(C(J)/3.0+Q(J)/3.0+H(J)/5.0)+

    +2.0*S(I)*(E(J)/3.0+3.0*S(J)/5.0+R(J)/5.0)+2.0*R(I)*(E(J)/5.0+

    +S(J)/5.0+R(J)/7.0)

    SS=2.0*SS

    RS=2.0*B(I)*(C(J)+H(J)/3.0+Q(J))+4.0*D(I)*(E(J)/3.0+R(J)/5.0+

$+S(J)/3.0)+4.0*E(I)*F(J)/3.0+2.0*G(I)*(C(J)+3.0*H(J)/5.0+Q(J))+$

$+8.0*H(I)*P(J)/9.0+2.0*P(I)*(C(J)/3.0+H(J)/9.0+3.0*Q(J)/5.0)+$

$+4.0*R(I)*F(J)/3.0+4.0*S(I)*F(J)/5.0$

RS=2.0*RS

SR=2.0*C(I)*(B(J)+P(J)/3.0+G(J))+4.0*F(I)*(E(J)/3.0+S(J)/5.0+

$+R(J)/3.0)+4.0*E(I)*D(J)/3.0+2.0*Q(I)*(B(J)+3.0*P(J)/5.0+G(J))+$

$+8.0*P(I)*H(J)/9.0+2.0*H(I)*(B(J)/3.0+P(J)/9.0+3.0*G(J)/5.0)+$

$+4.0*S(I)*D(J)/3.0+4.0*R(I)*D(J)/5.0$

SR=2.0*SR

RRRR=8.0*D(I)*D(J)+24.0*G(I)*G(J)+8.0*H(I)*H(J)/3.0+8.0*S(I)*S(J)

RRRR=2.0*RRRR

SSSS=8.0*F(I)*F(J)+24.0*Q(I)*Q(J)+8.0*P(I)*P(J)/3.0+8.0*S(I)*S(J)

SSSS=2.0*SSSS

RRSS=8.0*D(I)*F(J)+8.0*G(I)*P(J)+8.0*H(I)*Q(J)+8.0*R(I)*S(J)

RRSS=2.0*RRSS

SSRR=8.0*F(I)*D(J)+8.0*P(I)*G(J)+8.0*Q(I)*H(J)+8.0*S(I)*R(J)

SSRR=2.0*SSRR

RSRS=2.0*E(I)*(E(J)+R(J)+S(J))+8.0*H(I)*H(J)/3.0+8.0*P(I)*P(J)/

$+3.0+2.0*R(I)*(E(J)+9.0*R(J)/5.0+S(J))+2.0*S(I)*(E(J)+R(J)+9.0*$

$+S(J)/5.0)$

RSRS=2.0*RSRS

RRRS=4.0*D(I)*(E(J)+R(J)+S(J))+8.0*G(I)*H(J)+8.0*H(I)*P(J)/3.0

RRRS=2.0*RRRS

RSRR=4.0*D(J)*(E(I)+R(I)+S(I))+8.0*H(I)*G(J)+8.0*P(I)*H(J)/3.0

RSRR=2.0*RSRR

```fortran
      SSRS=4.0*F(I)*(E(J)+R(J)+S(J))+8.0*Q(I)*P(J)+8.0*P(I)*H(J)/3.0
      SSRS=2.0*SSRS
      RSSS=4.0*F(J)*(E(I)+R(I)+S(I))+8.0*P(I)*Q(J)+8.0*H(I)*P(J)/3.0
      RSSS=2.0*RSSS



      ST(I,J)=D11*RRRR+D12*SSRR+D16*RSRR+D12*RRSS+D22*SSSS+D26
     *RSSS+
     +D16*RRRS+D26*SSRS+D66*RSRS
      ST(I,J)=ST(I,J)*NEJ**2
      ZT(I,J)=PX*RR/ASR+PXY*(RS+SR)+PY*ASR*SS
  110 CONTINUE

      DO 40 I=1,NE
      DO 40 J=1,12
      L=ED(I,J)
      DO 40 K=1,12
      T=ED(I,K)
      IF(L.NE.0.AND.T.NE.0) THEN
      ESM(L,T)=ESM(L,T)+ST(J,K)
      EMM(L,T)=EMM(L,T)+ZT(J,K)
      ENDIF
   40 CONTINUE
      RETURN
      END
```

```
C***********************************************************

C***

      SUBROUTINE LUCOM(A,N,INDX,FLAG,M1)
      PARAMETER (M11=500, TINY=1.0E-20)
      INTEGER FLAG
      DIMENSION A(M1,M1),VV(M11),INDX(M1)


      FLAG=1
      D=1.0
      DO 12 I=1,N
      AMAX=0
      DO 11 J=1,N
      IF(ABS(A(I,J)).GT.AMAX) AMAX=ABS(A(I,J))
   11 CONTINUE
      IF(AMAX.EQ.0.0) THEN
      WRITE(*,*)'Singular matrix in subroutine LUCOM'
      FLAG=0
      RETURN
      ENDIF
      VV(I)=1.0/AMAX
   12 CONTINUE
      DO 19 J=1,N
      DO 14 I=1,J-1
      SUM=A(I,J)
      DO 13 K=1,I-1
```

```
      SUM=SUM-A(I,K)*A(K,J)
13 CONTINUE
   A(I,J)=SUM
14 CONTINUE
   AMAX=0.0
   DO 16 I=J,N
   SUM=A(I,J)
   DO 15 K=1,J-1
   SUM=SUM-A(I,K)*A(K,J)
15 CONTINUE
   A(I,J)=SUM
   DUM=VV(I)*ABS(SUM)
   IF(DUM.GE.AMAX) THEN
   IMAX=I
   AMAX=DUM
   ENDIF
16 CONTINUE
   IF(J.NE.IMAX) THEN
   DO 17 K=1,N
   DUM=A(IMAX,K)
   A(IMAX,K)=A(J,K)
   A(J,K)=DUM
17 CONTINUE
   D=-D
   VV(IMAX)=VV(J)
```

```fortran
      ENDIF

      INDX(J)=IMAX

      IF(A(J,J).EQ.0.0) A(J,J)=TINY

      IF(J.NE.N) THEN

      DUM=1.0/A(J,J)

      DO 18 I=J+1,N

      A(I,J)=A(I,J)*DUM

   18 CONTINUE

      ENDIF

   19 CONTINUE

      RETURN

      END
```

C***

```fortran
      SUBROUTINE LUSOL(A,N,INDX,X,M1)

      DIMENSION A(M1,M1),INDX(M1),X(M1,M1)


      DO 191 IT=1,N

      DO 192 J=1,N

      IF(IT.EQ.J) THEN

      X(J,IT)=1.0

      ELSE

      X(J,IT)=0.0

      ENDIF

  192 CONTINUE
```

```fortran
      II=0
      DO 12 I=1,N
      LL=INDX(I)
      SUM=X(LL,IT)
      X(LL,IT)=X(I,IT)
      IF(II.NE.0) THEN
      DO 11 J=II,I-1
      SUM=SUM-A(I,J)*X(J,IT)
11    CONTINUE
      ELSE IF(SUM.NE.0) THEN
      II=I
      ENDIF
      X(I,IT)=SUM
12    CONTINUE
      DO 14 I=N,1,-1
      SUM=X(I,IT)
      DO 13 J=I+1,N
      SUM=SUM-A(I,J)*X(J,IT)
13    CONTINUE
      X(I,IT)=SUM/A(I,I)
14    CONTINUE
191   CONTINUE
      RETURN
      END
```

```
C*****************************************
C***  This subroutine computes the product of two square
C***  matrices

      SUBROUTINE MULT(A,B,C,N,M1)
      DIMENSION A(M1,M1),B(M1,M1),C(M1,M1)

      DO 15 I=1,N
      DO 15 J=1,N
      SUM=0.0
      DO 10 K=1,N
      SUM=SUM+A(I,K)*B(K,J)
   10 CONTINUE
      C(I,J)=SUM
   15 CONTINUE
      RETURN
      END
C*****************************************
C***  This subroutine balances the plate matrix
      SUBROUTINE BAL(A,N,M1)
      INTEGER LAST
      DIMENSION A(M1,M1)

      RADX=2
```

```fortran
      SQRADX=RADX**2

    1 CONTINUE
      LAST=1
      DO 14 I=1,N
      C=0.0
      R=0.0
      DO 11 J=1,N
      IF(J.NE.I) THEN
      C=C+ABS(A(J,I))
      R=R+ABS(A(I,J))
      ENDIF
   11 CONTINUE
      IF(ABS(C).GT.0.AND.ABS(R).GT.0) THEN
      G=R/RADX
      F=1.0
      S=C+R

    2 IF(C.LT.G) THEN
      F=F*RADX
      C=C*SQRADX
      GO TO 2
      ENDIF

      G=RADX
```

```
   3 IF(C.GT.G) THEN

     F=F/RADX

     C=C/SQRADX

     GO TO 3

     ENDIF


     IF((C+R)/F.LT.0.95*S) THEN

     LAST=0

     G=1.0/F

     DO 12 J=1,N

     A(I,J)=A(I,J)*G

  12 CONTINUE

     DO 13 J=1,N

     A(J,I)=A(J,I)*F

  13 CONTINUE

     ENDIF

     ENDIF

  14 CONTINUE

     IF(LAST.EQ.0) GO TO 1

     RETURN

     END

C***************************************************

C    This subroutine reduces a general matrix to Heisenberg form

     SUBROUTINE HES(A,N,M1)

     DIMENSION A(M1,M1)
```

```
      DO 17 M=2,N-1

      X=0.0

      I=M

      DO 11 J=M,N

      IF(ABS(A(J,M-1)).GT.ABS(X)) THEN

      X=A(J,M-1)

      I=J

      ENDIF

   11 CONTINUE

      IF(I.NE.M) THEN

      DO 12 J=M-1,N

      Y=A(I,J)

      A(I,J)=A(M,J)

      A(M,J)=Y

   12 CONTINUE

      DO 13 J=1,N

      Y=A(J,I)

      A(J,I)=A(J,M)

      A(J,M)=Y

   13 CONTINUE

      ENDIF

      IF(X.NE.0) THEN

      DO 16 I=M+1,N

      Y=A(I,M-1)
```

```fortran
      IF(Y.NE.0) THEN

      Y=Y/X

      A(I,M-1)=Y

      DO 14 J=M,N

      A(I,J)=A(I,J)-Y*A(M,J)

14 CONTINUE

      DO 15 J=1,N

      A(J,M)=A(J,M)+Y*A(J,I)

15 CONTINUE

      ENDIF

16 CONTINUE

      ENDIF

17 CONTINUE

      RETURN

      END
```

C***

C   This subroutine uses the QR algorithm to find eigenvalues.

```fortran
      SUBROUTINE HQR(A,WR,WI,N,FLAG,M1)

      INTEGER FLAG

      DIMENSION A(M1,M1),WR(M1),WI(M1)


      FLAG=1

      ANORM=0

      DO 10 I=1,N
```

```
        DO 10 J=MAX(I-1,1),N

        ANORM=ANORM+ABS(A(I,J))

10 CONTINUE


    NN=N

    T=0.0

 1 IF(NN.GE.1) THEN

    ITS=0

 2 DO 13 L=NN,2,-1

    S=ABS(A(L-1,L-1))+ABS(A(L,L))

    IF(S.EQ.0) S=ANORM

    IF(ABS(A(L,L-1))+S.EQ.S) THEN

    A(L,L-1)=0.0

    GO TO 3

    ENDIF

13 CONTINUE

    L=1

 3 X=A(NN,NN)

    IF(L.EQ.NN) THEN

    WR(NN)=X+T

    WI(NN)=0.0

    NN=NN-1

    ELSE

    Y=A(NN-1,NN-1)

    W=A(NN,NN-1)*A(NN-1,NN)
```

```
      IF(L.EQ.NN-1) THEN

      P=0.5*(Y-X)

      Q=P**2+W

      Z=SQRT(ABS(Q))

      X=X+T

      IF(Q.GE.0.0) THEN

      Z=P+SIGN(Z,P)

      WR(NN)=X+Z

      WR(NN-1)=WR(NN)

      IF(ABS(Z).GT.0) WR(NN)=X-W/Z

      WI(NN)=0.0

      WI(NN-1)=0.0

      ELSE

      WR(NN)=X+P

      WR(NN-1)=WR(NN)

      WI(NN)=Z

      WI(NN-1)=-Z

      ENDIF

      NN=NN-2

      ELSE

C     IF(ITS.EQ.30) THEN

C     WRITE(*,*)'Iterations exceeded 30 in HQR subroutine'

C     FLAG=0

C     RETURN

C     ENDIF
```

```fortran
      IF(ITS.EQ.10.OR.ITS.EQ.20) THEN
      T=T+X
      DO 14 I=1,NN
      A(I,I)=A(I,I)-X
   14 CONTINUE
      S=ABS(A(NN,NN-1))+ABS(A(NN-1,NN-2))
      X=0.75*S
      Y=X
      W=-0.4375*S**2
      ENDIF
      ITS=ITS+1
      DO 15 M=NN-2,L,-1
      Z=A(M,M)
      R=X-Z
      S=Y-Z
      P=(R*S-W)/A(M+1,M)+A(M,M+1)
      Q=A(M+1,M+1)-Z-R-S
      R=A(M+2,M+1)
      S=ABS(P)+ABS(Q)+ABS(R)
      P=P/S
      Q=Q/S
      R=R/S
      IF(M.EQ.L) GO TO 4
      U=ABS(A(M,M-1))*(ABS(Q)+ABS(R))
      V=ABS(P)*(ABS(A(M-1,M-1))+ABS(Z)+ABS(A(M+1,M+1)))
```

```fortran
      IF(U+V.EQ.V) GO TO 4
   15 CONTINUE
    4 DO 16 I=M+2,NN
      A(I,I-2)=0.0
      IF(I.NE.M+2) A(I,I-3)=0.0
   16 CONTINUE
      DO 19 K=M,NN-1
      IF(K.NE.M) THEN
      P=A(K,K-1)
      Q=A(K+1,K-1)
      R=0.0
      IF(K.NE.NN-1) R=A(K+2,K-1)
      X=ABS(P)+ABS(Q)+ABS(R)
      IF(ABS(X).GT.0) THEN
      P=P/X
      Q=Q/X
      R=R/X
      ENDIF
      ENDIF
      S=SIGN(SQRT(P**2+Q**2+R**2),P)
      IF(ABS(S).GT.0) THEN
      IF(K.EQ.M) THEN
      IF(L.NE.M) A(K,K-1)=-A(K,K-1)
      ELSE
      A(K,K-1)=-S*X
```

```fortran
      ENDIF

      P=P+S

      X=P/S

      Y=Q/S

      Z=R/S

      Q=Q/P

      R=R/P

      DO 17 J=K,NN

      P=A(K,J)+Q*A(K+1,J)

      IF(K.NE.NN-1) THEN

      P=P+R*A(K+2,J)

      A(K+2,J)=A(K+2,J)-P*Z

      ENDIF

      A(K+1,J)=A(K+1,J)-P*Y

      A(K,J)=A(K,J)-P*X

   17 CONTINUE

      DO 18 I=L,MIN(NN,K+3)

      P=X*A(I,K)+Y*A(I,K+1)

      IF(K.NE.NN-1) THEN

      P=P+Z*A(I,K+2)

      A(I,K+2)=A(I,K+2)-P*R

      ENDIF

      A(I,K+1)=A(I,K+1)-P*Q

      A(I,K)=A(I,K)-P

   18 CONTINUE
```

```fortran
      ENDIF
   19 CONTINUE
      GO TO 2
      ENDIF
      ENDIF
      GO TO 1
      ENDIF
      RETURN
      END
C*******************************************
C***  This subroutine arrange loads in descending order.

      SUBROUTINE ESORT(LAMBDA,VAL,DOF,M1)
      REAL LAMBDA
      INTEGER DOF
      DIMENSION LAMBDA(M1),VAL(M1)

      DO 14 I=1,DOF-1
      K=I
      P=LAMBDA(I)
      DO 11 J=I+1,DOF
      IF(LAMBDA(J).LE.P)THEN
      K=J
      P=LAMBDA(J)
      ENDIF
```

```fortran
   11 CONTINUE
      IF(K.NE.I)THEN
      LAMBDA(K)=LAMBDA(I)
      LAMBDA(I)=P
      ENDIF
   14 CONTINUE
      DO 15 I=1,DOF
      VAL(I)=LAMBDA(I)
   15 CONTINUE
      RETURN
      END
```

C**

C*** This subroutine computes the eigenvectors.

```fortran
      SUBROUTINE SIL(A,X,VAL,NN,FLAG,M1,M5)
      PARAMETER (M11=500)
      INTEGER FLAG
      DIMENSION
A(M1,M1),B(M11),X(M1,M5),VAL(M1),ALFA(M11,M11)

      FLAG=1
      DO 109 I=1,NN
      DO 109 J=1,NN
      ALFA(I,J)=A(I,J)
  109 CONTINUE
```

```fortran
C***  Solution of system equations.
      DO 200 IT=1,M5
      IF(IT.GT.1) THEN
      DO 210 I=1,NN
      DO 210 J=1,NN
      A(I,J)=ALFA(I,J)
  210 CONTINUE
      ENDIF

      DO 110 I=1,NN
      X(I,IT)=0.0
      B(I)=-A(I,NN)
      A(I,I)=A(I,I)-VAL(IT)
  110 CONTINUE

      N=NN-1
C***  Gaussian elimination
      DO 170 K=1,N-1

C***  Pivoting routine
      IF(A(K,K).EQ.0.0)THEN
      K1=0
      DO 121 L=K+1,N
      IF(A(L,K).NE.0.0)K1=L
      IF(K1.EQ.L)GO TO 130
```

```fortran
121 CONTINUE
130 DO 140 J=1,N
    AS=A(K,J)
    A(K,J)=A(K1,J)
    A(K1,J)=AS
140 CONTINUE
    BS=B(K)
    B(K)=B(K1)
    B(K1)=BS
    ENDIF


    IF(A(K,K).EQ.0.0) THEN
    WRITE(*,*) 'Divide by zero in subroutine SIL'
    FLAG=0
    RETURN
    ENDIF


    M=K
    DO 170 I=M,N-1
    R=A(I+1,K)/A(K,K)
    B(I+1)=B(I+1)-R*B(K)
    DO 170 J=M,N
    A(I+1,J)=A(I+1,J)-R*A(K,J)
170 CONTINUE
```

C*** Backward substitution

```
      X(N,IT)=B(N)/A(N,N)
      DO 190 I=N-1,1,-1
      SUM=0.0
      DO 180 J=I+1,N
      SUM=A(I,J)*X(J,IT)+SUM
  180 CONTINUE
      X(I,IT)=(B(I)-SUM)/A(I,I)
  190 CONTINUE
      X(NN,IT)=1.0
  200 CONTINUE
      RETURN
      END
```

C***

C*** This subroutine arrange the eigenvectors.

```
      SUBROUTINE
PNATF(A,DOF,NEI,NEJ,EE,WD,PHID,THID,M1,M4,M5,M6,
   +M7,M8,NODE)
      INTEGER DOF,COUNT,EE,ELEMENT
      PARAMETER (M11=500, M66=121, M55=7, M44=180)
      DIMENSION
A(M1,M5),W(M66,M55),PHI(M66,M55),THI(M66,M55),NX(M11),

+EE(M4,M8),NODE(M4,M7),WD(M5,M6,M6),PHID(M5,M6,M6),THID(M
5,M6,M6),
   +WF(M44,M55),PHIF(M44,M55),THIF(M44,M55)
```

```fortran
      NE=NEI*NEJ

      NODES=NODE(NE,3)

      NALL=3*NODES


      COUNT=0

      DO 310 I=1,NEJ

      DO 310 J=1,2

      L=NODE(I,J)

      DO 310 K=1,3

      COUNT=COUNT+1

      NX(COUNT)=EE(L,K)

  310 CONTINUE

      DO 314 J=3,4

      L=NODE(NEJ,J)

      DO 314 K=1,3

      COUNT=COUNT+1

      NX(COUNT)=EE(L,K)

  314 CONTINUE


      N=2

      DO 315 I=NEJ+1,NE

      J=1

      L=NODE(I,J)

      DO 311 K=1,3
```

```fortran
      COUNT=COUNT+1
      NX(COUNT)=EE(L,K)
  311 CONTINUE
      IEQ=N*NEJ
      IF(I.EQ.IEQ) THEN
      N=N+1
      J=3
      L=NODE(I,J)
      DO 319 K=1,3
      COUNT=COUNT+1
      NX(COUNT)=EE(L,K)
  319 CONTINUE
      ENDIF
  315 CONTINUE

      DO 31 I=DOF+1,NALL
      DO 31 J=1,M5
      A(I,J)=0.0
   31 CONTINUE

      DO 330 K=1,M5
      DO 330 I=1,NALL
      IF(NX(I).EQ.0) THEN
      DO 340 J=NALL-1,I,-1
      A(J+1,K)=A(J,K)
```

```
340 CONTINUE

   A(I,K)=0.0

   ENDIF

330 CONTINUE


   DO 350 K=1,M5

   I1=1

   DO 350 I=1,NALL,3

   W(I1,K)=A(I,K)

   PHI(I1,K)=A(I+1,K)

   THI(I1,K)=A(I+2,K)

   I1=I1+1

350 CONTINUE


   DO 380 K=1,M5

   PW=0.0

   PP=0.0

   PT=0.0

   DO 390 I=1,NODES

   PW=MAX(ABS(W(I,K)),PW)

   PP=MAX(ABS(PHI(I,K)),PP)

   PT=MAX(ABS(THI(I,K)),PT)

390 CONTINUE


   IF(PW.GT.0) THEN
```

```fortran
      DO 402 I=1,NODES

      W(I,K)=W(I,K)/PW

402 CONTINUE

      ENDIF

      IF(PP.GT.0) THEN

      DO 403 I=1,NODES

      PHI(I,K)=PHI(I,K)/PP

403 CONTINUE

      ENDIF

      IF(PT.GT.0) THEN

      DO 404 I=1,NODES

      THI(I,K)=THI(I,K)/PT

404 CONTINUE

      ENDIF

380 CONTINUE


      DO 515 N=1,M5

      I1=0

      DO 510 I=1,NEJ

      DO 510 J=1,2

      L=NODE(I,J)

      I1=I1+1

      WF(L,N)=W(I1,N)

      PHIF(L,N)=PHI(I1,N)

      THIF(L,N)=THI(I1,N)
```

```
510 CONTINUE

   I=NEJ

   DO 514 J=3,4

   L=NODE(I,J)

   I1=I1+1

   WF(L,N)=W(I1,N)

   PHIF(L,N)=PHI(I1,N)

   THIF(L,N)=THI(I1,N)

514 CONTINUE


   M=2

   DO 515 I=NEJ+1,NE

   J=1

   L=NODE(I,J)

   I1=I1+1

   WF(L,N)=W(I1,N)

   PHIF(L,N)=PHI(I1,N)

   THIF(L,N)=THI(I1,N)

   IEQ=M*NEJ

   IF(I.EQ.IEQ) THEN

   M=M+1

   J=3

   L=NODE(I,J)

   I1=I1+1

   WF(L,N)=W(I1,N)
```

```fortran
      PHIF(L,N)=PHI(I1,N)

      THIF(L,N)=THI(I1,N)

      ENDIF

515   CONTINUE


      DO 425 K=1,M5

      DO 425 I=1,NEI+1

      IF(I.GT.NEI) THEN

      I1=NEI

      ELSE

      I1=I

      ENDIF

      ELEMENT=(I1-1)*NEJ+1

      IF(I.GT.NEI) THEN

      LMIN=NODE(ELEMENT,1)

      ELSE

      LMIN=NODE(ELEMENT,2)

      ENDIF

      LMAX=LMIN+NEJ

      DO 410 L=LMIN,LMAX

      J=L-LMIN+1

      WD(K,I,J)=WF(L,K)

      PHID(K,I,J)=PHIF(L,K)

      THID(K,I,J)=THIF(L,K)

410   CONTINUE
```

```
     425 CONTINUE

         RETURN

         END

C*****************************************

C***  Arrange critical loads in descending order.


         SUBROUTINE PRINT(VAL,DOF,NLOAD,W,PHI,THI,NEI,NEJ,
        +M1,M5,M6)

         PARAMETER(M11=11)

         INTEGER DOF

         DIMENSION
VAL(M1),W(M5,M6,M6),PHI(M5,M6,M6),THI(M5,M6,M6),
        +X(M11),Y(M11)


      20 FORMAT(I3,1X,7(F8.4,2X))


C***  Write results

         IF(NLOAD.GT.DOF) NLOAD=DOF

         DO 310 I=1,NLOAD

         WRITE(6,20)I,VAL(I)

     310 CONTINUE


C***  Arrange the eigenvectors.


         DO 100 J=1,NEJ+1

         X(J)=(J-1.0)/NEJ
```

```fortran
      100 CONTINUE


         DO 101 I=1,NEI+1

         Y(I)=(I-1.0)/NEI

      101 CONTINUE


C    Arrange the eigenvectors.


      21 FORMAT(F4.2,1X,8(F7.4,2X))

      23 FORMAT(5X,8(F5.2,4X))

      22 FORMAT('Buckling load',2X,7(F7.4,2X))
C***  write buckling modes (eigenvectors)
         WRITE(6,*)

         WRITE(6,*)' * The first seven buckling modes are as follows:'


         DO 1000 K=1,M5

         WRITE(6,22) VAL(K)


         WRITE(6,*)

         WRITE(6,*)'* Out-of-plane normalized displacements W'

         WRITE(6,23)(X(J),J=1,NEJ+1)

         DO 322 I=1,NEI+1

         WRITE(6,21)Y(I),(W(K,I,J),J=1,NEJ+1)

      322 CONTINUE
```

```fortran
      WRITE(6,*)
      WRITE(6,*)'* Normalized rotations PHI'
      WRITE(6,23)(X(J),J=1,NEJ+1)
      DO 323 I=1,NEI+1
      WRITE(6,21)Y(I),(PHI(K,I,J),J=1,NEJ+1)
  323 CONTINUE

      WRITE(6,*)
      WRITE(6,*)'* Normalized rotations THI'
      WRITE(6,23)(X(J),J=1,NEJ+1)
      DO 3231 I=1,NEI+1
      WRITE(6,21)Y(I),(THI(K,I,J),J=1,NEJ+1)
 3231 CONTINUE
      WRITE(6,*)

 WRITE(6,*)'*********************************************'
      WRITE(6,*)
 1000 CONTINUE
      RETURN
      END
```